EMERGING INFECTIOUS DISEASES

A Peer-Reviewed Journal Tracking and Analyzing Disease Trends Vol.6, No.3, May–Jun 2000

Hantavirus Geographic Information Systems Bat Lyssavirus

DEPARTMENT OF HEALTH AND HUMAN SERVICES

CDC
CENTERS FOR DISEASE CONTROL AND PREVENTION

In Index Medicus/Medline, Current Contents, Excerpta Medica, and other databases

Electronic Access

Retrieve the journal electronically on the World Wide Web (WWW) at http://www.cdc.gov/eid or from the CDC home page (http://www.cdc.gov).

Announcements of new table of contents can be automatically e-mailed to you. To subscribe, send an e-mail to listserv@cdc.gov with the following in the body of your message: subscribe EID-TOC.

Emerging Infectious Diseases

Emerging Infectious Diseases is published six times a year by the National Center for Infectious Diseases, Centers for Disease Control and Prevention (CDC), 1600 Clifton Road, Mailstop D 61, Atllanta, GA 30333, USA. Telephone 404-371-5329, fax 404-371-5449, e-mail eideditor@cdc.gov.

EMERGING INFECTIOUS DISEASES

A Peer-Reviewed Journal Tracking and Analyzing Disease Trends Vol.6, No.3, May–Jun 2000

The journal is distributed electronically and in hard copy and is available **at no charge**.

☐ YES, I would like to receive Emerging Infectious Diseases.

Please print your name and business address in the box and return by fax to 404-371-5449 or mail to
EID Editor
CDC/NCID/MS D 61
1600 Clifton Road, NE
Atlanta, GA 30333

Moving? Please give us your new address (in the box) and print the number of your old mailing label here_____

EMERGING INFECTIOUS DISEASES

A Peer-Reviewed Journal Tracking and Analyzing Disease Trends Vol.6, No.3, May–Jun 2000

Cover: Detail of Sonoran Desert. First in the Nature in America series. Stamp Design ©1999 U.S. Postal Service. Reproduced with permission. All rights reserved.

Letters

Perspectives

Research

EMERGING INFECTIOUS DISEASES

A Peer-Reviewed Journal Tracking and Analyzing Disease Trends Vol.6, No.3, May–Jun 2000

Dispatches

Electronic Access

Retrieve the journal electronically on the World Wide Web (WWW) at http://www.cdc.gov/eid or from the CDC home page (http://www.cdc.gov).

Announcements of new table of contents can be automatically e-mailed to you. To subscribe, send an e-mail to listserv@cdc.gov with the following in the body of your message: subscribe EID-TOC.

Research, cont'd

News and Notes

EMERGING INFECTIOUS DISEASES

A Peer-Reviewed Journal Tracking and Analyzing Disease Trends Vol.6, No.3, May–Jun 2000

Remote Sensing and Human Health: New Sensors and New Opportunities

Louisa R. Beck,*† Bradley M. Lobitz,† and Byron L. Wood†
California State University, Monterey Bay, California, USA;
NASA Ames Research Center, Moffett Field, California, USA

Since the launch of Landsat-1 28 years ago, remotely sensed data have been used to map features on the earth's surface. An increasing number of health studies have used remotely sensed data for monitoring, surveillance, or risk mapping, particularly of vector-borne diseases. Nearly all studies used data from Landsat, the French Système Pour l'Observation de la Terre, and the National Oceanic and Atmospheric Administration's Advanced Very High Resolution Radiometer. New sensor systems are in orbit, or soon to be launched, whose data may prove useful for characterizing and monitoring the spatial and temporal patterns of infectious diseases. Increased computing power and spatial modeling capabilities of geographic information systems could extend the use of remote sensing beyond the research community into operational disease surveillance and control. This article illustrates how remotely sensed data have been used in health applications and assesses earth-observing satellites that could detect and map environmental variables related to the distribution of vector-borne and other diseases.

Remote sensing data enable scientists to study the earth's biotic and abiotic components. These components and their changes have been mapped from space at several temporal and spatial scales since 1972. A small number of investigators in the health community have explored remotely sensed environmental factors that might be associated with disease-vector habitats and human transmission risk. However, most human health studies using remote sensing data have focused on data from Landsat's Multispectral Scanner (MSS) and Thematic Mapper (TM), the National Oceanic and Atmospheric Administration (NOAA)'s Advanced Very High Resolution Radiometer (AVHRR), and France's Système Pour l'Observation de la Terre (SPOT). In many of these studies (Table 1), remotely sensed data were used to derive three variables: vegetation cover, landscape structure, and water bodies.

International space agencies are planning an estimated 80 earth-observing missions in the next 15 years (29). During these missions >200 instruments will measure additional environmental features such as ocean color and other currently detectable variables, but at much higher spatial and spectral resolutions. The commercial sector is also planning to launch several systems in the next 5 years that could provide complementary data (30). These new capabilities will improve spectral, spatial, and temporal resolution, allowing exploration of risk factors previously beyond the capabilities of remote sensing. In addition, advances in pathogen, vector, and reservoir and host ecology have allowed assessment of a greater range of environmental factors that promote disease transmission, vector production, and the emergence and maintenance of disease foci, as well as risk for human-vector contact. Advances in computer processing and in geographic information system and global positioning system technologies facilitate integration of remotely sensed environmental parameters with health data so that models for disease surveillance and control can be developed.

In 1998, the National Aeronautics and Space Administration's (NASA) Center for Health Applications of Aerospace Related Technologies (CHAART)[1] evaluated current and planned

Address for correspondence: Louisa R. Beck, Earth Systems Science and Policy, California State University, Monterey Bay, MS 242-4, NASA Ames Research Center, Moffett Field, CA 94035-1000, USA; fax: 650-604-4680; e-mail: lrbeck@gaia.arc.nasa.gov.

[1]CHAART was established at Ames Research Center by NASA's Life Sciences Division, within the Office of Life & Microgravity Sciences & Applications, to make remote sensing, geographic information systems, global positioning systems, and computer modeling available to investigators in the human health community.

Table 1. Research using remote sensing data to map disease vectors[a]

Disease	Vector	Location	Sensor	Ref.
Dracunculiasis	***Cyclops*** spp.	Benin	TM	1
	Cyclops spp.	Nigeria	TM	2
Eastern equine encephalomyelitis	***Culiseta melanura***	Florida, USA	TM	3
Filariasis	***Culex pipiens***	Egypt	AVHRR	4
	Cx. pipiens	Egypt	TM	5,6
Leishmaniasis	***Phlebotomus papatasi***	SW Asia	AVHRR	7
Lyme disease	***Ixodes scapularis***	New York, USA	TM	8,9
	I. scapularis	Wisconsin, USA	TM	10
Malaria	***Anopheles albimanus***	Mexico	TM	11
	An. albimanus	Belize	SPOT	12
	An. albimanus	Belize	SPOT	13
	An. albimanus	Mexico	TM	14
	An. spp.	Gambia	AVHRR, Metosat	15,16
	An. albimanus	Mexico	TM	17,18
Rift Valley fever	***Aedes*** & ***Cx***. spp.	Kenya	AVHRR	19,20
	Cx. spp.	Kenya	TM, SAR	21
	Cx. spp.	Senegal	SPOT, AVHRR	22
Schistosomiasis	***Biomphalaria*** spp.	Egypt	AVHRR	23
Trypanosomiasis	***Glossina*** spp.	Kenya, Uganda	AVHRR	24
	Glossina spp.	Kenya	TM	25
	Glossina spp.	West Africa	AVHRR	26
	Glossina spp.	Africa	AVHRR	27
	Glossina spp.	Southern Africa	AVHRR	28

[a]See Appendix A for explanation of sensor acronyms

satellite sensor systems as a first step in enabling human health scientists to determine data relevant for the epidemiologic, entomologic, and ecologic aspects of their research, as well as developing remote sensing-based models of transmission risk. This article discusses the results of the evaluation and presents two examples of how remotely sensed data have been used in health-related studies. The first example, a terrestrial application, illustrates how a single Landsat TM image was used to characterize the spatial patterns of key components of the Lyme disease transmission cycle in New York. The second example, which focuses on the coastal environment, shows how remote sensing data from different satellite systems can be combined to characterize and map environmental variables in the Bay of Bengal that are associated with the temporal patterns of cholera cases in Bangladesh. These examples demonstrate how remote sensing data acquired at various scales and spectral resolutions can be used to study infectious disease patterns.

Lyme Disease in the Northeastern United States

During the past 10 years, NASA's Ames Research Center has been collaborating with the New York Medical College and the Yale School of Medicine to develop remote sensing-based models for mapping Lyme disease transmission risk in the northeastern United States (31,32). The first study compared Landsat TM data with canine seroprevalence rate (CSR) data summarized at the municipality level (31). The canine data were used as a measure of human exposure risk, the assumption being that dogs were more likely to acquire tick bites on or near their owner's property. The second study used TM data to map relative tick abundance on residential properties by using TM-derived indices of vegetation greenness and wetness (32). Figure 1 shows a subset of the TM data used in both studies, as well as some of the products (e.g., maps) derived from the data. Each product illustrated Lyme disease transmission variables, such as vector and reservoir habitats, as well as human risk for disease. Figure 1a shows raw Landsat-5 TM data, which are recorded in six spectral bands (excluding a seventh thermal band) at a spatial resolution of 30 m. These data were processed to derive the products shown in Figures 1b-d.

The image in Figure 1b was used to explore the relationship between forest patch size and deer distribution. Because white-tailed deer

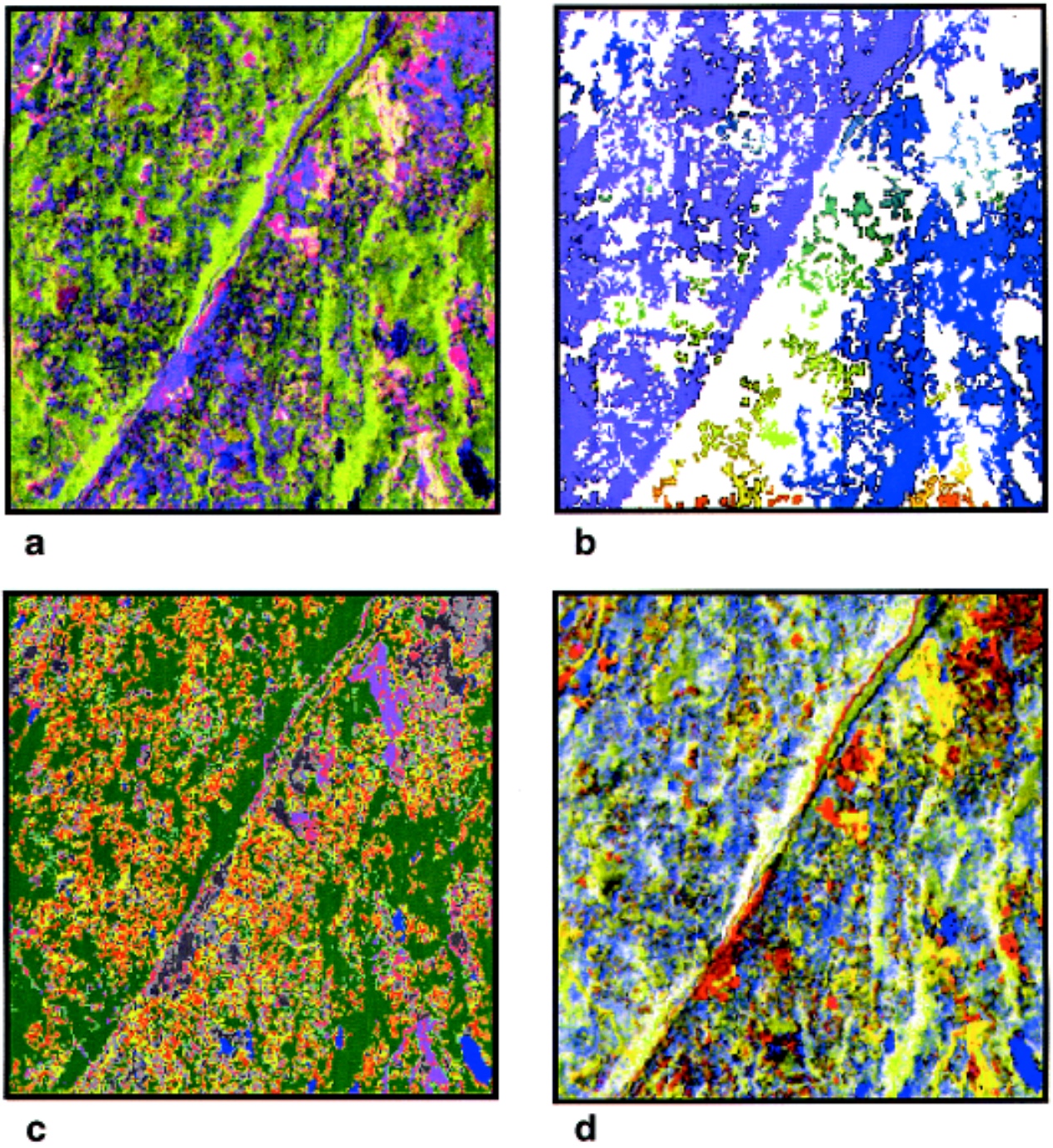

Figure 1. Landsat Thematic Mapper (TM) satellite data for a 6x6-km area in Westchester County, New York. Shown are the raw data (a), as well as products (e.g., maps) derived from the data (b-d) that might be used for modeling Lyme disease transmission risk. a) Raw Landsat TM image composed of bands 5, 4, and 3 (mid-infrared, near-infrared, and red bands). Vegetation is shown in shades of green, with bare soil and urban areas shown in shades of pink and purple. The spatial resolution of these data is 30x30 m. b) Map showing contiguous forest patches, derived from a Landsat TM classification. Colors represent discrete patches, with white indicating the absence of contiguous forest. c) A 12-class land cover map derived from the Landsat TM data. d) Composite image of three spectral indices derived from the Landsat TM data, showing the contributions of scene brightness in red, greenness in green, and wetness in blue.

serve as a major host of the adult tick as well as its primary mode of transportation, deer distribution was a potentially important factor in a Lyme disease risk model.

Figure 1c shows 12 classes used in two separate analyses of risk at two different scales (31). These classes include water, evergreen trees/vegetation, sparse deciduous trees, dense deciduous trees, clearings, golf courses (managed grass), urban/commercial, miscellaneous urban, residential-lawn, residential-sparse vegetation, residential-medium vegetation, and residential high-vegetation. In the first scale, the amount of remotely sensed deciduous forest was positively correlated (r-0.82) with canine exposure to ***Borrelia burgdorferi***, as indicated by CSR data summarized by municipality. In the second analysis, a linear regression of the residential-high vegetation pixels (i.e., wood-edge) and CSR data resulted in a correlation coefficient of 0.84—indicating that human-host contact risk (e.g., deer leaving the forest to feed on residential ornamental vegetation) might be a good measure of human-vector contact risk.

The image in Figure 1d was derived from the Landsat TM data by a Tasseled Cap Transformation (33). Tasseled Cap greenness and wetness were positively correlated with tick abundance on residential properties in this study area (32).

Cholera in Bangladesh

The second example of the use of remotely sensed data to provide information for health research and applications concerns cholera in Bangladesh. In this study, described by Lobitz et al. (34), remotely sensed datasets, downloaded from the Internet at no cost, were used to search for temporal patterns in the Bay of Bengal associated with cholera outbreaks in Bangladesh.

Figure 2a shows a color-infrared image of the Ganges River, where it empties into the Bay of Bengal. These data, which were acquired by NOAA's AVHRR sensor, have a spatial resolution of 1.1 km. The sediment load, transported to the Bay of Bengal by the Ganges and Brahmaputra rivers, includes nutrients that could support plankton blooms. Plankton is an important marine reservoir of ***Vibrio cholerae***, which attaches primarily to zooplankton, which, in turn, is associated with phytoplankton (35).

In Figure 2b, the AVHRR data shown in Figure 2A were processed to show sea surface temperature (SST) (36). Because these data are for large-area studies, they have been processed at a spatial resolution of 18 km. Figure 2c represents sea surface height (SSH) anomaly data derived from the TOPEX/Poseidon satellite (37). These data have a spatial resolution of 1 degree. Increases in SST and SSH have preceded cholera outbreaks in Bangladesh (34).

In the next 15 years, new sensors will provide valuable data for studies of infectious diseases similar to the ones described here. For Lyme disease, new sensors could provide similar information about ecotones, human settlement patterns, or forests. These sensors include ARIES-1, scheduled for launch by Australia; CCD and IR/MSS sensors onboard CBERS, launched by China and Brazil in late 1999; Ikonos, a commercial satellite with 4-m spatial resolution; LISS III, onboard the orbiting Indian IRS-1C and –1D satellites; and ASTER, onboard the recently launched Terra satellite. Information from these sensors could also be used to address other vector-borne diseases, such as malaria, schistosomiasis, trypanosomiasis, and hantavirus, whose patterns are likewise influenced by environmental variables.

SeaWiFS, the Sea-Viewing Wide Field-of-View Sensor, with its increased spectral resolution of 1.1 km, is already providing imagery critical to understanding the temporal and spatial pattern of cholera risk (35). This sensor was specifically designed to gather information about ocean color (38) (Figure 2d).

Sensor Evaluation Project[2]

CHAART evaluated data from current and planned satellite instruments for mapping, surveillance, prediction, and control of human disease transmission activities, including vector ecology, reservoir and host ecology, and human settlement patterns. From hundreds of potential sensors, 54 were identified that were current (or would be launched within the next 5 years), operational (not reserved for the scientific community), and digital (not photographic).

Beginning in 1985, NASA has held a series of workshops to elicit input from the health community on the use of remote sensing in the areas of entomology, ecology, epidemiology, vector control, and infectious diseases. In addition, NASA has participated in sessions on remote sensing and health at professional meetings sponsored by national and international health

[2]The information gathered during the CHAART sensor evaluation process is available at http://geo.arc.nasa.gov/sge/health/sensor/sensor.html.

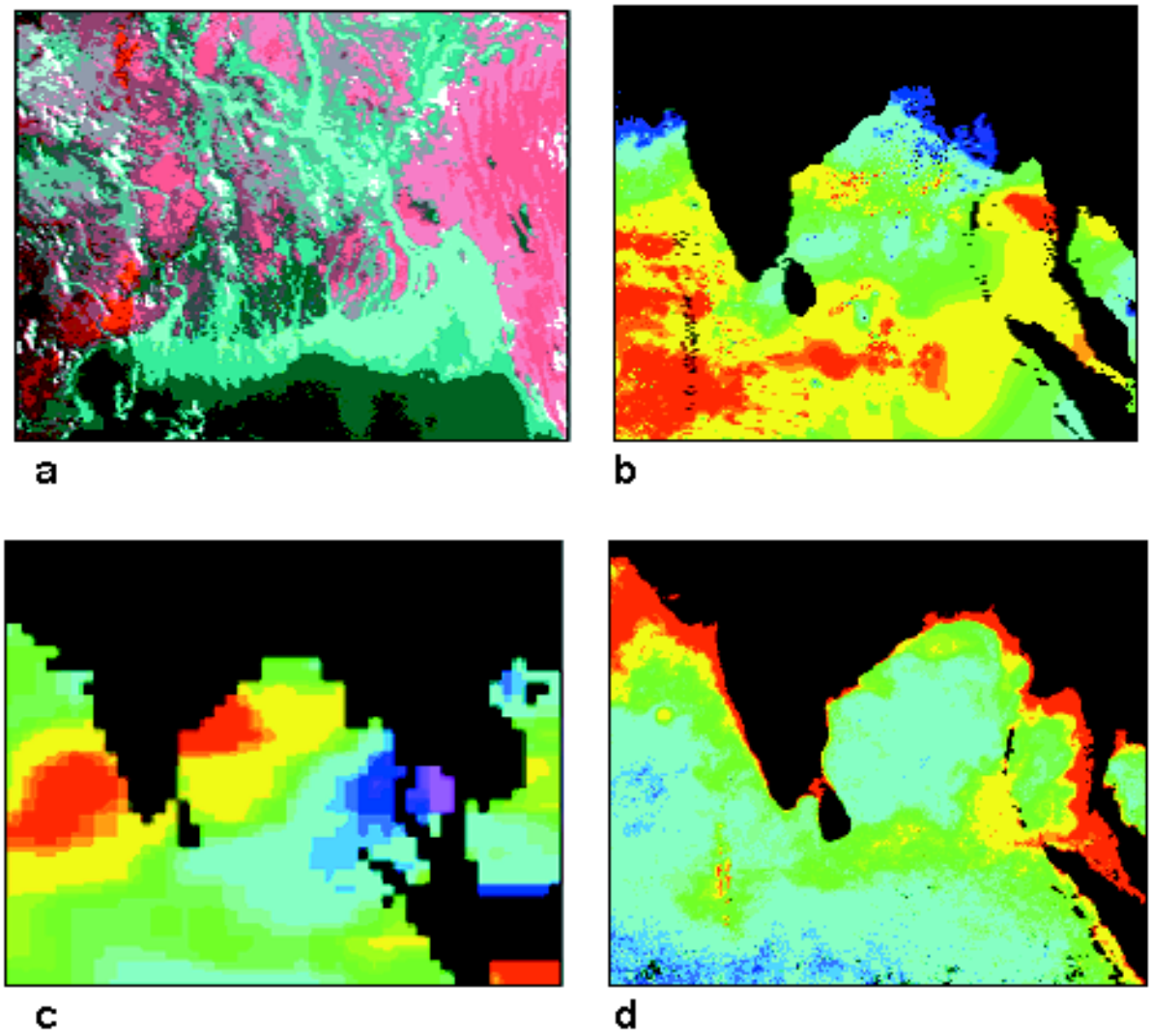

Figure 2. Datasets used to model the temporal patterns of cholera outbreaks in Bangladesh. a) Advanced Very High Resolution Radiometer (AVHRR) satellite image showing the mouth of the Ganges River and the Bay of Bengal. Vegetation is shown in shades of red and water in shades of blue. The spatial resolution of these data is 1.1 km. b) Sea surface temperature data, derived from AVHRR thermal bands. Temperatures range from low (purple) to high (red). c) Sea surface height data, derived from TOPEX/Poseidon satellite data. The spatial resolution of these data is 1 degree. d) Image derived from the Sea-Viewing Wide Field-of-View Sensor (SeaWiFS) showing chlorophyll concentration, ranging from low (blue) to high (red). These satellite data have a nominal spatial resolution of 1.1 km.

organizations. On the basis of this experience as well as a review of the scientific literature (Table 1), there does not appear to be consensus in the health community regarding requirements for a remote sensing system. Some investigators use remotely sensed data to resolve questions regarding the relationship between an aspect of disease transmission and an environmental variable. Other researchers already have a model of disease transmission and have specific spatial, temporal, or spectral requirements for the remotely sensed variables.

No single spatial, temporal, or spectral resolution is universally appropriate for understanding the transmission risk for any disease, given the variety of vectors, reservoirs, hosts,

geographic locations, and environmental variables associated with that disease. Therefore, in evaluating the existing sensors, CHAART used an approach that allowed individual investigators to identify satellite data appropriate for their own needs. This approach defined 16 groups of physical factors that could be used for both research and applications. Each factor is essentially an environmental variable that might have a direct or indirect bearing on the survival of pathogens, vectors, reservoirs, and hosts. These factors may also affect many types of non-vector-borne diseases, such as waterborne diseases. The factors are vegetation or crop type, vegetation green-up, ecotones, deforestation, forest patches, flooded forests, general flooding, permanent water, wetlands, soil moisture, canals, human settlements, urban features, ocean color, SST, and SSH. Precipitation, humidity, and surface temperature were not included because deriving these measurements from raw data requires highly specialized processing and calibration, routinely performed by qualified groups who often make the information available on Internet websites (Appendix B).

The sensor evaluation project generated a series of tables that associated each of the 16 factors with the 54 sensors according to spatial, temporal, and spectral characteristics. For example, factors requiring frequent monitoring, such as vegetation green-up, are linked with sensors with shorter repeat overpasses. Similarly, factors requiring very high spatial resolution, such as mapping urban features, are linked with sensors having a spatial resolution of 10 m or less, regardless of their temporal or spectral resolutions.

Perhaps the broadest use of Landsat and SPOT data has been to identify and map vegetation or crop types. This factor is important because the distribution of vegetation types integrates the combined impact of rainfall, temperature, humidity, topographic effects, soil, water availability, and human activities. Nearly all vector-borne diseases are linked to the vegetated environment during some aspect of their transmission cycle; in many cases, this vegetation can be sensed remotely from space. The spatial and temporal distribution of vector or reservoir and host species may relate to the occurrence and distribution of specific vegetation or crop types, not simply to whether an area has forests or grasslands. For example, food and cover preferences of the white-tailed deer, the host for adult ticks that transmit Lyme disease in the northeastern United States, might well encourage deer to live near certain types of forest. Crop-type information may also be important for studying the effects of pesticides (e.g., vector resistance; illnesses caused by exposure to toxins).

The sensor evaluation procedure has identified many potentially useful sensors for mapping vegetation and crop type beyond the Landsat and SPOT systems (Table 2). A ground resolution threshold of 30 m was used as the upper limit for exploring the relationship between vegetation (or crop) type and disease vectors, reservoirs, and hosts; above 30 m, vegetation and crop type are more difficult to ascertain. Many of the sensors could also be used for mapping the boundary

Table 2. Current and proposed sensor systems for identifying and mapping vegetation and crop type[a]

Temporal resolution (d)	Spatial resolution[b] (m) 1-5	6-10	11-30
Daily	(QuickBird)[c]		
2-7	(Orbview-3,4) (QuickBird)	(Almaz-1b MSU-E2) (ALOS AVNIR-2) (Orbview-4) (SPOT-5a,b 3xHRG)	(ALOS AVNIR-2) (ARIES-1) SPOT-4 2xHRVIR
8-14	Ikonos	Priroda/Mir MOMS-2P	Priroda/Mir MOMS-2P
15-30			Terra ASTER IRS-1C,D LISS III Landsat TM Landsat-7 ETM+ SPOT-2 2xHRV
>30		(ALOS AVNIR-2)	(ALOS AVNIR-2)

[a]This matrix is the output from an interactive search with the search engine located at http://geo.arc.nasa.gov/sge/health/sensor/senchar.html.
[b]See Appendix A for explanations of sensor acronyms.
[c]Sensors in parentheses have not yet been launched.

between vegetation types, or ecotones, which provide habitat for insects and animals critical to the maintenance and transmission of vector-borne diseases. These edges may be areas for increased risk for vector-human contact, as indicated by the relationship between Lyme disease transmission and suburban encroachment into forested areas in the northeastern United States. The movement of humans into forested edges where potential vectors are established could also be important for predicting malaria or yellow fever transmission.

The list of 16 factors used in the CHAART evaluation includes some that have not yet been quantified because available sensors do not provide adequate spatial, spectral, or temporal resolutions. Two of these factors are briefly described below to illustrate how remotely sensed data might be used to explore their potential links to human health. More links between the factors and various diseases are listed in Table 3.

Table 3. Potential links between remotely sensed factors and disease

Factor	Disease	Mapping opportunity
Vegetation/crop type	Chagas disease	Palm forest, dry & degraded woodland habitat for triatomines
	Hantavirus	Preferred food sources for host/reservoirs
	Leishmaniasis	Thick forests as vector/reservoir habitat in Americas
	Lyme disease	Preferred food sources and habitat for host/reservoirs
	Malaria	Breeding/resting/feeding habitats; crop pesticides → vector resistance
	Plague	Prairie dog and other reservoir habitat
	Schistosomiasis	Agricultural association with snails, use of human fertilizer
	Trypanosomiasis	***Glossina*** habitat (forests, around villages, depending on species)
	Yellow fever	Reservoir (monkey) habitat
Vegetation green-up	Hantavirus	Timing of food sources for rodent reservoirs
	Lyme disease	Habitat formation and movement of reservoirs, hosts, vectors
	Malaria	Timing of habitat creation
	Plague	Locating prairie dog towns
	Rift Valley fever	Rainfall
	Trypanosomiasis	***Glossina*** survival
Ecotones	Leishmaniasis	Habitats in and around cities that support reservoir (e.g., foxes)
	Lyme disease	Ecotonal habitat for deer, other hosts/reservoirs; human/vector contact risk.
Deforestation	Chagas disease	New settlements in endemic-disease areas
	Malaria	Habitat creation (for vectors requiring sunlit pools)
		Habitat destruction (for vectors requiring shaded pools)
	Yellow fever	Migration of infected workers into forests where vectors exist
		Migration of disease reservoirs (monkeys) in search of new habitat
Forest patches	Lyme disease	Habitat requirements of deer and other hosts, reservoirs
	Yellow fever	Reservoir (monkey) habitat, migration routes
Flooded forests	Malaria	Mosquito habitat
Flooding	Malaria	Mosquito habitat
	Rift Valley fever	Flooding of dambos, breeding habitat for mosquito vector
	Schistosomiasis	Habitat creation for snails
	St. Louis encephalitis	Habitat creation for mosquitoes
Permanent water	Filariasis	Breeding habitat for ***Mansonia*** mosquitoes
	Malaria	Breeding habitat for mosquitoes
	Onchocerciasis	***Simulium*** larval habitat
	Schistosomiasis	Snail habitat
Wetlands	Cholera	***Vibrio cholerae*** associated with inland water
	Encephalitis	Mosquito habitat
	Malaria	Mosquito habitat
	Schistosomiasis	Snail habitat
Soil moisture	Helminthiases	Worm habitat
	Lyme disease	Tick habitat
	Malaria	Vector breeding habitat
	Schistosomiasis	Snail habitat
Canals	Malaria	Dry season mosquito-breeding habitat; ponding; leaking water
	Onchocerciasis	***Simulium*** larval habitat
	Schistosomiasis	Snail habitat
Human settlements	Diseases	Source of infected humans; populations at risk for transmission in general
Urban features	Chagas disease	Dwellings that provide habitat for triatomines
	Dengue fever	Urban mosquito habitats
	Filariasis	Urban mosquito habitats
	Leishmaniasis	Housing quality
Ocean color (Red tides)	Cholera	Phytoplankton blooms; nutrients, sediments
Sea surface temp.	Cholera	Plankton blooms (cold water upwelling in marine environment)
Sea surface height	Cholera	Inland movement of ***Vibrio***-contaminated tidal water

Urban Features

The detection of urban features requires higher spatial resolution systems than needed for detecting the presence of human settlements. Some disease vectors are associated with specific urban features such as housing type, which can only be detected by sensors with very high spatial resolution. In the future, new sensors may be able to provide information on the urban environment (Table 4).

Table 4. Current and proposed sensor systems for identifying and mapping urban features[a]

Temporal resolution (d)	Spatial resolution[b] (m) 1-5	6-10
Daily	(QuickBird)[c]	
2-7	(ALOS AVNIR-2)	(Almaz-1b MSU-E2)
	(Orbview-3,4)	(ALOS AVNIR-2)
	(QuickBird)	(ARIES-1)
	(SPOT-5a,b 3xHRVIR)	IRS-1C,D PAN
		(Orbview-4)
		SPOT-4 2xHRVIR
		(SPOT-5a,b 3xHRVIR)
8-15	Ikonos	IRS-1C,D PAN
		Priroda/Mir MOMS-2P
15-30		IRS-1C,D PAN
		SPOT-2 2xHRV
>30	(ALOS AVNIR-2)	(ALOS AVNIR-2)

[a]This matrix is the output from an interactive search with the search engine located at http://geo.arc.nasa.gov/sge/health/sensor/senchar.html
[b]See Appendix A for explanations of sensor acronyms.
[c]Sensors in parentheses have not yet been launched.

Soil Moisture

Wet soils indicate a suitable habitat for species of snails, mosquito larvae, ticks, and worms. Several types of sensors can detect soil moisture, including synthetic aperture radars (SARs), shortwave-infrared, and thermal-infrared sensors (Table 5). SARs are particularly important for sensing ground conditions in areas of cloud cover or vegetation canopy cover, two factors commonly found in the tropics.

Conclusions

The extent to which remotely sensed data are used for studying the spatial and temporal patterns of disease depends on a number of obstacles and opportunities. Many of the obstacles—including cost, inadequate spatial, spectral, or temporal resolutions, and long turnaround times for products—have restricted the use of remote sensing within the user community as a whole. Many of these barriers will be addressed by new sensor systems in the next 5 years. The recently launched Landsat-7 ETM+ sensor, for example, is now providing 30-m multispectral data, a 15-m panchromatic band, and an improved 60-m thermal infrared band, all at a cost that is an order of magnitude less than current Landsat-5 TM data.

With the higher spatial and spectral resolutions, more frequent coverage, lower price,

Table 5. Current and proposed sensor systems for identifying and mapping soil moisture[a]

Temporal resolution (d)	Spatial Resolution[b] (m) 11-30	101-500	501-1,000	1,001-4,000
Daily				NOAA AVHRR
2-7	(Almaz-1b SAR-70)[c]		(ADEOS II GLI)	
	(ARIES-1)		(Almaz-1b MSU-SK)	
	(ENVISAT-1 ASAR)		(Almaz-1b SROSM)	
	Radarsat		(ENVISAT-1 AATSR)	
	SPOT-4 2xHRVIR		Terra MODIS	
			(EOS PM-1 MODIS)	
			Resurs-01 N2,3	
			MSU-SK	
8-14	(LightSAR)			
	Priroda/Mir MOMS-2P		Priroda/Mir MSU-SK	
15-30	Terra ASTER	Landsat TM TIR		
	ERS-1,2 AMI-SAR			
	Landsat TM			
	Landsat-7 ETM+			
>30	ERS-1,2 AMI-SAR			

[a]This matrix is the output from an interactive search with the search engine located at http://geo.arc.nasa.gov/sge/health/sensor/senchar.html.
[b]See Appendix A for explanations of sensor acronyms.
[c]Sensors in parentheses have not yet been launched.

and increased availability offered by the range of new sensors, human health investigators should be able to extract many more environmental variables than previously realized. These improvements will provide new opportunities to extend the uses of remote sensing technology beyond a few vector-borne diseases to studies of water- and soil-borne diseases (for example, cholera and schistosomiasis [waterborne] and the helminthiases) and the mapping of human settlements at risk. The next generation of earth-observing remote sensing systems will also allow investigators in the human health community to characterize an increasing range of variables key to understanding the spatial and temporal patterns of disease transmission risk. These improved capabilities, when combined with the increased computing power and spatial modeling capabilities of geographic information systems, should extend remote sensing into operational disease surveillance and control.

Acknowledgment

The CHAART staff acknowledges the contributions made to the sensor project by their colleague Michael A. Spanner (1952-1998).

Funding for the sensor evaluation project was provided by the Office of Earth Science at NASA Headquarters, RW#179. Funding for the Lyme disease and cholera examples described in this article was provided by NASA's Life Sciences Division and the NASA Ames Director's Discretionary Fund.

References

1. Clarke KC, Osleeb JR, Sherry JM, Meert JP, Larsson RW. The use of remote sensing and geographic information systems in UNICEF's dracunculiasis (Guinea worm) eradication effort. Prev Vet Med 1990;11:229-35.
2. Ahearn SC, De Rooy C. Monitoring the effects of dracunculiasis remediation on agricultural productivity using satellite data. International Journal of Remote Sensing 1996;17:917-29.
3. Freier JW. Eastern equine encephalomyelitis. Lancet 1993;342:1281-3.
4. Thompson DF, Malone JB, Harb M, Faris R, Huh OK, Buck AA, et al. Bancroftian filariasis distribution and diurnal temperature differences in the southern Nile Delta. Emerg Infect Dis 1996;2:234-5.
5. Hassan AN, Beck LR, Dister S. Prediction of villages at risk for filariasis transmission in the Nile Delta using remote sensing and geographic information system technologies. J Egypt Soc Parasitol 1998;28:75-87.
6. Hassan AN, Dister S, Beck L. Spatial analysis of lymphatic filariasis distribution in the Nile Delta in relation to some environmental variables using geographic information system technology. J Egypt Soc Parasitol 1998;28:119-31.
7. Cross ER, Newcomb WW, Tucker CJ. Use of weather data and remote sensing to predict the geographic and seasonal distribution of ***Phlebotomus paptasi*** in Southwest Asia. Am J Trop Med Hyg 1996;54:530-6.
8. Dister SW, Beck LR, Wood BL, Falco R, Fish D. The use of GIS and remote sensing technologies in a landscape approach to the study of Lyme disease transmission risk. Proceedings of GIS '93: Geographic Information Systems in Forestry, Environmental and Natural Resource Management; 1993 Feb 15-18; Vancouver, B.C., Canada. 1993.
9. Dister SW, Fish D, Bros S, Frank DH, Wood BL. Landscape characterization of peridomestic risk for Lyme disease using satellite imagery. Am J Trop Med Hyg 1997;57:687-92.
10. Kitron U, Kazmierczak JJ. Spatial analysis of the distribution of Lyme disease in Wisconsin. Am J Epidemiol 1997;145:558-66.
11. Pope KO, Rejmánková E, Savage HM, Arredondo-Jimenez JI, Rodríguez MH, Roberts DR. Remote sensing of tropical wetlands for malaria control in Chiapas, Mexico. Ecological Applications 1993;4:81-90.
12. Rejmánková E, Roberts DR, Pawley A, Manguin S, Polanco J. Predictions of adult ***Anopheles albimanus*** densities in villages based on distance to remotely sensed larval habitats. Am J Trop Meg Hyg 1995;53 (5):482-488.
13. Roberts DR, Paris JF, Manguin S, Harbach RE, Woodruff R, Rejmánková E, et al. Predictions of malaria vector distribution in Belize based on multispectral satellite data. Am J Trop Med Hyg 1996;54:304-8.
14. Rodríguez AD, Rodríguez MH, Hernández JE, Dister SW, Beck LR, Rejmánková E, et al. Landscape surrounding human settlements and malaria mosquito abundance in southern Chiapas, Mexico. J Med Entomol 1996;33:39-48.
15. Thomson MC, Connor SJ, Milligan PJM, Flasse SP. The ecology of malaria-as seen from Earth-observation satellites. Ann Trop Med Parasitol 1996;90:243-64.
16. Thomson MC, Connor SJ, Milligan PJM, Flasse SP. Mapping malaria risk in Africa: what can satellite data contribute? Parsitology Today 1997;13:313-8.
17. Beck LR, Rodríguez MH, Dister SW, Rodríguez AD, Rejmánková E, Ulloa A, et al. Remote sensing as a landscape epidemiologic tool to identify villages at high risk for malaria transmission. Am J Trop Med Hyg 1994;51:271-80.
18. Beck LR, Rodríguez MH, Dister SW, Rodríguez AD, Washino RK, Roberts DR, et al. Assessment of a remote sensing based model for predicting malaria transmission risk in villages of Chiapas, Mexico. Am J Trop Med Hyg 1997;56:99-106.
19. Linthicum KJ, Bailey CL, Davies FG, Tucker CJ. Detection of Rift Valley Fever viral activity in Kenya by satellite remote sensing imagery. Science 1987;235:1656-9.
20. Linthicum KJ, Bailey CL, Tucker CJ, Mitchell KD, Logan TM, Davies FG, et al. Applications of polar-orbiting, meteorological satellite data to detect flooding in Rift Valley Fever virus vector mosquito habitats in Kenya. Med Vet Entomol 1990;4:433-8.

21. Pope KO, Sheffner EJ, Linthicum KJ, Bailey CL, Logan TM, Kasischke ES, et al. Identification of central Kenyan Rift Valley Fever virus vector habitats with Landsat TM and evaluation of their flooding status with Airborne Imaging Radar. Remote Sensing Environment 1992;40:185-96.
22. Linthicum KJ, Bailey CL, Tucker CJ, Gordon SW, Logan TM, Peters CJ, et al. Man-made ecological alterations of Senegal River basin on Rift Valley Fever transmission. Sistema Terra 1994;45-7.
23. Malone JB, Huh OK, Fehler DP, Wilson PA, Wilensky DE, Holmes RA, et al. Temperature data from satellite images and the distribution of schistosomiasis in Egypt. Am J Trop Med Hyg 1994;50:714-22.
24. Rogers DJ. Satellite imagery, tsetse and trypanosomiasis. Prev Vet Med 1991;11:201-20.
25. Kitron U, Otieno LH, Hungerford LL, Odulaja A, Brigham WU, Okello OO, et al. Spatial analysis of the distribution of tsetse flies in the Lambwe Valley, Kenya, using Landsat TM satellite imagery and GIS. Journal of Animal Ecology 1996;65:371-80.
26. Rogers DJ, Randolph SE. Mortality rates and population density of tsetse flies correlated with satellite imagery. Nature 1991;351:739-41.
27. Rogers DJ, Williams BG. Monitoring trypanosomiasis in space and time. Parasitology 1993;106 Suppl:77-92.
28. Robinson TP, Rogers DJ, Williams B. Mapping tsetse habitat suitability in the common fly belt of Southern Africa using multivariate analysis of climate and remotely sensed data. Med Vet Entomol 1997;11:235-45.
29. Committee on Earth Observation Satellites. Coordination for the Next Decade (1995 CEOS Yearbook). European Space Agency. Smith System Engineering Ltd, UK; 1995.
30. Stoney WE. The Pecora legacy-land observation satellites in the next century. Proceedings of the Pecora 13 Symposium; 1996 Aug 20-22; Sioux Falls, SD; Bethesda, MD: American Society for Photogrammetry and Remote Sensing; 1998. p. 260-74.
31. Dister SW, Beck LR, Wood BL, Falco R, Fish D. The use of GIS and remote sensing technologies in a landscape approach to the study of Lyme disease transmission risk. In: Proceedings of GIS '93: Geographic Information Systems in Forestry, Environmental and Natural Resource Management. Vancouver, B.C., Canada; 1993.
32. Dister SW, Fish D, Bros S, Frank DH, Wood BL. Landscape characterization of peridomestic risk for Lyme disease using satellite imagery. Am J Trop Med Hyg 1997;57:687-92.
33. Crist EP, Cicone RC. A physically based transformation of Thematic Mapper data—The TM Tasseled Cap. IEEE Trans Geosciences and Remote Sensing 1984;22:256-63.
34. Lobitz B, Beck L, Huq A, Wood B, Fuchs G, Faroque ASG, et al. Climate and infectious disease: use of remote sensing for detection of ***Vibrio cholerae*** by indirect measurement. Proc National Academy Sciences 2000;97:1438-43.
35. Huq A, Colwell RR. Vibrios in the marine and estuarine environments. J Marine Biotechnology 1995;3:60-3.
36. NASA Jet Propulsion Laboratory, Physical Oceanography Distributed Active Archive Center. Pasadena, California; 1996. Archived data available at the following URL: http://podaac.jpl.nasa.gov
37. Center for Space Research. University of Texas, Austin; 1996. Archived data available at the following URL: http://www.csr.utexas.edu
38. NASA Goddard Distributed Active Archive Center, Greenbelt, Maryland; 1996. Archived data available at the following URL: http://seawifs.gsfc.nasa.gov/cgibrs/level3.pl

Appendix A. Acronyms used in the text and tables

Acronym	Mission	Instruments	Country
ADEOS II	Advanced Earth Observation Satellite	GLI	Japan
ALOS	Advanced Land Observing Satellite	AVNIR	Japan
ARIES	Australian Resource Information & Environment Satellite	ARIES	Australia
CBERS	China-Brazil Earth Resources Satellite	CCD, IR/MSS	China/Brazil
ENVISAT	Environmental Satellite	AATSR, ASAR	Europe
EOS	Earth Observation System	ASTER, MODIS	USA
ERS-2	ESA (European Space Agency) Remote Sensing	AMI-SAR	Europe
IRS	Indian Remote Sensing Satellite	PAN, LISS	India
NOAA	National Oceanographic & Atmospheric Administration	AVHRR	USA
SPOT	Système Pour l'Observation de la Terre	HRV, HRVIR	France
Acronym	**Instrument**	**Mission**	**Country**
AATSR	Advanced Along Track Scanning Radiometer	ENVISAT 1	ESA
AMI-SAR	Active Microwave Instrumentation Synthetic Aperture Radar	ERS-1, 2	ESA
ASAR	Advanced Synthetic Aperture Radar	ENVISAT 1	ESA
ASTER	Advanced Spaceborne Thermal Emission & Reflection Radiometer	Terra	USA
AVHRR	Advanced Very High Resolution Radiometer	NOAA	USA
AVNIR	Advanced Visible & Near Infrared Radiometer	ALOS	Japan
CCD	Charged Couple Device Camera	CBERS	China/Brazil
ETM+	Enhanced Thematic Mapper Plus	Landsat-7	USA
GLI	Global Land Imager	ADEOS II	Japan
HRV	High Resolution Visible	SPOT 1, 2	France
HRVIR	High Resolution Visible & Infrared	SPOT 4, 5	France
IR-MSS	Infrared-Multispectral Scanner	CBERS	China/Brazil
LISS III	Linear Imaging Self-Scanning System	IRS-1C, D	India
MODIS	Moderate Resolution Imaging Spectro Radiometer	Terra, EOS PM 1-3	USA
MOMS-2P	Modular Optoelectronic Multispectral Scanner	Priroda/Mir	Russia
MSU-E2	Multizone High-Resolution Electronic Scanner	Almaz-1B	Russia
MSU-SK	Multizone Middle-Resolution Optomechanical Scanner	Almaz-1B	Russia
		Priroda	Russia
		Resurs-O1, O2	Russia
PAN	Panchromatic	IRS-1C, D	India
PAN	Panchromatic	Ikonos-2	Space Imaging
SAR-70	Synthetic Aperture Radar (70 cm)	Almaz-1B	Russia
SeaWiFS	Sea-Viewing Wide Field-of-View Sensor	TOPEX/Poseidon	France/USA
SROSM	Spectroradiometer for Ocean Satellite Monitoring	Almaz-1B	Russia
TM	Thematic Mapper	Landsat	USA
Acronym	**Miscellaneous**		
ESA	European Space Agency		
TIR	Thermal Infrared		

Appendix B. Partial list of Internet locations that contain (or will contain) products derived from remotely sensed precipitation, moisture, relative humidity, and surface temperature data

Parameter	Mission/ sensor[a]	Spatial	Temporal[b]	Web site
Precipitation	TRMM/TMI	10 km	D	daac.gsfc.nasa.gov/CAMPAIGN_DOCS/hydrology/hd_main.html
Precipitation	TRMM/TMI	5°	M	daac.gsfc.nasa.gov/CAMPAIGN_DOCS/hydrology/hd_main.html
Precipitation	Terra[c]/DAS[d]	1°	8-day	eos-am.gsfc.nasa.gov
Precipitation	GOES/Sounder	10 km	hr	www.nndc.noaa.gov/phase3/productaccm.htm
Precipitation rate	Terra[c]/DAS[d]	2°	8/day	eos-am.gsfc.nasa.gov
Precipitation amount	TOVS/MSU	0.5°	D, M, Y	ghrc.msfc.nasa.gov/ghrc/list.html
Moisture	GOES/Imager	8 km	hr	www.nndc.noaa.gov/phase3/productaccm.htm
Relative humidity	Terra[c]/DAS[d]	2°	4/day	eos-am.gsfc.nasa.gov
Surface temperature	Terra[c]/MODIS	1 km	D	eos-am.gsfc.nasa.gov
Surface temperature	Terra[c]/MODIS	1°	D, 8-day, M	eos-am.gsfc.nasa.gov
Surface temperature	Terra[c]/DAS[d]	2°	8/day	eos-am.gsfc.nasa.gov
Surface temperature	Envisat/AATSR	17 km	D	envisat.estec.esa.nl/envisat-welcom.html
Surface temperature	Envisat/AATSR	50 km	D	envisat.estec.esa.nl/envisat-welcom.html
Surface temperature	ERS/ATSR	1 km	W	earth1.esrin.esa.it/ERS
Surface temperature	Meteosat/VISSR	5 km	48/day	www.eumetsat.de/en
Surface temperature	GOES/Imager	4 km	hr	www.nndc.noaa.gov/phase3/productaccm.htm

[a]See Appendix A for explanation of sensor acronyms.
[b]hr, hourly; D, daily; W, weekly; M, monthly; Y, yearly.
[c]Future launch.
[d]Data Assimilation System.

A Dynamic Transmission Model for Predicting Trends in *Helicobacter pylori* and Associated Diseases in the United States

Marcia F.T. Rupnow,* Ross D. Shachter,* Douglas K. Owens,*† and Julie Parsonnet*
*Stanford University, Stanford, California, USA; †Department of Veterans Affairs Health Care System, Palo Alto, California, USA

To assess the benefits of intervention programs against ***Helicobacter pylori*** infection, we estimated the baseline curves of its incidence and prevalence. We developed a mathematical (compartmental) model of the intrinsic dynamics of ***H. pylori***, which represents the natural history of infection and disease progression. Our model divided the population according to age, infection status, and clinical state. Case-patients were followed from birth to death. A proportion of the population acquired ***H. pylori*** infection and became ill with gastritis, duodenal ulcer, chronic atrophic gastritis, or gastric cancer. We simulated the change in transmissibility consistent with the incidence of gastric cancer and duodenal ulcer over time, as well as current ***H. pylori*** prevalence. In the United States, transmissibility of ***H. pylori*** has decreased to values so low that, should this trend continue, the organism will disappear from the population without targeted intervention; this process, however, will take more than a century.

Helicobacter pylori, a common human bacterial pathogen (1), causes peptic ulcer disease, gastric cancer, and gastric mucosa-associated lymphoid tissue lymphoma. Current U.S. guidelines from the National Institutes of Health recommend antimicrobial treatment only for ***H. pylori*** patients with peptic ulcer disease (2). Because asymptomatic infection is very common, treatment of all asymptomatic persons would be expensive and might promote antibiotic resistance. Prophylactic and therapeutic vaccines against ***H. pylori*** are being developed (3,4); however, if vaccines are to be cost-effective, companies must take into account the changing epidemiology of ***H. pylori*** and related diseases. Knowledge of these trends can also allow health agencies to predict resource allocations needed for these diseases.

In industrialized countries, ***H. pylori*** incidence has been decreasing in successive generations, without any targeted intervention (5-7). Quantifying the benefits of intervention in reducing disease incidence or cost requires an analytical model that estimates the natural course of ***H. pylori*** and associated diseases. The model could then estimate the decrease in ***H. pylori*** incidence that would result from an intervention strategy, relative to the natural course of infection.

We present an analytical framework to model ***H. pylori*** transmission dynamics and its subsequent disease progression. Our goal is to estimate future trends of ***H. pylori*** and associated diseases in the United States based solely on its natural history (i.e., without intervention).

Address for correspondence: Marcia F.T. Rupnow, Health Research and Policy T221, Stanford, CA 94305-5405, USA; fax: 650-725-6951; e-mail: marcia.rupnow@stanfordalumni.org.

Methods

Model Description and Epidemiologic Assumptions

Our analysis is based on a dynamic compartmental model, a technique in which the population is divided into compartments and mathematical equations describe the transfer of persons from one compartment to another (8). In this technique, the incidence of ***H. pylori*** infection

is calculated as a function of the number of susceptible and infected persons in the population and a constant called the transmission parameter (***ß***). We sought transmission parameters that would best explain historical trends and allow estimates of future trends of ***H. pylori*** prevalence and the incidence of ***H. pylori***–associated gastric cancer (GC) and duodenal ulcer (DU).

We developed a compartmental model that captures the age-dependence of ***H. pylori*** infection and disease progression in infected persons (Figure 1)(6,9-17). The population was compartmentalized according to three factors:

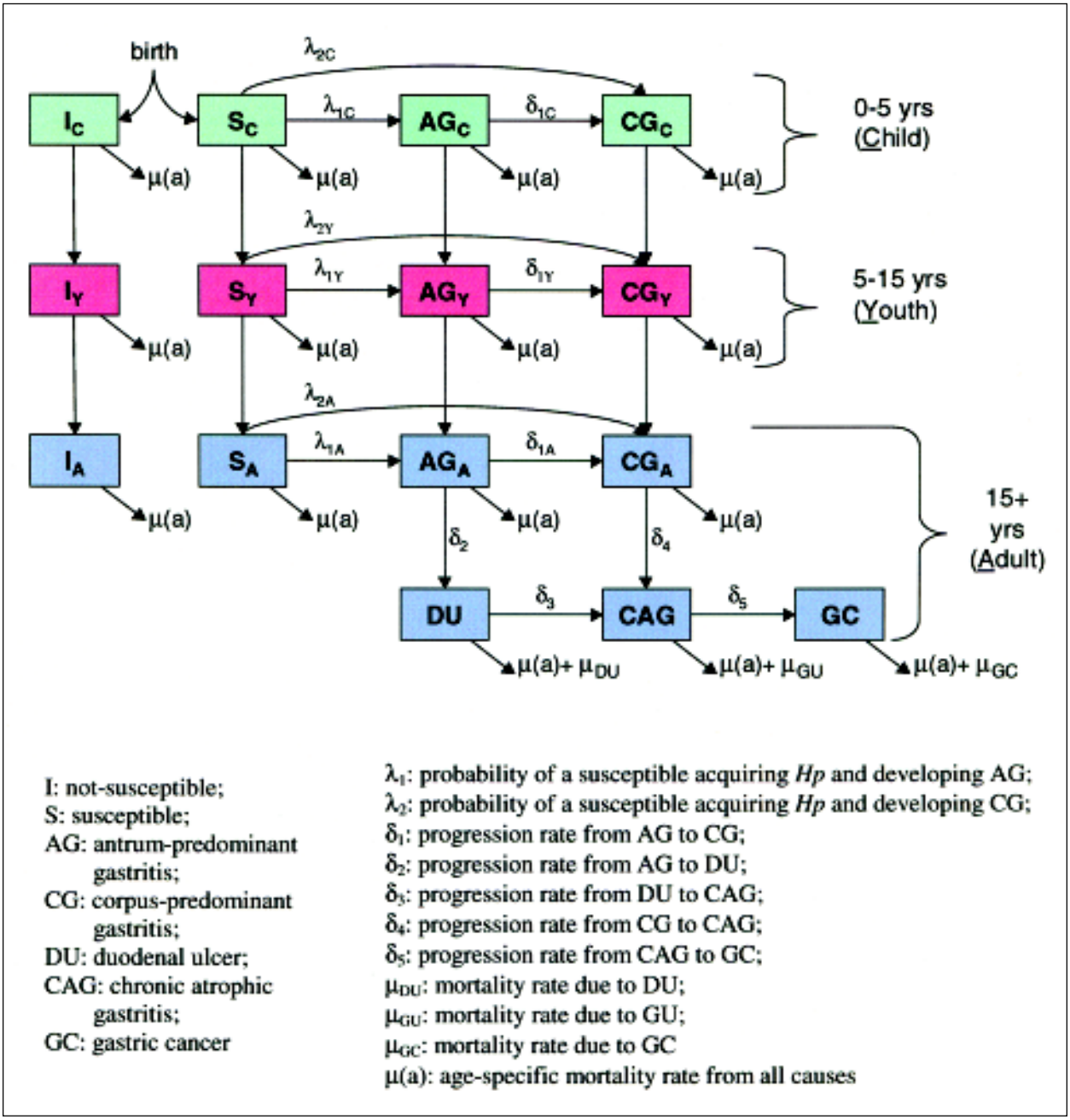

Figure 1. Compartmental model of ***Helicobacter pylori*** transmission and disease progression. In this model, the population is divided into compartments according to age, infection status, and clinical state. Boxes represent population subgroups and arrows indicate transitions between subgroups, as well as flow into and out of the population (birth and death).

age (child [4 years old], youth [5 to 14 years old], and adult [>15 years old]); infection state (uninfected and infected); and clinical state (normal stomach, antrum-predominant gastritis, corpus-predominant gastritis, DU, chronic atrophic gastritis [CAG], and GC) (Appendix). DU and GC states corresponded to persons whose illnesses were caused by ***H. pylori*** infection (***H. pylori***–associated DU and GC). We excluded from our model DU and GC not related to ***H. pylori***. Computer simulation was used to solve the system of equations numerically and calculate the number of persons in each compartment over time.

We modeled the possibility of being born susceptible or not susceptible to ***H. pylori*** (Figure 1). The nonsusceptible or "isolated" group comprised persons who could not become infected for physiologic, physical, or immunologic reasons. This conforms with epidemiologic studies indicating that, even within populations at high risk, a small percentage (10% to 20%) does not become infected with ***H. pylori*** (9,10).

A susceptible person could become infected with ***H. pylori*** at any age and either antrum- or corpus-predominant gastritis could develop. The model represents the net flow from one clinical state to the other. Thus, we represented a positive flow from antrum gastritis to corpus gastritis because this progression is much larger than the reverse. From the gastritis states, we modeled the possibility of further clinical progression to DU, CAG, and GC. The model is consistent with previously reported outcomes in that persons with antrum-predominant gastritis are at higher risk for DU, while those who have corpus-predominant gastritis are at higher risk for CAG, GU, and GC (11,12-17). We also incorporated the possibility of CAG and GC developing in DU patients.

Input Data and Sources

Input assumptions are divided into disease and population parameters (Table). We adopted a constant demographic characteristic of birth and death rates, to eliminate complexities associated

Table. Input variables and sources

Symbol	Description	Value	Explanation	Source
Population parameters				
μ(a)	Death rate (per person per year)	Age-specific		18
Z	Population size (persons)	200,000		Assumption
Π	Birth rate (persons per year)	2,962	Derived from disease-free equilibrium simulation	
p_I	Proportion (%) nonsusceptible	20	Based on data from developing countries	Assumption
Disease parameters				
p_C	Proportion (%) of children with antrum (vs. corpus) gastritis	5		Assumption
p_Y	Proportion (%) of youths with antrum (vs. corpus) gastritis	75	Based on simulation	Assumption
p_A	Proportion (%) of adults with antrum (vs. corpus) gastritis	95		Assumption
δ_{1C}	AG_C to CG_C (per person per year)	0		Assumption
δ_{1Y}	AG_Y to CG_Y (per person per year)	0		Assumption
δ_{1A}	AG_A to CG_A (per person per year)	0.0010	1% progression in 10 yrs	Assumption
δ_2	AG_A to DU (per person per year)	0.0046	14% progression in 32 yrs	22
δ_3	DU to CAG (per person per year)	0.0020	2% progression in 10 yrs	15
δ_4	CG_A to CAG (per person per year)	0.0112	30% progression in 32 yrs	22
δ_5	CAG to GC (per person per year)	0.0030	3% progression in 10 yrs	13
μ_{DU}	Mortality rate due to DU (per person per year)	0.0050		23
μ_{GU}	Mortality rate due to GU (per person per year)	0.0100		24
μ_{GC}	Mortality rate due to GC (per person per year)	0.3219	80% death in 5 yrs	25

GC = Gastric cancer; DU = Duodenal ulcer; CG = Corpus-predominant gastritis; AG = Antrum-predominant gastritis; CAG = Chronic atrophic gastritis.

with changing demographics (8). Baseline demographics were characteristic of the general U.S. population in 1950. The age-specific death rates from all causes were derived from the survival curve of the Vital Statistics Report (18). We assumed an initial population of 200,000, which corresponds to the population of a medium-sized city in the United States (19). The birth rate was set so that the size of the population remained constant when ***H. pylori***–associated diseases were not present. This birth rate was derived from a disease-free simulation exercise in which we assumed zero infection with ***H. pylori***.

The proportion of isolated (nonsusceptible) persons in the population, p_I, is an assumption based on data from developing countries, in which the prevalence of ***H. pylori*** among adults achieves an asymptote of approximately 80% by age 30 (1,20). We assumed that earlier acquisition of ***H. pylori*** is associated with development of corpus-predominant gastritis and subsequent CAG, GU, and GC, and that acquisition at older ages is more likely to lead to antrum-predominant gastritis and subsequent DU (11,12,21). Therefore, we adopted 5% and 95% for the proportions of gastritis initially restricted to the antrum in children and adults, respectively. We chose 75% as the proportion of antrum gastritis in youths; this estimation had to be closer to that of adults than to that of children for the delay of ***Hp*** acquisition to result in more persons with antrum-predominant gastritis and subsequent DU.

We derived the rates of clinical progression from gastritis to cancer from published information (13,15,22-25). The model also incorporated deaths from DU, GU, and GC. GU is not an explicit compartment in our model; instead, we modeled the possibility that a person with CAG would die of GU, in accordance with previous studies that documented an increased risk for GU in persons with CAG (12,16).

Transmission Parameters, Validation of the Model, and Future Trends

We calculated incidence as a function of the number of susceptible and infected persons in the population and the transmission parameter, ß, which is a constant that characterizes infectivity of the pathogen. The number of infected persons at each period was determined by adding the number of persons with antrum- and corpus-predominant gastritis, DU, and CAG. We multiplied the number of CAG patients by a factor (<1), to reflect the fact that the infection may subside (or ***H. pylori*** density may be lower) as a result of atrophy (26), and therefore would contribute less to the transmission of ***H. pylori***. Furthermore, we assumed that the role of GC patients as a source of infection was negligible.

ß may differ according to the population, age of infective and susceptible persons, environmental conditions, household sanitary and hygiene practices, and genetic characteristics of the organism itself (e.g., strain differences). Direct measurement of ß is not possible for most infections (8). However, the value of ß and its change over time must be estimated to assess the impact of public health programs against ***H. pylori***. Since the incidence and prevalence of ***H. pylori*** have been decreasing in the absence of a vaccine (which would decrease the number of susceptible persons) or widespread eradication therapies (which would decrease the number of infected persons), the historical decrease in ***H. pylori*** incidence must represent a decrease in ß. Thus, we estimated the value of ß in the 19th century by simulating an endemic equilibrium condition of ***H. pylori*** in the U.S. population. We then estimated the change in ß that would account for the observed patterns of DU and GC. Finally, we extrapolated ß for the 21st century to estimate the future trends in ***H. pylori***–associated DU and GC.

We set up the model with nine transmission parameters, according to the age groups of infected and susceptible persons. To find ß*s* in mid-1800s, we assumed that the pattern of infection in the United States at that time was similar to that in developing countries today, i.e., rapid acquisition of ***H. pylori*** at younger ages (up to 5 years old) and subsequent slower acquisition rate, achieving a maximum prevalence of approximately 80%. In personal interviews, four experts in ***H. pylori*** epidemiology provided an assessment of the transmissibility among different age groups; they estimated transmission among children to be 5 to 10 times higher than among adults (Hazell SL, Megraud F, Blaser M, Correa P, unpub. comm.). No assessment could be obtained for the different inter-age group transmissions ($ß_{CY}$, $ß_{CA}$, $ß_{YC}$, $ß_{YA}$, $ß_{AC}$, $ß_{AY}$). For the baseline analysis, we assumed that inter-age group transmissions are negligible compared with intra-age group transmissions ($ß_{CC}$, $ß_{YY}$, $ß_{AA}$) because on average, interaction among persons of the same age group is the highest.

Once we established transmission parameters for the mid-1800s, we estimated changes in transmissibility that could explain the historical patterns of GC and DU. GC incidence and deaths have been decreasing since the beginning of the 20th century (25,27,28). DU, however, is characterized by a rise and fall within the 19th century (29-31). For DU, long-term estimates were based on other statistics, such as deaths, physician visits, and hospitalized patients.

Investigators have postulated that the different patterns of GC and DU could be explained by a more rapid decline in childhood than in adult incidence, thereby decreasing the proportion of new infections acquired in childhood (10,32). We evaluated whether changes in ß consistent with this hypothesis could reasonably explain disease patterns. We then extrapolated the transmissibility values into the year 2100 on the basis of our projections for future socioeconomic changes that would affect the dynamics of ***H. pylori*** transmission, and estimated the future trends in ***H. pylori*** prevalence, as well as the incidence of ***H. pylori***–associated GC and DU.

Model Implementation

We implemented the model using the software package Powersim Constructor Version 2.5 (Powersim Corp., Herndon, VA), integrated with Microsoft Excel 97 (Microsoft Corp., Redmond, VA). We set Powersim to use Runge-Kutta 4th-order integration method and time-step of 1 year.

To obtain correct flows of age groups, at the implementation level we further subdivided the child and youth groups by 1-year age increments (i.e., birth through first birthday, 1 year of age through second birthday . . . 14 years of age through 15th birthday). We subdivided the adult compartments by 5-year age increments up to 85 years of age (15 years of age through 20th birthday . . . 80 years of age through 85th birthday, 85+), which allowed us to program the age-specific death rate and track the aging of cohorts with relative accuracy.

Results

Transmissibility of *H. pylori* in 1850

The values of transmissibility most consistent with the endemic pattern of infection were: $ß_{CC} = 0.000055$, $ß_{YY} = 0.000011$, and $ß_{AA} = 0.0000012$. This translated into Potential Transmission Rates (PTR, defined as the average number of secondary infections per unit of time that an infected person would produce in an infection-free population) of $PTR_{CC} = 0.6$ for children (one infected child would be expected to transmit the pathogen to 0.6 susceptible child per year), $PTR_{YY} = 0.25$ for youths, and $PTR_{AA} = 0.15$ for adults. In real populations, these transmission parameters would result in lower incidence rates, since no population is infection free.

Change in Transmissibility from 1850 to 1995

We estimated the change in transmissibility from 1850 to 1995 that was most consistent with the historical trends of DU and GC and with current ***H. pylori*** prevalence in the United States (Figure 2). The fastest decrease occurred in the latter half of the 19th century. Transmissibility then leveled off at $ß_{CC} = 0.000042$, $ß_{YY} = 0.0000044$, and $ß_{AA} = 0.0000009$. Only a pronounced decrease in ß at the end of the 19th century could explain the decline in GC incidence and deaths observed. Such a plateau in transmissibility was necessary

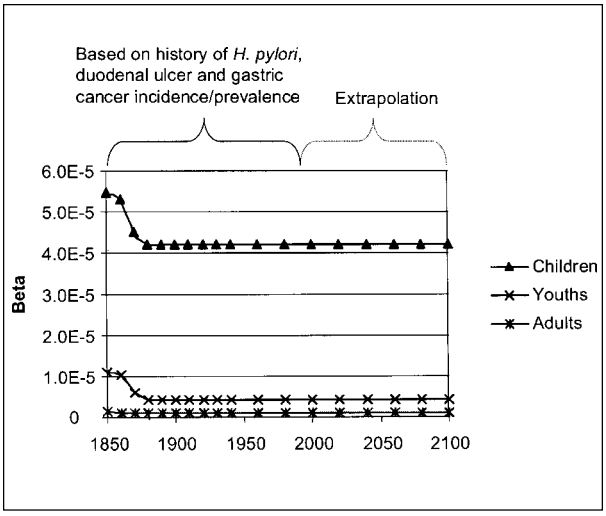

Figure 2. Temporal change in transmission parameters. The transmissibility values in 1850 yielded a pattern of infection similar to that observed in developing countries today (rapid acquisition in younger ages and lower acquisition in older ages). The rapid decline of transmissibility in the latter half of the 19th century is consistent with GC and DU patterns. Although the graph does not show the decrease in $ß_{AA}$ because of the scale ($ß_{AA}$ ***is*** much smaller than $ß_{CC}$ and $ß_{YY}$), $ß_{AA}$ also decreased over time. Constant extrapolation of transmissibility assumes no change in standards of living that would affect ***H. pylori*** transmission.

for the prevalence of ***H. pylori*** infection to coincide with current rates. An S-shaped Gompertz curve (33)—in which the decrease is slow initially, accelerates, and slows down again, trending to a stable level—best illustrates the past trends in ***H. pylori*** and associated DU and GC.

H. pylori Prevalence, DU Incidence, and GC Incidence

We simulated the temporal trend of ***H. pylori*** prevalence in the general U.S. population by age category (Figure 3a). Among children, prevalence decreased from 30% in 1850 to 1% by the end of the 20th century; among youths, prevalence decreased from approximately 70% to 5%, and among adults, from approximately 80% to less than 20% in the same period. We compared the simulation outputs with available U.S. data on incidence of GC and DU (Figure 3b). According to the two sources on GC incidence and deaths (25,28), total GC incidence declined from approximately 34 per 100,000 in 1930 to 6.6 per 100,000 in 1995. In comparison, ***H. pylori***-associated GC, estimated from the simulation, decreased from 24 per 100,000 in 1930 to 5.8 per 100,000 in 1995. Kurata and colleagues, based on data from a large health-maintenance organization in southern California from 1977 to 1980, estimated the incidence of DU to be 58 per 100,000 (34). In comparison, our model estimated ***H. pylori***-associated DU incidence to be 47 per 100,000 in 1980.

To extend the simulation through 2100, we assumed that the transmissibility of ***H. pylori*** would remain stable at the level in 1995 (Figure 2) and kept the input parameters constant. ***H. pylori*** prevalence, as well as the associated DU and GC, would continue to decrease in the 21st century. By 2100, the model predicted incidences of 1.3 and 12.2 per 100,000 population for ***H. pylori***-associated DU and GC, respectively, with overall ***H. pylori*** prevalence decreasing to 4.2%.

Sensitivity Analyses

We tested the model by using different input assumptions. For each change in the input assumptions, we generated curves of ***H. pylori*** prevalence and incidences of ***H. pylori***-associated GC and DU.[1] The most sensitive variables were the proportion of persons with antrum- (vs.

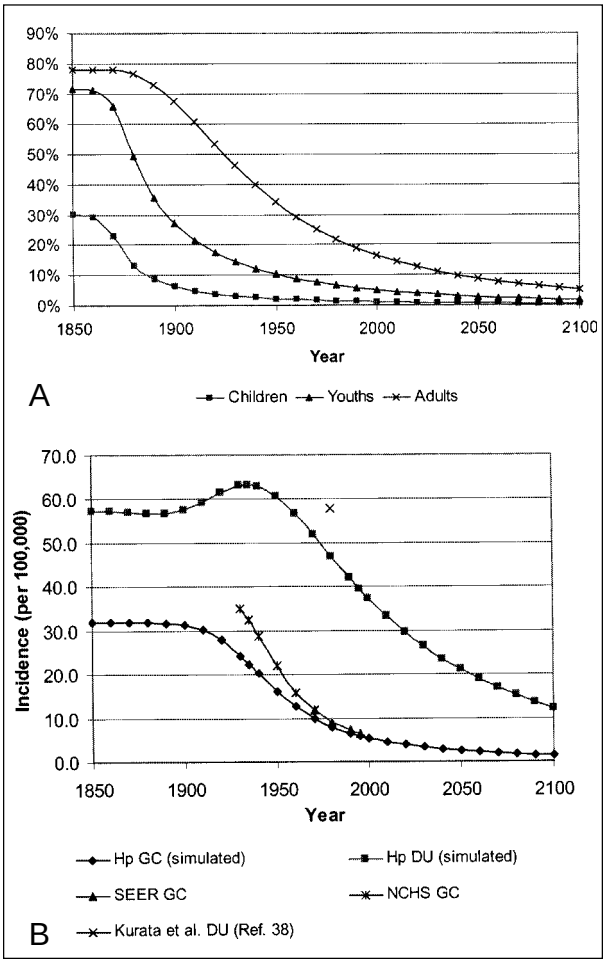

Figure 3. Simulated temporal change in ***Helicobacter pylori*** and associated diseases. a) Prevalence of ***H. pylori*** in the U.S. population by age category (simulation output). b) Incidence of DU and GC per 100,000 U.S. population. "Hp GC" and "Hp DU" are simulation outputs. "SEER GC" represents incidence of GC from all cases, from the Surveillance, Epidemiology, and End Results report (25). "NCHS GC" represents incidence of GC from all cases, derived from the mortality statistics published by the National Center for Health Statistics and the Bureau of the Census (28). "Kurata et al. DU" represents incidence of DU from all cases, based on data from a large health maintenance organization in southern California (34). The simulation model predicted that the prevalence of ***H. pylori***, as well as incidence of ***H. pylori***-associated DU and GC, would continue to decrease in the 21st century.
GC = gastric cancer; DU = duodenal ulcer; NCHS = National Center for Health Statistics; SEER = Surveillance, Epidemiology, and End Results system.

[1]Specific graphs can be made available to readers upon request.

corpus-) predominant gastritis, rate of progression from AG to DU, and rate of progression from CAG to GC. For example, when the rate of progression from CAG to GC was 0.0035, the incidence of ***H. pylori***-associated GC decreased from 6.7 per 100,000 in 1995 to 1.5 per 100,000 in 2100; when the rate was assumed to be 0.0025, the incidence in 1995 was 4.9 per 100,000, decreasing to 1.1 per 100,000 by the end of the 21st century. Overall, we found that ***H. pylori*** prevalence would decrease to <10% in the general U.S. population and the incidence of ***H. pylori***-associated DU and GC would decrease to <20 and 1.5 per 100,000 population, respectively, by the end of the 21st century.

Discussion

This work provides insights into the intrinsic dynamics of ***H. pylori*** and associated diseases, applying and extending the basic principles of mathematical modeling used extensively in infectious disease analysis. First, we found that in the United States, transmissibility of ***H. pylori*** has already become so low that the incidence and prevalence of the organism will continuously decrease in the foreseeable future, without any targeted intervention. The disappearance of ***H. pylori***, however, would take more than a century without intervention. Second, we found that only a rapid decline in ***H. pylori*** transmissibility during the second half of the 19th century could explain the rapid decrease in GC incidence observed in the 20th century. We tested different curves of decrease in ***H. pylori*** transmissibility and found that a Gompertz curve best fits the past trends of ***H. pylori*** and associated GC and DU. Gompertz curves have been used to describe decline of living organisms, as well as mechanical devices (33). Our findings suggest that those curves could also be used to represent waning of transmissibility (infectivity or transmission potential) of an organism in a given host population.

The decline in transmissibility paralleled the rapid improvement in sanitation and hygiene that occurred in the 19th and early 20th centuries in the United States. In a history of hygiene in the United States, Hoy describes how the United States, once a country with poor sanitary conditions, became one with exemplary cleanliness (35). The author states that "in 1850, cleanliness in the United States, north and south, rural and urban, stood at Third World levels." During the Civil War era, appreciation for cleanliness expanded. Frequent washing of clothes and bathing with soap, expanded availability of clean running water, and development of a sewage network in the late 19th century were among improvements in personal hygiene. Although we cannot rule out other causes, this massive improvement in sanitary and hygienic conditions (better household hygiene and community sanitation projects, including water purification systems), which was responsible for reducing the incidence of infectious diseases such as shigellosis and typhoid, could also explain the decrease in transmissibility of ***H. pylori***.

This model attempted to explain quantitatively how the shift in age of ***H. pylori*** acquisition could have produced the different patterns of DU and GC outcomes. We cannot rule out other factors (such as change in ***H. pylori*** strains), not included in our model, which could have been responsible for the rise and fall of DU and the parallel decrease in GC.

We can indirectly estimate ***H. pylori***–associated GC from National Center for Health Statistics (NCHS) and Surveillance, Epidemiology, and End Results (SEER) curves showing GC incidence from all cases, based on attributable risk (Figure 3b). Since attributable risk for ***H. pylori*** is believed to have decreased because the proportion of proximal GC is higher today than it was at the beginning of the 20th century, the total GC curve underestimates the decline in ***H. pylori***-associated GC. Thus, the incidence of ***H. pylori-***associated GC from our simulation is higher than the one estimated by the method of attributable risk applied to NCHS/SEER data. This discrepancy can be explained by the existence of other factors acting in conjunction with ***H. pylori*** to promote the development of GC. The discrepancy, however, does not affect our conclusions about future decreasing trends in ***H. pylori*** and associated diseases.

In this study, we did not model the demographic changes—such as increase in birth rate and life expectancy—that occurred in the United States from 1850 to the present. Demographic changes affect the epidemiology and disease statistics in many ways. For example, an increase in birth rate would affect population density and crowding, depending on availability of land. Change in the size of a family unit could also affect the transmission dynamics.

The model quickly becomes too complex and intractable. We therefore fixed the population parameters as in other infectious disease transmission models (8,36,37). Because our simulation covers a long time span (1850 to 2100), to compromise between the past, present, and future, we derived the population characteristics from the demographic data of 1950. In sensitivity analyses, we also tested different birth and death rates, but the predictions for future ***H. pylori*** prevalence and incidence of ***H. pylori***-associated DU and GC did not differ significantly from the base case.

In our baseline model, we assumed that 20% of the population would not become infected with ***H. pylori***. This is based on studies from developing countries, where prevalence in older adults is typically 70% to 90%. Given the high rates of transmission in childhood required to account for this high endemicity, the prevalence of nonsusceptible persons (because they are either immune or physically isolated) is critical in explaining why 100% prevalence has not been observed in any population. The model, however, can accommodate a range of values, including 100% prevalence.

We simplified the quantification of transmission parameters by considering only transmission between persons in the same age group. In reality, transmission can also occur between adults and children or adults and youths. However, no data are available on the magnitude of transmission between or among different age groups. Therefore, we also tested the model by using positive numbers for inter-age group transmission, but the predictions for future ***H. pylori*** prevalence and incidence of associated GC and DU did not differ significantly from our base case results.

Given the model estimation that ***H. pylori*** transmissibility has remained relatively constant since the beginning of 20th century, despite many recent developments and changes in lifestyle, we assumed that maintenance of the current ***H. pylori*** transmissibility would be a reasonable extrapolation for the next century. Despite this assumption of constant transmissibility, the model predicted that ***H. pylori*** prevalence, as well as ***H. pylori***-associated DU and GC, would continue to decrease without intervention. Thus, the decreasing trends indicate that transmissibility of ***H. pylori*** has already declined below the threshold value needed to maintain the organism endemic in the population. Without any targeted intervention, however, the disappearance of ***H. pylori*** from the U.S. population will take more than a century.

Acknowledgments

The authors thank S.L. Hazell, F. Megraud, and M. Blaser for helpful comments and information on the epidemiology and transmission of ***H. pylori***; D. Graham, M. Dixon, J.I. Wyatt, and P. Correa on the natural history of ***H. pylori*** infection; S.M. Blower and M.M. Tanaka on the infectious disease modeling; and P. Glynn on the mathematical formulation.

This study was supported in part by the Centers for Disease Control and Prevention, grant no. 97FEDO9763. Marcia F.T. Rupnow was supported by a scholarship from CNPq Agency, Brazilian Ministry of Education, grant number 20.0724/96-7. Douglas K. Owens is supported by a career development award from the Department of Veterans Affairs Health Services Research and Development Service.

Dr. Rupnow is a senior analyst of strategic modeling with OrthoBiotech, Inc. Her professional interests include mathematical modeling of disease processes and interventions, medical decision analysis, and pharmacoeconomics.

References

1. Taylor DN, Parsonnet J. Epidemiology and natural history of ***Helicobacter pylori*** infection. In: Blaser MJ, Smith PD, Ravdin JI, Greenberg HB, Guerrant RL, editors. Infections of the gastrointestinal tract. New York: Raven Press; 1995. p. 551-63.
2. NIH Consensus Conference. ***Helicobacter pylori*** in peptic ulcer disease. NIH Consensus Development Panel on ***Helicobacter pylori*** in Peptic Ulcer Disease. JAMA 1994;272:65-9.
3. Telford JL, Ghiara P. Prospects for the development of a vaccine against ***Helicobacter pylori***. Drugs 1996;52:799-804.
4. Lee A. Vaccination against ***Helicobacter pylori***. J Gastroenterol 1996;31 Suppl 9:69-74.
5. Parsonnet J, Blaser MJ, Perez-Perez GI, Hargrett-Bean N, Tauxe RV. Symptoms and risk factors of ***Helicobacter pylori*** infection in a cohort of epidemiologists. Gastroenterology 1992;102:41-6.
6. Banatvala N, Mayo K, Megraud F, Jennings R, Deeks JJ, Feldman RA. The cohort effect and ***Helicobacter pylori***. J Infect Dis 1993;168:219-21.
7. Parsonnet J. The incidence of ***Helicobacter pylori*** infection. Aliment Pharmacol Ther 1995;9 Suppl 2:45-51.
8. Anderson RM, May RM. Infectious diseases of humans: dynamics and control. New York: Oxford University Press; 1991.
9. Kuipers EJ. ***Helicobacter pylori*** and the risk and management of associated diseases: gastritis, ulcer disease, atrophic gastritis and gastric cancer. Aliment Pharmacol Ther 1997;11 Suppl 1:71-88.

10. Graham DY. ***Helicobacter pylori***: its epidemiology and its role in duodenal ulcer disease. J Gastroenterol Hepatol 1991;6:105-13.
11. Schultze V, Hackelsberger A, Günther T, Miehlke S, Roessner A, Malfertheiner P. Differing patterns of ***Helicobacter pylori*** gastritis in patients with duodenal, prepyloric, and gastric ulcer disease. Scand J Gastroenterol 1998;33:137-42.
12. Sonnenberg A. Temporal trends and geographical variations of peptic ulcer disease. Aliment Pharmacol Ther 1995;9 Suppl 2:3-12.
13. Sipponen P, Kekki M, Haapakoski J, Ihamäki T, Siurala M. Gastric cancer risk in chronic atrophic gastritis: statistical calculations of cross-sectional data. Int J Cancer 1985;35:173-7.
14. Sipponen P. ***Helicobacter pylori*** gastritis—epidemiology. J Gastroenterol 1997;32:273-7.
15. Hansson LE, Nyrén O, Hsing AW, Bergström R, Josefsson S, Cho WH, et al. The risk of stomach cancer in patients with gastric or duodenal ulcer disease. N Engl J Med 1996;335:242-9.
16. Blaser MJ, Chyou PH, Nomura A. Age at establishment of ***Helicobacter pylori*** infection and gastric carcinoma, gastric ulcer, and duodenal ulcer risk. Cancer Res 1995;55:562-5.
17. Correa P, Cuello C, Duque E, Burbano LC, Garcia F, Bolanos O, et al. Gastric cancer in Colombia. III. Natural history of precursor lesions. J Natl Cancer Inst 1976;57:1027-35.
18. U.S. National Office of Vital Statistics. Abridged life tables—United States, 1950. Vital Statistics—Special Reports 1953;37:333-43.
19. Gibson C. Population of the 100 largest cities and other urban places in the United States: 1790 to 1990: U.S. Census Bureau, 1998. Available from: URL: http://www.census.gov/population/www/documentation/twps0027.html.
20. Feldman RA, Eccersley AJ, Hardie JM. Epidemiology of ***Helicobacter pylori***: acquisition, transmission, population prevalence and disease-to-infection ratio. British Medical Bulletin 1998;54:39-53.
21. Graham DY. ***Helicobacter pylori*** infection in the pathogenesis of duodenal ulcer and gastric cancer: a model. Gastroenterology 1997;113:1983-91.
22. Valle J, Kekki M, Sipponen P, Ihamäki T, Siurala M. Long-term course and consequences of ***Helicobacter pylori*** gastritis. Results of a 32-year follow-up study. Scand J Gastroenterol 1996;31:546-50.
23. Bonnevie O. The incidence of duodenal ulcer in Copenhagen county. Scand J Gastroenterol 1975;10:385-93.
24. Bonnevie O. The incidence of gastric ulcer in Copenhagen county. Scand J Gastroenterol 1975;10:231-9.
25. SEER Cancer Statistics Review 1973-1995, 1998. Available from: URL: http://www-seer.ims.nci.nih.gov/Publications/CSR7395.
26. Karnes WE, Samloff IM, Siurala M. Positive serum antibody and negative tissue staining for ***Helicobacter pylori*** in subjects with atrophic body gastritis. Gastroenterology 1991;101:167-74.
27. American Cancer Society. Cancer facts and figures—1998. New York: The Society; 1998.
28. Garfinkel L. Cancer statistics and trends. In: Murphy GP, Lawrance W Jr, Lenhard RE Jr, editors. American Cancer Society textbook of clinical oncology. Atlanta: American Cancer Society; 1995. p. 1-9.
29. Susser M. Causes of peptic ulcer. A selective epidemiologic review. Journal of Chronic Diseases 1967;20:435-56.
30. Sonnenberg A. Factors which influence the incidence and course of peptic ulcer. Scand J Gastroenterol Suppl 1988;155:119-40.
31. Sonnenberg A. Geographic and temporal variations in the occurrence of peptic ulcer disease. Scand J Gastroenterol Suppl 1985;110:11-24.
32. Kuipers EJ, Thijs JC, Festen HP. The prevalence of ***Helicobacter pylori*** in peptic ulcer disease. Aliment Pharmacol Ther 1995;9 Suppl 2:59-69.
33. Olshansky SJ, Carnes BA. Ever since Gompertz. Demography 1997;34:1-15.
34. Kurata JH, Honda GD, Frankl H. The incidence of duodenal and gastric ulcers in a large health maintenance organization. Am J Public Health 1985;75:625-9.
35. Hoy S. Chasing dirt. New York: Oxford University Press; 1995.
36. Williams JR, Nokes DJ, Medley GF, Anderson RM. The transmission dynamics of hepatitis B in the UK: a mathematical model for evaluating costs and effectiveness of immunization programmes [published erratum appears in Epidemiol Infect 1996 Oct;117:409]. Epidemiol Infect 1996;116:71-89.
37. Porco TC, Blower SM. Quantifying the intrinsic transmission dynamics of tuberculosis. Theor Popul Biol 1998;54:117-32.

Appendix

The mathematical equations underlying our compartmental model of *H. pylori* is a system of partial differential equations:

$$\frac{\partial I}{\partial t}+\frac{\partial I}{\partial a}=-\mu(a)\cdot I(a,t)$$
$$\frac{\partial S}{\partial t}+\frac{\partial S}{\partial a}=-[\lambda_1(a,t)+\lambda_2(a,t)+\mu(a)]\cdot S(a,t)$$
$$\frac{\partial AG}{\partial t}+\frac{\partial AG}{\partial a}=\lambda_1(a,t)\cdot S(a,t)-[\delta_1(a)+\delta_2(a)+\mu(a)]\cdot AG(a,t)$$
$$\frac{\partial CG}{\partial t}+\frac{\partial CG}{\partial a}=\lambda_2(a,t)\cdot S(a,t)-[\delta_4(a)+\mu(a)]\cdot CG(a,t)$$
$$\frac{\partial DU}{\partial t}+\frac{\partial DU}{\partial a}=\delta_2(a)\cdot AG(a,t)-[\delta_3(a)+\mu_{DU}+\mu(a)]\cdot DU(a,t)$$
$$\frac{\partial CAG}{\partial t}+\frac{\partial CAG}{\partial a}=\delta_3(a)\cdot DU(a,t)+\delta_4(a)\cdot CG(a,t)-[\delta_5(a)+\mu_{GU}+\mu(a)]\cdot CAG(a,t)$$
$$\frac{\partial GC}{\partial t}+\frac{\partial GC}{\partial a}=\delta_5(a)\cdot CAG(a,t)-[\mu_{GC}+\mu(a)]\cdot GC(a,t)$$

where:

$$\lambda_1(a,t)=p(a)\cdot\int_0^{\infty}\beta(a',a)\cdot[AG(a',t)+CG(a',t)+DU(a',t)+\alpha\cdot CAG(a',t)+GC(a',t)]da'$$

$$\lambda_2(a,t)=(1-p(a))\cdot\int_0^{\infty}\beta(a',a)\cdot[AG(a',t)+CG(a',t)+DU(a',t)+\alpha\cdot CAG(a',t)+GC(a',t)]da$$

The boundary conditions are:

$$I(0,t)=p_I\cdot\Pi$$
$$S(0,t)=(1-p_I)\cdot\Pi$$
$$AG(0,t)=CG(0,t)=DU(0,t)=CAG(0,t)=GC(0,t)=0$$

Notation:

a, a'	age index
t	time index
Π	birth rate per unit time
I(a,t)	number of isolated (not-susceptible) individuals of age *a*, at time *t*
S(a,t)	number of susceptible individuals of age *a*, at time *t*
AG(a,t)	number of infected individuals of age *a* with antrum-predominant gastritis, at time *t*
CG(a,t)	number of infected individuals of age *a* with corpus-predominant gastritis, at time *t*
DU(a,t)	number of individuals of age *a* with duodenal ulcer, at time *t*
CAG(a,t)	number of individuals of age *a* with chronic atrophic gastritis, at time *t*
GC(a,t)	number of individuals of age *a* with gastric cancer, at time *t*
p_I	proportion of population that is not-susceptible at birth
$\lambda_1(a,t)$	rate at which one susceptible of age *a* acquire infection and develop antrum-predominant gastritis
$\lambda_2(a,t)$	rate at which one susceptible of age *a* acquire infection and develop corpus-predominant gastritis
$\beta(a',a)$	transmission parameter; probability that an infective of age *a'* will infect a susceptible of age *a*
p(a)	proportion of newly infected individuals of age *a* developing antrum (vs. corpus) predominant gastritis
$\delta_1(a)$	transition rate from antrum- to corpus-predominant gastritis in age group *a*
$\delta_2(a)$	progression rate from antrum-predominant gastritis to duodenal ulcer in age group *a*
$\delta_3(a)$	transition rate from duodenal ulcer to chronic atrophic gastritis in age group *a*
$\delta_4(a)$	progression rate from corpus-predominant gastritis to chronic atrophic gastritis in age group *a*
$\delta_5(a)$	progression rate from chronic atrophic gastritis to gastric cancer in age group *a*
$\mu(a)$	age-specific background mortality rate due to all cases
μ_{DU}	mortality rate due to duodenal ulcer
μ_{GU}	mortality rate due to gastric ulcer
μ_{GC}	mortality rate due to gastric cancer

Using Remotely Sensed Data To Identify Areas at Risk For Hantavirus Pulmonary Syndrome

Gregory E. Glass,* James E. Cheek,† Jonathan A. Patz,* Timothy M. Shields,* Timothy J. Doyle,‡ Douglas A. Thoroughman,† Darcy K. Hunt,† Russell E. Enscore,§ Kenneth L. Gage,§ Charles Irland,† C. J. Peters,¶ and Ralph Bryan§

*The Johns Hopkins School of Hygiene and Public Health, Baltimore, Maryland, USA; †Indian Health Service, Albuquerque, New Mexico, USA; ‡Centers for Disease Control and Prevention, Albuquerque, New Mexico, USA; §Centers for Disease Control and Prevention, Ft. Collins, Colorado, USA; and ¶Centers for Disease Control and Prevention, Atlanta, Georgia, USA

The 1993 U.S. hantavirus pulmonary syndrome (HPS) outbreak was attributed to environmental conditions and increased rodent populations caused by unusual weather in 1991-92. In a case-control study to test this hypothesis, we estimated precipitation at 28 HPS and 170 control sites during the springs of 1992 and 1993 and compared it with precipitation during the previous 6 years by using rainfall patterns at 196 weather stations. We also used elevation data and Landsat Thematic Mapper satellite imagery collected the year before the outbreak to estimate HPS risk by logistic regression analysis. Rainfall at case sites was not higher during 1992-93 than in previous years. However, elevation, as well as satellite data, showed association between environmental conditions and HPS risk the following year. Repeated analysis using satellite imagery from 1995 showed substantial decrease in medium- to high-risk areas. Only one case of HPS was identified in 1996.

In 1993, a disease characterized by acute respiratory distress with a high death rate (>50%) among previously healthy persons was identified in the southwestern United States. This disease, hantavirus pulmonary syndrome (HPS), was traced to infection with an unrecognized, directly transmissible virus—Sin Nombre virus (SNV) (Bunyaviridae; Hantavirus) (1). The virus was maintained and transmitted primarily within populations of a common native rodent, the deer mouse (***Peromyscus maniculatus***) (2), and transmission to humans occurred through contact with secretions and excretions of infected mice (3).

It has been hypothesized that the El Niño Southern Oscillation (ENSO) of 1991-92 was the major climatic factor producing environmental conditions leading to the outbreak of HPS in 1993. Unseasonable rains in 1991 and 1992 during the usually dry spring and summer and the mild winter of 1992 are thought to have created favorable conditions for an increase in local rodent populations (4,5).

This hypothesis is based primarily on the following observations: 1) ENSO tends to influence the timing and abundance of precipitation in the southwestern United States. 2) Some ***Peromyscus*** populations increased dramatically in areas where precipitation was above average but remained near normal levels where precipitation did not increase—this observation is based on comparison of data from only two study areas: the University of New Mexico's Sevilleta Long-Term Ecological Research station (90 km south of Albuquerque, NM), where precipitation was 2 to 3 times the previous

Address for correspondence: Gregory E. Gurri Glass, Molecular Microbiology & Immunology, The Johns Hopkins School of Public Health, 615 N. Wolfe Street, Baltimore, MD 21205, USA; fax: 410-955-0105; e-mail: gurriglass@msn.com.

20-year average, and Moab, Utah, where precipitation was at or below normal in the summer of 1992. Before and during the HPS outbreak, populations of ***P. maniculatus*** did not increase in Moab, while at sites on the Long-Term Ecological Research station they were 10 to 15 times higher than normal. Moreover, both Moab and the research station were 200 km to 300 km from the epicenter of the 1993 HPS outbreak, making comparison with conditions where disease occurred uncertain. 3) 1993 case studies found that rodent abundance varied dramatically over short distances. Rodent populations were higher at HPS households than at neighboring households without disease or randomly selected households at least 25 km away (6); however, these one-time case studies provide little information on the responses of rodent populations to changes in environmental conditions. Although associating weather with HPS outbreaks is consistent with these observations, supporting data are limited. This reflects the situation for many emerging diseases, as active surveillance for unidentified diseases is rare.

Current attempts to understand the factors leading to HPS outbreaks focus on detailing the chain of events from weather, through changes in vegetation, to virus maintenance and transmission within rodent populations, culminating in changes in human disease risk (trophic cascade hypothesis) (4,5,7). An impediment to this approach, however, is the focal nature of SNV within local populations of ***P. maniculatus***. Among local rodent populations the rates of infection vary, and some populations appear uninfected (8). The reason for this is uncertain but may be related to the stochastic loss of the horizontally transmitted viruses within local populations of the reservoir (9). Alternatively, the dynamics of local populations may be such that SNV cannot be maintained at very low population numbers. Under either circumstance, responses of local populations to environmental fluctuations could substantially alter human risk. Given the sporadic nature of HPS outbreaks, ongoing, longitudinal monitoring of rodent populations in the vicinity of subsequent cases is unlikely (6). Consequently, inferring human disease risk from rodent-SNV population dynamics will again require extrapolating from studies in regions other than the site of the outbreak.

In this article, we examine the relationship of the environment to HPS risk by using locations of HPS cases as sites where people were associated with infected rodents. This approach avoids the immediate need to establish the conditions that lead some reservoir populations to be uninfected by SNV. We compare the environmental characteristics of sites where people were infected with those at sites where people were not infected. Differences in environmental conditions could indicate factors that influence either the abundance of rodents or the occurrence of virus, creating testable hypotheses of environmental conditions that influence SNV infection patterns in reservoir populations. As a partial test of our method, the analysis was repeated when cases of HPS were uncommon. Under these conditions, the identified environmental factors should indicate low levels of disease risk.

Two sources of information were used as measures of the local environmental conditions preceding the HPS outbreak: 1) Monthly patterns of precipitation from March to June (generated from archived weather station data in the region to estimate local precipitation patterns at both case and control sites) and 2) satellite imagery (obtained before the HPS outbreak and used as a measure of variable, local environmental conditions and HPS risk evaluated by epidemiologic analysis).

Methods

Study Population and Region

The epidemiologic analysis was performed as a case-control study. Twenty-eight (93.3%) of 30 sites with confirmed cases of HPS identified in the region between November 1992 (identified retrospectively) and November 1994 were selected. Inclusion criteria were based on clinical disease consistent with the Centers for Disease Control and Prevention case definition that was confirmed by serologic, nucleic acid, or immunohistochemical tests (1). One case was excluded because the likely site of exposure could not be established, and a second case because we could not confirm that the proper geographic location of the site was recorded during data collection.

Sites of exposure were established previously by investigation of each case-patient's activities and, for most fatal cases, demonstration of sequence homology of polymerase chain reaction (PCR)-amplified regions of SNV nucleic acids obtained from case-patients and rodents collected at the imputed sites of exposure (1,2). Sites

of exposure for the HPS cases were at or in the immediate vicinity of households, and there usually was a history of activities that could have generated exposure to contaminated aerosols (1).

To control for issues related to access to care and socioeconomic conditions, controls were selected randomly from all households that used the same health clinics as the HPS patients during the same period as the HPS patients. Controls were randomly selected among persons without HPS. A total of 170 persons with different residential addresses were identified from a listing of visits to all the clinics during the time of the HPS outbreak. This represented an approximately 2% random sample of addresses of the patient population. A previous study showed that subclinical infection with SNV was not observed among controls (10). Geographic locations of case and control sites were established by using global positioning system (GPS) receivers to record latitude and longitude at each site.

The study area of 105,200 km^2 was located in the southwestern United States, incorporating the region of the original HPS outbreak (1,2). Epidemiologic surveillance was part of the HPS outbreak investigation.

Environmental Characterization of Sites

Monthly precipitation data recorded at 196 weather stations throughout the region from 1986 to 1993 were from the U.S. National Oceanic and Atmospheric Administration's National Climatic Data Center. Spring precipitation at the weather stations was calculated by aggregating monthly precipitation for March through June. Spring precipitation at individual case and control sites was estimated by interpolation among the nearest weather stations to each case or control site. Interpolation procedures used the eight nearest weather stations to estimate precipitation by applying trend surface algorithms from the GIS software (IDRISI, 11). Spring precipitation during 1992 to 1993 at each site was compared with spring precipitation during previous years by paired differences tests, with correction for multiple tests. The null hypothesis for each case or control site was that there was no increase in precipitation during the spring of 1992 to 1993 compared with the previous years. We also used satellite imagery to develop detailed characterization of local environmental conditions. We selected three archived Landsat Thematic Mapper (TM) images originally recorded in mid-June 1992 for analysis. TM records digital numbers (DN) from reflected light in six bands, three in visible and three in infrared (IR) portions of the electromagnetic (EM) spectrum. (An additional band of thermal IR energy also is recorded but was not used.)

The TM images were merged to form the study area of 105,200 km^2. Nominal pixel resolution was 30 m. Images were geometrically and radiometrically corrected by the U.S. Geological Survey (USGS) Earth Resources Observation Systems (EROS) Data Center. The images were imported into a raster-based geographic information system (GIS) for geographic registration by using control points obtained from USGS quadrangle maps (11). The images were resampled by a bilinear resampling procedure with a quadratic mapping function (11). Corrections for atmospheric scattering of bands one to three were performed by the method of Chavez (12). Latitude and longitude positions of case and control households were imported as a data layer in IDRISI GIS. Additional environmental variables incorporated in GIS included elevation, slope, and aspect of the case and control sites. Elevation was derived from the USGS digital elevation models (1:250,000 scale), while slope and aspect were generated from these data by using software in GIS.

Three satellite images from mid-June 1995 were selected to further validate the analysis of the 1992 imagery. There was no ENSO from 1994 to 1996, and we predicted that any relationship between the satellite imagery in 1992 and the case and control sites would indicate reduced risk in 1995. DNs for selected locations on the 1992 and 1995 images were compared to determine any significant changes in sensor calibration.

Epidemiologic Analysis of HPS by Satellite Imagery

The spatial distribution of HPS sites (cases) was compared with that of control sites to determine if cases were spatially aggregated within the study region (13). Then, the relationship between HPS and environmental factors measured by TM imagery was examined. Because the analysis used three tiled images, the strategy for model development involved model fitting by using a portion of the study region, followed by external validation (14). A sample of HPS sites and control sites was selected for

analysis, by using logistic regression to examine the relationship between the odds of a site being an HPS site (outcome variable) and the DN in each TM band, elevation, slope, and aspect (predictor variables). The analysis was then repeated by using the remaining HPS and control sites to validate the model. Identifying the same model in the two analyses would indicate that the HPS risk model was robust for that period.

The initial model used a test area of 12,279 km^2 from the east-central region of the study area. This area included 14 case and 36 control sites and was entirely within one TM image. The validation analysis used the remaining sites (14 case and 134 control sites) and incorporated all or parts of the three TM images covering 92,921 $km.^2$ The average DN for each of the six TM bands used in the analysis was calculated with a 3 x 3 pixel filter centered on the location for each case or control site. This sampled a local region of approximately 8,100 m^2 around each case or control site.

We used logistic regression analysis to identify the best combination of TM bands and environmental variables associated with HPS status (14). Elevation was dichotomized at the median elevation for case and control sites, combined. Inclusion of remotely sensed variables was based on the statistical significance of their coefficients in the model. Elevation was retained in all models because of its observed association with ***P. maniculatus*** abundance (8). The logistic model was evaluated with the Deviance and the Hosmer-Lemeshow goodness of fit statistics (C) for deciles of risk. To examine the accuracy of the model predictions, we evaluated the sensitivity and specificity by creating a Receiver Operator Characteristic function (15). The function compares the true-positive rate (sensitivity) against the false-positive rate (1 – specificity) of a model by using various predicted values as thresholds identifying case and control sites. In addition to examining spring precipitation, we evaluated the trophic cascade hypothesis by examining the relationship between HPS risk and vegetation growth before the HPS outbreak (5), regardless of habitat type. We used data from the near infrared (band 4) and red (band 3) portions of the spectrum to generate a normalized difference vegetation index of the region. The index is a standard algorithm used as a measure of vegetative growth. We compared the index and the TM bands identified in the initial epidemiologic analysis for estimating HPS risk by comparing the Receiver Operator Characteristic's generated by each analysis.

Results

Cases and controls occupied the same general, geographic area with the greatest difference of most extreme sites of 20 km in the north-south and 13 km in east-west directions. Despite the broad geographic overlap, cases of HPS were not randomly distributed within the area. HPS cases were spatially clustered (Table 1). Despite this clustering, HPS sites were widely separated geographically. The average distance between case sites was 50.3 km (SD = 23.8 km), and the nearest neighboring sites (k = 1; Table 1) were not themselves likely to be case sites.

Table 1. Spatial clustering of households with hantavirus pulmonary syndrome

k	T[k]	z	P
1	6	0.91	0.181
2	14	1.88	0.030
3	24	3.05	0.001
4	33	3.71	<0.001
5	40	3.87	<0.001
6	50	4.57	<0.001
7	64	5.85	<0.001
8	75	6.50	<0.001
9	79	6.14	<0.001
10	86	6.21	<0.001

Cuzick and Edwards' test (13), T[k], its z score under the null hypothesis and the p value using Simes correction for multiple tests (16). Results show significant spatial clustering among case households for the second through tenth nearest neighbors (k= 2,...,10).

Spring precipitation patterns showed substantial interannual variation at case and control sites (Figure 1). From 1986 through 1993, precipitation was 4.5 mm (1989) to 110 mm (1992). Spring precipitation decreased markedly between 1992 and 1993 (Figure 1). Overall, precipitation at control sites tended to be lower (65 mm) than at case sites (72 mm) during the spring each year, but there was broad overlap among sites, and yearly variation at control sites tracked that of the case sites (Figure 1). None of the case sites had higher precipitation during 1992 to 1993 than during the preceding 6 years ($p > 0.05$).

There was a significant relationship between local environmental conditions and HPS risk as measured by the statistical association between

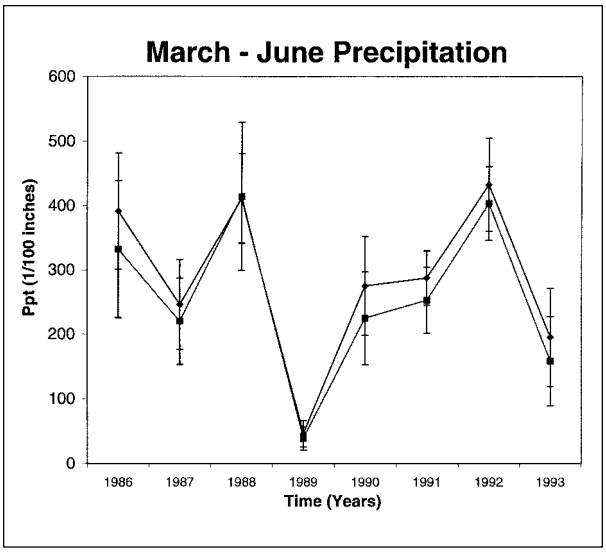

Figure 1. March–June precipitation patterns at case sites (solid symbols) and control sites (open symbols) from 1986 through 1993. Vertical bars are 1 standard deviation in precipitation values.

the DN recorded by the satellite in 1992 and HPS risk the following year. The logistic regression analysis developed for the training area fit the observed data well (Deviance = 45.45; p = 0.49, df = 46; Hosmer Lemeshow C = 6.62; p = 0.58, df = 8), and none of the sites were obvious outliers. Higher level interactions between the independent variables did not change the results. Three of the six bands from the TM images (1, 5, and 7) were associated with the odds of HPS (Table 2). Sites above the median elevation (2,094 m) were marginally associated with risk in the training area, but elevation was retained because of the relatively small sample sizes used to estimate the parameters, as well as the biologic rationale outlined elsewhere (8).

High DN values in the blue (band 1) and mid-infrared (band 7) portions of the EM spectrum were associated with decreased risk for HPS, while high values in the mid-infrared (band 5) portion of the spectrum were a risk factor for HPS (Table 2). The DN values were approximately 58 to 233 units. Each unit change in the average DN around sites altered the odds of HPS risk by 6% (band 1), 15% (band 7). Sites above 2,094 m in the test area were >4 times as likely to be HPS sites as sites below 2,094 m. Slope and aspect at the sites were not associated with risk.

The Receiver Operator Characteristic graph of sensitivity and specificity of the predictor function showed that at least 95% of the case sites were correctly identified until the proportion of control sites correctly identified exceeded 56% (20 of 36 control sites) (Figure 2). The same predictor variables from the TM imagery were identified when the analysis was repeated for the validation area. The coefficients of the validation analysis did not differ significantly from those for the training area (Table 2). This model also fit the data well (Deviance = 74.49; p = 1.00, df = 144; Hosmer Lemeshow C = 6.78; p =0.56, df = 8).

Because the logistic models did not differ between the training and validation areas, all the

Table 2. Logistic regression analysis of LANDSAT Thematic Mapper data and elevation

	Training area			Validation area			
Predictor	Odds ratio	95% CI	P	Odds ratio	95% CI	P	t
Band 1	0.94	(0.89, 0.99)	0.027	0.95	(0.90, 0.99)	0.019	ns
Band 5	1.14	(1.03, 1.26)	0.013	1.08	(1.01, 1.17)	0.034	ns
Band 7	0.85	(0.73, 0.99)	0.039	0.90	(0.80, 1.00)	0.046	ns
Elevation	4.63	(0.88, 24.29)	0.070	2.56	(0.77, 8.43)	0.123	ns

	Overall			Controls		Cases	
Predictor	Odds ratio	95% CI	p	Mean	Range	Mean	(Range)
Band 1	0.96	(0.93, 0.99)	0.012	111.9	(70.6, 164.0)	97.8	(72.0, 134.3)
Band 5	1.07	(1.01, 1.13)	0.013	170.6	(110.7, 253.3)	160.7	(110.2,226.2)
Band 7	0.91	(0.84, 0.99)	0.015	102.6	(60.6, 163.3)	93.1	(58.2, 140.4)
Elevation	4.60	(1.96, 10.79)	0.005	1935	(1465, 2500)	2081	(1825, 2341)

Odds ratios, 95% confidence intervals, and statistical significance of HPS predictor variables. Odds ratios of the Thematic Mapper bands indicate the change in risk for each unit change in digital number recorded by the satellite sensor. Elevation was divided as either above or below 2,094 m for the analysis. There was no difference between the Training and Validation areas, as tested by t-test (t). The Controls and Cases columns show the mean and range of values at the control and case sites, respectively.
ns=not shown.

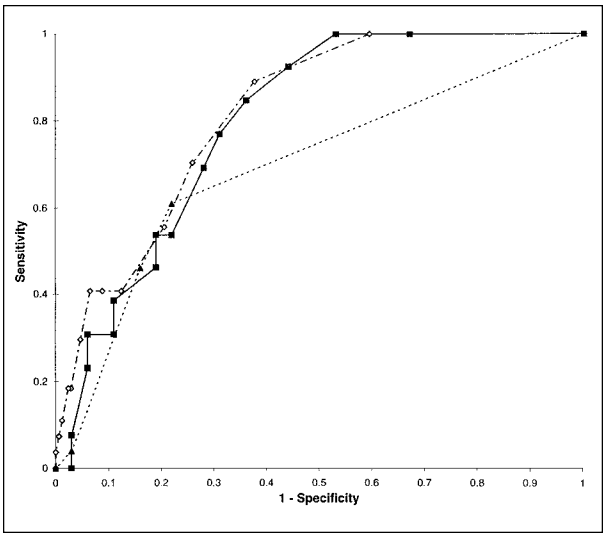

Figure 2. Receiver Operator Characteristic (ROC) function of the logistic model for HPS risk in the training area (closed squares) and overall for 1992 (open diamonds) as the threshold for predicted case households was varied from p = 0.00 - 0.85 in 0.05 increments. The ROC for normalized difference vegetation index model (triangles) had p values of 0.00 to 0.40 and multiple points occurred together. The early rapid loss of sensitivity for the NDVI model was the result of poor model specification.

sites were combined to give an overall model (Table 2). The overall Receiver Operator Characteristic (Figure 2) had a sensitivity and specificity similar to those of the test area (95% sensitivity, 62% specificity). This threshold corresponded to a predicted value for HPS of approximately 0.10. Thus, using a predicted log odds ratio of at least 0.10 as a threshold for increased risk included 95% of the case sites and excluded 62% of the control sites.

The logistic function was applied to each pixel in the study area to produce a map of predicted risk (Figure 3) (17). The analysis was repeated by using satellite images from June 1995 to predict HPS risk for 1996 (Figure 3). There was a near elimination of predicted high-risk areas in the 1995 imagery and a broad expansion of low-risk areas compared with the 1992 images. The single case of HPS reported from the region in 1996 occurred at a site with a predicted risk of 0.16 (i.e., above the HPS threshold).

Areas of high vegetation growth in 1992, as measured by the normalized difference vegeta-

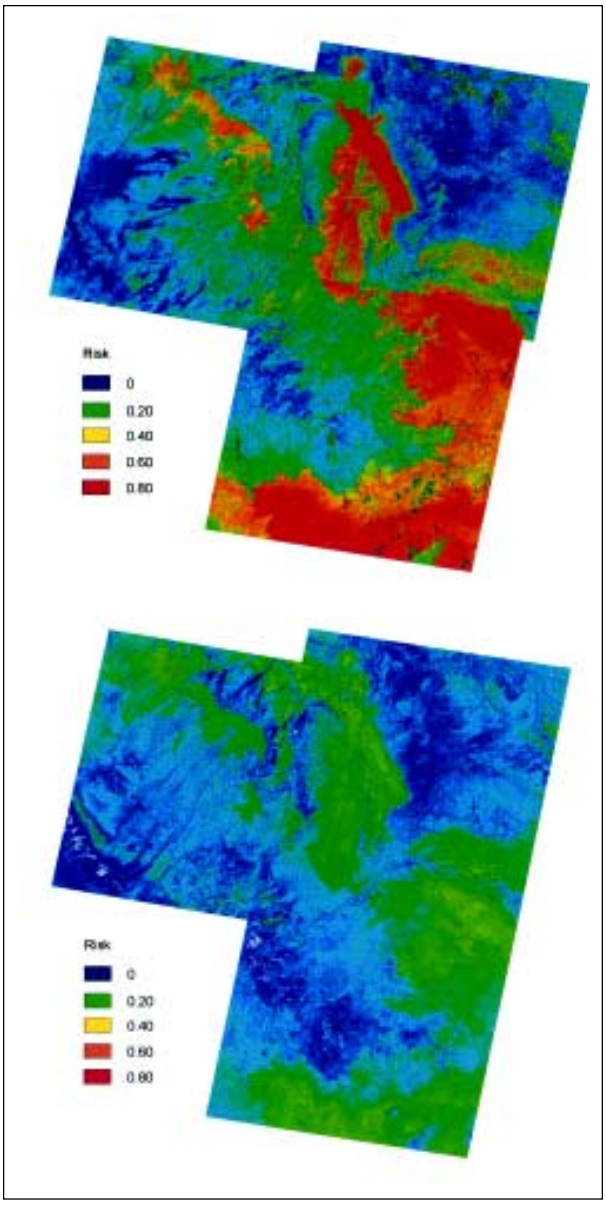

Figure 3. Comparison of predicted HPS risk for 1993 (top) and 1996 (bottom) by satellite imagery taken in 1992 and 1995, respectively, in the study area. Low-risk areas are in dark blue and high-risk areas are in red and yellow. There was a significant reduction in predicted high-risk areas in 1996 compared with 1993.

tion index (Figure 4) incorporated only a portion of the HPS high-risk areas (Figure 3). We evaluated vegetation growth, as measured by the index, as a predictor of HPS risk by modeling the case-control data, using the index and elevation as predictor variables. The vegetation growth model that best fit the observed data included an

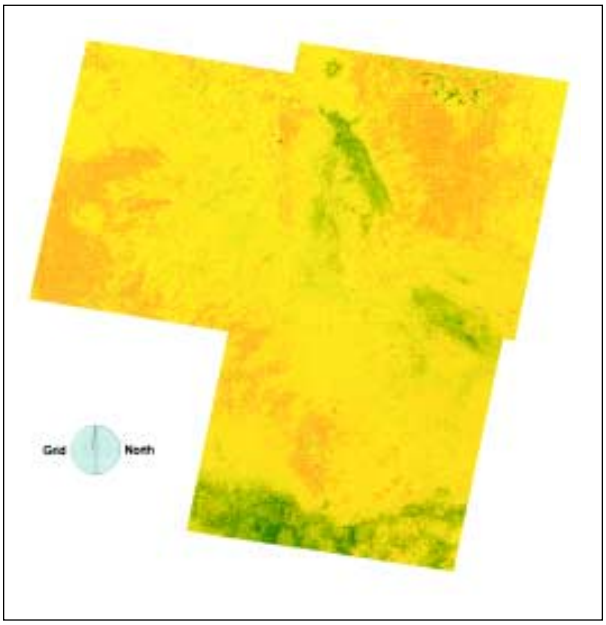

Figure 4. The normalized difference vegetation index (NDVI) scores of the study area by Thematic Mapping bands 3 and 4. Vegetation growth increased from brown through yellow to green. There was a substantial portion of high-risk area (especially the eastern portion of the image) where the NDVI image pixels did not obviously correspond to high-risk areas (see Figure 3 for comparison).

exponential transformation of the normalized difference vegetation index and sites above the median elevation. This index model accounted for a significant part of the variation in the HPS risk (deviance = 147.62; p = 0.99, df = 196) but did not accurately model the odds of HPS. In this analysis 11 (39.3%) of 28 case sites had standardized residuals exceeding three standard deviations, suggesting a poor fit to the data—an interpretation supported by the Hosmer Lemeshow statistic (C = 20.09; p = 0.01, df = 8), which indicated that the form of risk model fit the data poorly. The receiver operator characteristic of the vegetation index analysis (Figure 2) also lost sensitivity more rapidly than the analysis using TM bands 1, 5, and 7, especially over the range of values near the threshold of increasing HPS risk.

Conclusions

Satellite imagery, combined with epidemiologic surveillance, retrospectively identified areas at high risk for HPS associated with ***Peromyscus*** populations over broad geographic regions during the 1993 outbreak. TM data identified environmental conditions near HPS sites that were measurably different from conditions in rural, populated sites where disease did not occur for nearly 1 year before the outbreak. These environmental conditions varied with the presence of ENSO (Figure 3). The geographic extent and general level of predicted HPS risk were higher during ENSO, supporting the view that El Niño may increase the likelihood of HPS outbreaks. The hypothesized pathway between ENSO, increased spring precipitation leading to increased vegetation growth, and subsequent HPS risk, however, was not strongly supported by the data. Possible reasons for this lack of support are discussed below.

In this study, we used a retrospective epidemiologic approach to risk assessment (15). Therefore, odds ratios of the environmental characteristics were used to estimate the population's relative risk for HPS. This approach is valid when the cases used in the study are representative of all cases, the controls are representative of the general population, and the disease is relatively rare. Under these conditions, odds ratios approximate relative risk (15).

HPS is rare–fewer than 1,000 cases have been identified in North America, although most occurred in the southwestern region of the United States. In this study, the cases included nearly all (28 of 30) sites in the region where HPS occurred during the outbreak. Although bias induced from this factor is unlikely, we cannot be certain that environmental factors identified with outbreaks of HPS are similar to those with the sporadic, single cases of HPS reported each year. However, the accurate identification of the site where the single case of HPS was observed in 1996 suggests that the classification may also identify risk characteristics for this group. Issues related to personal privacy make accessing these data difficult, however, because geographic locations of residences, for example, are considered personal identifiers.

The selection of controls focused on a population from the same socioeconomic and geographic region as the HPS cases. Although HPS cases were clustered, the maximal geographic extent of both cases and controls was similar, suggesting that the enrollment procedure adequately fulfilled this goal. Random selection of controls also was intended to control

for access to care in a region where travel may be difficult. Restricting controls to those using the same health-care facilities again raises the issue of the applicability of the results to areas with different socioeconomic and cultural conditions and probably excluded much of the population within urban areas of the study site.

These are relatively minor potential problems. HPS cases are rare in urban areas because the primary reservoir species in North America rarely occur within urban settings. Moreover, surveys of rural housing show that infestations by ***Peromyscus*** are nearly ubiquitous in the absence of focused rodent exclusion methods (6,18).

Absence of a significant difference in spring precipitation at case sites during 1992-93 and the previous 6 years (Figure 1) may reflect either the absence of an effect (contradicting the trophic cascade hypothesis) or practical problems with estimating precipitation and incorporating conditions associated with past HPS outbreaks. Although nearly 200 weather stations were used in estimating spring precipitation at case and control sites, this still represents a relatively sparse network of sampling locations; therefore, localized precipitation could have been at too fine a spatial scale to detect. However, when we estimated precipitation at weather stations by using the surrounding stations and comparing the results with the observed precipitation, we found no difference between observed and predicted results in 1992-93. A more likely possibility is that the relatively short time series of precipitation data used makes demonstrating a statistical effect difficult. Additionally, if ENSO is a triggering event, outbreaks of HPS must have occurred in the past. Therefore, previous ENSO events may "contaminate" comparisons with past precipitation data because they include unrecognized HPS outbreaks.

The trophic cascade hypothesis predicts that ENSO leads to increased precipitation that affects vegetation growth, subsequently influencing HPS risk. The association between HPS risk and vegetation growth, as measured by the normalized difference vegetation index, was inconsistent. Areas with a high index (Figure 4) did correspond to areas at highest risk for HPS (Figure 3) in 1992. Similarly, areas at low risk were generally those with low normalized difference vegetation indexes. However, broad regions of moderate- to high-risk areas did not relate to the vegetation index, and the logistic regression model did not perform well (Figure 2).

The failure of the normalized difference vegetation index to predict HPS risk may indicate that the ecologic connections hypothesized by the trophic cascade hypothesis are complex and modulated by intervening ecologic variables. Alternatively, the normalized difference vegetation index, which is the normalized difference of DN in red and near-infrared portion of the EM spectrum, may have difficulty accurately characterizing vegetation growth in semi-arid areas that contain a complex mixture of vegetation and bare ground (19). Further, detailed studies incorporating "ground truthing" to establish the relationship between local ecological dynamics of plant and rodent populations and satellite sensor readings will be needed to determine which of these alternatives may apply (19,20).

Field validation of interpretations, which is critical to testing hypotheses derived from satellite data, should also be applied to the epidemiologic analyses of HPS risk. Our approach associates three TM bands and elevation with human risk. Interpretation of what these bands detect in the environment varies (soil moisture, soil type, and vegetation structure) (19). Our classification is being used to identify other sites with similar reflectance patterns in the same bands and characterize the structure and dynamics of rodent reservoir populations. Preliminary analyses show a good relationship between HPS risk predicted from satellite imagery and ***P. maniculatus*** population abundance ($r = 0.92$).

The case-control model using high-resolution spatial data from satellite imagery supports previous epidemiologic observations indicating that changes in rodent population densities and HPS risk could occur dramatically over relatively short distances (6). Although extensive areas of high and low risk were evident (Figure 3), substantial interdigitation of these zones at higher resolution created a mosaic of high- and low-risk areas. This suggests possibly widespread "environmental islands" of suitable reservoir habitat imbedded within less suitable habitat and may account for the apparently focal nature of HPS outbreaks and the near random distribution of cases relative to their nearest neighbors observed in this study (Table 1, $k = 1$).

The results also support epidemiologic investigations indicating that the only measurable risk factor around HPS sites during the 1993 epidemic was the abundance of ***P. maniculatus*** (6).

Satellite imagery analysis provides an efficient survey of large geographic regions for environmental indicators of disease risk affecting human populations and has the potential to make surveillance of disease risk for rare zoonotic and vectorborne diseases practical for public health applications (18,20-26). For many diseases, the basis for the supposition that remotely sensed data will be useful for anticipating disease risk is that pathogen transmission is facilitated by arthropods, whose survival and reproduction are influenced by variations in temperature and humidity. The effect of climatic variability, however, on directly transmissible zoonotic agents maintained in vertebrate, especially mammalian reservoirs, is less certain and has received little attention.

Additionally, although the reason to assume a relationship between climate variability and infectious disease outbreaks is clear (27), few studies have evaluated whether this presumed relationship actually exists. This study indicates that if these relationships do occur, they are modulated by a number of poorly understood ecologic and social conditions that will require substantial detailed studies of the pathways influencing disease risk.

Acknowledgments

We thank Anne Grambsch for assistance in the early development and planning of this project and to the state and local Outbreak Response Teams, CDC, IHS, and environmental health specialists and biologists from health departments and universities in New Mexico, Arizona, and Colorado, who collected the epidemiologic data with such care.

Dr. Glass was supported in part by an Intergovernmental Personnel Agreement from the Centers for Disease Control and Prevention and NASA 97CAN01-0048. Drs. Patz and Shields were supported by the U.S. Environmental Protection Agency ORD STAR grant 96-NCERQA-1B and Dr. Patz received additional support from a cooperative agreement from the U.S. EPA Climate Policy and Assessment Division. Satellite imagery and supplies were provided through cooperative agreement CR823143 and grant 96-NCERQA-1B from EPA and cooperative agreement 97CAN01-0048 from NASA.

Dr. Glass is associate professor, W. H. Feinstone Department of Molecular Microbiology and Immunology, with a joint appointment in the Department of Epidemiology, The Johns Hopkins School of Public Health; he is director of the Spatial Information Systems Unit, Program on Health Effects of Global Environmental Change. His area of interest is the ecology of rodent-borne zoonotic diseases.

References

1. Nichol ST, Spiropoulou CF, Morzunov S, Rollin PE, Ksiazek TG, Feldmann HS, et al. Genetic identification of a hantavirus associated with an outbreak of acute respiratory illness. Science 1993;262:615-8.
2. Childs JE, Ksiazek TG, Spriopoulou CF, Krebs JW, Morzunov S, Maupin GO, et al. Serologic and genetic identification of ***Peromyscus maniculatus*** as the primary rodent reservoir for a new hantavirus in the southwestern United States. J Infect Dis 1994;169:1271-80.
3. Glass GE. Hantaviruses. Current Opinion in Infectious Diseases 1997;10:362-6.
4. Engelthaler D, Mosley D, Bryan R, Cheek J, Levy C, Komatsu K, et al. Investigation of climatic and environmental patterns in hantavirus pulmonary syndrome cases in the Four Corners states. Emerg Infect Dis 1999;5:87-94.
5. Parmenter RR, Brunt JW, Moore DI, Ernest S. The hantavirus epidemic in the Southwest: rodent population dynamics and the implications for transmission of hantavirus-associated adult respiratory distress syndrome (HARDS) in the Four Corners region. 41:1-44. University of New Mexico: Sevilleta LTER Publication; 1993.
6. Childs JE, Krebs JW, Ksiazek TG, Maupin GO, Gage KL, Rollin PE, et al. A household-based, case-control study of environmental factors associated with hantavirus pulmonary syndrome in the southwestern United States. Am J Trop Med Hyg 1995;52:393-7.
7. Mills JN, Ksiazek TG, Peters CJ, Childs JE. Long-term studies of hantavirus reservoir populations in the southwestern United States: a synthesis. Emerg Infect Dis 1999;5:135-42.
8. Mills JN, Ksiazek TG, Ellis BA, Rollin PE, Nichol ST, Yates TL, et al. Patterns of association with host and habitat: antibody reactive with Sin Nombre virus in small mammals in the major biotic communities of the southwestern United States. Am J Trop Med Hyg 1997;56:273-84.
9. Anderson RM, May RM. Infectious diseases of humans: dynamics and control. Oxford: Oxford University Press; 1991.
10. Simonsen L, Dalton MJ, Breiman RF, Hennessy T, Umland ET, Sewell M, et al. Evaluation of the magnitude of the 1993 hantavirus outbreak in the southwestern United States. J Infect Dis 1995;172:729-33.
11. Eastman JR. IDRISI for Windows. Worcester (MA): Clark University; 1995.
12. Chavez PS. Atmospheric, solar, and MTF corrections for ERTS digital imagery. American Society of Photogrammetry and Remote Sensing, Proceedings. 1975.
13. Cuzick J, Edwards R. Spatial clustering for in homogeneous populations. Journal of the Royal Statistical Society, Series B 1990;52:73-104.
14. Collett D. Modelling binary data. 2nd ed. London: Chapman & Hall; 1994.

15. Fletcher RH, Fletcher SW, Wagner EH. Clinical epidemiology–the essentials. Baltimore: Williams & Wilkins; 1982.
16. Simes RJ. An improved Bonferroni procedure for multiple tests of significance. Biometrika 1986;73:751-4.
17. Glass GE, Schwartz BS, Morgan JM, Johnson DT, Noy PM, Israel E. Environmental risk factors for Lyme disease identified with geographic information systems. Am J Public Health 1995;85:944-8.
18. Linthicum KJ, Bailey CL, Davies FG, Tucker CJ. Detection of Rift Valley fever viral activity in Kenya by satellite remote sensing imagery. Science 1987;235:1656-9.
19. Sabins FF. Remote sensing principles and interpretation. New York: W.H. Freeman and Company; 1997.
20. Beck LR, Rodriguez MH, Dister SW, Rodriguez A, Washino D, Roberts RK, et al. Assessment of a remote sensing-based model for predicting malaria transmission risk in villages of Chiapas, Mexico. Am J Trop Med Hyg 1997;56:99-106.
21. Kitron U, Bouseman, JK, Jones CJ. Use of the ARC/ INFO GIS to study the distribution of Lyme disease ticks in an Illinois county. Prevent Vet Med 1991;11:243-8.
22. Malone JB, Fehler DP, Loyacano AF, Zukowski SH. Use of LANDSAT MSS imagery and soil type in a geographic information system to assess site-specific risk of fascioliasis on Red River basin farms in Louisiana. Tropical Veterinary Medicine: Current Issues and Perspectives 1992;653:389-97.
23. Rogers DJ, Randolph SE. Distribution of tsetse and ticks in Africa: past, present and future. Parasitology Today 1993;9:266-71.
24. Kitron U, Otieno LH, Hungerford LL, Odulaja A, Brigham WU, Okello OO, et al. Spatial analysis of the distribution of tsetse flies in the Lambwe Valley, Kenya, using Landsat TM satellite imagery and GIS. Journal of Animal Ecology 1996;65:371-80.
25. Kitron U, Kazmierczak JJ. Spatial analysis of the distribution of Lyme disease in Wisconsin. Am J Epidemiol 1997;145:1-8.
26. Malone JB, Abdel-Rahman MS, El Bahy MM, Huh OK, Shafik M, Bavia M. Geographic information systems and the distribution of ***Schistosoma mansoni*** in the Nile delta. Parasitology Today 1997;13:112-9.
27. Patz JA, Epstein PR, Burke TA, Balbus JM. Global climate change and emerging infectious diseases. JAMA 1995;275:217-23.

Remote Sensing and Geographic Information Systems: Charting Sin Nombre Virus Infections in Deer Mice

John D. Boone,* Kenneth C. McGwire,† Elmer W. Otteson,*
Robert S. DeBaca,† Edward A. Kuhn,* Pascal Villard,*
Peter F. Brussard,* and Stephen C. St. Jeor*
*University of Nevada, Reno, Nevada, USA; and †Desert Research Institute, Biological Sciences Center, Reno, Nevada, USA

We tested environmental data from remote sensing and geographic information system maps as indicators of Sin Nombre virus (SNV) infections in deer mouse (***Peromyscus maniculatus***) populations in the Walker River Basin, Nevada and California. We determined by serologic testing the presence of SNV infections in deer mice from 144 field sites. We used remote sensing and geographic information systems data to characterize the vegetation type and density, elevation, slope, and hydrologic features of each site. The data retroactively predicted infection status of deer mice with up to 80% accuracy. If models of SNV temporal dynamics can be integrated with baseline spatial models, human risk for infection may be assessed with reasonable accuracy.

Remote sensing (RS) and geographic information systems (GIS) are map-based tools that can be used to study the distribution, dynamics, and environmental correlates of diseases (1,2). RS is gathering digital images of the earth's surface from airborne or satellite platforms and transforming them into maps. GIS is a data management system that organizes and displays digital map data from RS or other sources and facilitates the analysis of relationships between mapped features. Statistical relationships often exist between mapped features and diseases in natural host or human populations (1). Examples include malaria in southern Mexico and in Asia (3,4), Rift Valley fever in Kenya (5), Lyme disease in Illinois (6), African trypanosomiasis (7), and schistosomiasis in both humans (8) and livestock in the southeastern United States (9). RS and GIS may also permit assessment of human risk from pathogens such as Sin Nombre virus (SNV; family Bunyaviridae), the agent primarily associated with hantavirus pulmonary syndrome (HPS) in North America (10,11). RS and GIS are most useful if disease dynamics and distributions are clearly related to mapped environmental variables. For example, if a disease is associated with certain vegetation types or physical characteristics (elevation, average precipitation), RS and GIS could identify regions where risk is relatively high.

We examined whether RS and GIS data were useful indicators of the spatial pattern of SNV infections in populations of the primary rodent host, the deer mouse (***Peromyscus maniculatus***) (12-15). Our approach involved determining the infection status of rodents at 144 field sites, collecting RS and GIS data for each site, testing for statistical relationships between these data and infection, using the statistical relationships to retroactively classify infection status of rodents at these sites, and using the classifications to estimate prediction accuracy. Predictions derived from RS and GIS data could identify the ecologic settings where human exposure to SNV is most likely to occur.

SNV and its Host

Since the first recognized outbreak of HPS in the southwestern United States in 1993, approximately 240 cases have occurred, with a

Address for correspondence: John D. Boone, Dept. of Microbiology/320, University of Nevada, Reno, NV 89557, USA; fax: 775-784-1620; e-mail: boone@scsr.nevada.edu.

death rate of approximately 40% (J. Mills, pers. comm.) (16). Information about SNV host-virus-environment relationships is limited (16,17). No simple relationships have been found between host density and antibody seroprevalence (16-18), but more complex nonlinear relationships appear to exist (17). SNV infections also appear to be less frequent in relatively high- or low-elevation habitats (16,17).

Study Design

Types of Data

RS data are commonly used to generate maps of vegetation types. Vegetation types can be useful indicators of environmental characteristics, including moisture, soil type, and elevation. However, transforming RS images into vegetation maps can be subjective and imprecise (19,20); therefore, we supplemented our vegetation maps with other RS/GIS data, including elevation, slope, vegetation density, and hydrology.

We sampled rodents over four field seasons (June to October during 1995 to 1998). However, in 1997, population densities of deer mice in our study area averaged approximately 25% of 1995-96 and 1998 levels (unpub. data, Boone et al.). Most of the 47 sites sampled in 1997 had three or fewer deer mice, and 14 sites had none. Simple t-tests (SAS ver. 6.10) showed that the mean number of animals per site was statistically equivalent in 1995, 1996, and 1998 (11.1, 10.3, and 8.9 animals per site, respectively; $p > 0.10$ for all comparisons), but differed significantly in 1997 from all other years (2.4 animals per site; $p < 0.0001$ for all comparisons). In 1997, antibody-positive animals were significantly less likely to be positive by reverse transcription-polymerase chain reaction (RT-PCR) for viral RNA in the blood than in any other year, suggesting unusual infection patterns (25% were PCR positive in 1997 and >50% to 70% in other years; chi-square test, $p < 0.002$ for all comparisons of 1997 to other years; $p > 0.20$ for all comparisons of years excluding 1997). On the basis of these tests, we pooled data from 1995, 1996, and 1998 and excluded 1997 data from all analyses because host density and infection dynamics appeared atypical and likely to obscure the baseline spatial infection patterns we sought to identify (21).

Infection Status of Sites

Presence of SNV infections is commonly inferred by determining antibody seroprevalence in a host population (14,16-18,21-23). However, antibody prevalence at the same site may vary considerably (<5% to >60%) over relatively brief periods of <1 year (17,18,22,23), probably because of rapid turnover of rodent populations through death, reproduction, dispersal, and migration. We focused on the presence or absence of SNV infections inferred from antibody data, a more stable measure than antibody prevalence. However, determining infection status is complicated by several factors: animals may remain antibody-positive well after the transmissible phase of an infection (17); noninfectious but antibody-positive deer mice may migrate to a site where no active SNV infection is present; and detectable antibody response requires at least 1 to 2 weeks to develop in newly infected animals (17).

Because of these uncertainties, we used two criteria to demonstrate the effect of classification on analytical outcome. "Status 1" classified sites with one or more antibody-positive animals as positive (active infection present). This criterion may have falsely assigned positive status to some sites where no active, transmissible infections were present. "Status 2" required two or more antibody-positive deer mice or an overall antibody seroprevalence of at least 10% for a site to be classified positive. This criterion may have falsely assigned negative (active infection absent) status to some sites that had a single infectious animal.

Site Selection

Our study area was the Walker River Basin, a 10,200-km^2 region in western Nevada and east-central California northeast of Yosemite National Park (Figure 1). At least nine cases of HPS have occurred in the area since 1993. Major vegetation types in the river basin along an increasing elevational gradient (1,200 m to 3,760 m) are salt desert scrub, sagebrush-grass scrub, piñon-juniper woodland, coniferous forest, montane shrubland, and alpine tundra, with riparian habitat and meadows at a wide range of elevations (24).

We compiled a GIS database for the study area, including a second-generation map of vegetation types (Figure 1) (25). The vegetation

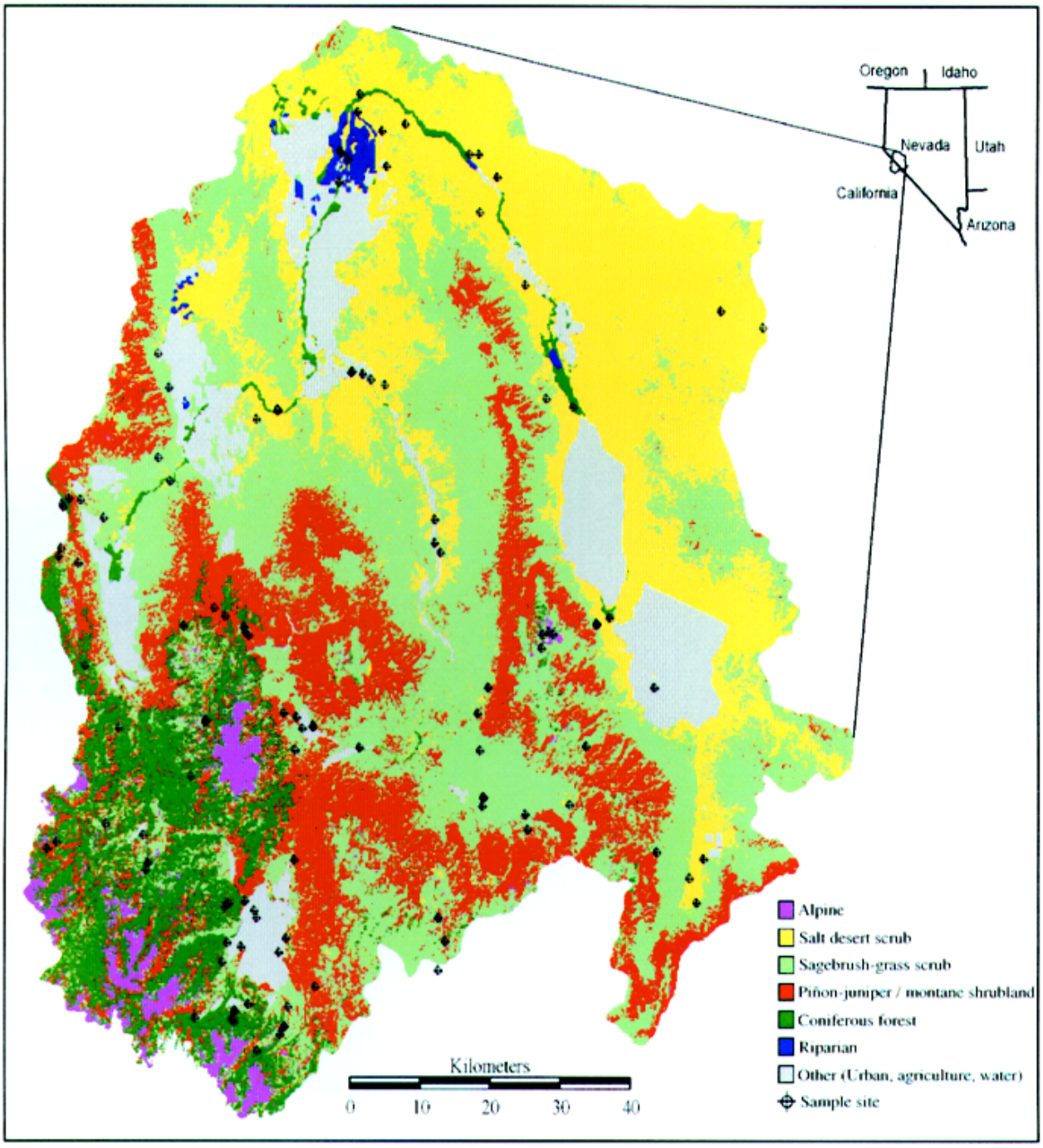

Figure 1. Location of Walker River Basin (17) and its eight major vegetation types, as well as developed areas. Piñon-juniper woodland and montane shrubland tend to be highly interspersed and were combined for visual clarity. Because meadows occurred in very small patches, they could not be represented on this map. Map generated at Utah State University as part of the GAP conservation mapping project.

map, which was generated from Landsat Thematic Mapper images and digital elevation data, had a 100-hectare mapping unit. We aggregated the 36 vegetation subtypes on the GAP map into the eight general vegetation types described above. To estimate vegetation density, we used the normalized difference vegetation index (NDVI), a transformation of near infrared (TM band 4) and red wavelengths (TM band 3) correlated with the amount and productivity, or rate of plant growth, of vegetation (5,26,27). The standard deviation of NDVI within a local area was calculated to estimate the uniformity of vegetation density at each field site. Elevation and slope (i.e., steepness) data were derived from the 2-arcsecond digital elevation model of the U.S. Geological Survey. Because riparian zones could influence rodent population densities and facilitate rodent dispersal across arid regions, we calculated proximity to streams and bodies of water on the U.S. Geological Survey's 1:100,000-scale digital line graph datasets.

In 1995, we sampled rodents at 42 sites before the GAP map became available. These sites were selected as representative of the five most common vegetation types in the Walker River Basin. In 1996 and 1998, full GIS datasets and the GAP map were used to distribute 102 new field sampling sites systematically across the widest possible range of environmental conditions. We categorized each GIS variable according to its relevance to each of the eight vegetation types. For example, 'distance to streams' was a meaningful distinction within salt desert but not within riparian habitat; elevation varied substantially within sagebrush scrub but not within alpine tundra. For each vegetation type, the relevant variables were divided into high and low ranges. The resulting binary classes for each variable were then intersected in GIS to produce distinct environmental "combinations," or strata, for each vegetation type (Figure 2). Randomly located sample sites were selected within each stratum so that they were within 0.5 km of a passable road and at least 1 km from any other sample site (Figures 1,3). The number of replicates within each stratum (including 1995 sites, which were included retroactively) was proportional to its spatial extent, with a minimum sample size of two. This GIS-based stratification is a more objective and randomized variation of the gradsect sampling method (28, 29).

All samples were collected from early June to early October to minimize seasonal effects on host density and antibody prevalence (17). Seasonal influences were minimized by sampling the replicate sites within each environmental stratum at different times throughout the field season.

Field and Laboratory Procedures

Deer mice were live-trapped at all field sites according to a fixed protocol (17). Each site had 48 live-traps in place for 3 days. A blood sample was collected from each deer mouse by retroorbital puncture with a heparinized capillary tube or Pasteur pipette. Blood samples were placed on dry ice and returned to the laboratory for enzyme-linked immunosorbent assay testing for immunoglobulin G antibody to SNV, which indicates current or past infections (14). Relative population density was estimated by counting the number of animals captured during a trapping session.

Analytical Methods

Of the 144 sites sampled in 1995, 1996, and 1998, 25 were excluded from analysis because no deer mice were captured. Status 1 classified 38 of the remaining 119 sites as negative and 81 as positive. Status 2 classified 70 sites as negative and 49 as positive (i.e., 32 sites had differing infection status under the two criteria). We tested (by chi-square, SAS ver. 6.10, PROC FREQ) for differences among the proportion of positive sites for each vegetation type. Then, with a canonical linear discriminant function analysis [DFA] [SAS ver. 6.10, PROC DISCRIM], we examined relationships between infection status and the alternate set of RS and GIS variables with slope, elevation, density and uniformity of vegetation, and distance from streams as indicators of SNV infection status (3,17). Prior probabilities were adjusted to reflect actual proportions of positive and negative sites.

The relationships derived from these two analyses were then used to classify sites retroactively according to their expected infection status. Because error rates were not distributed evenly among sites classified as positive and negative, we present these results separately. Classification accuracy is a general estimate of the prediction accuracy of each method if it were applied to new sites in a similar

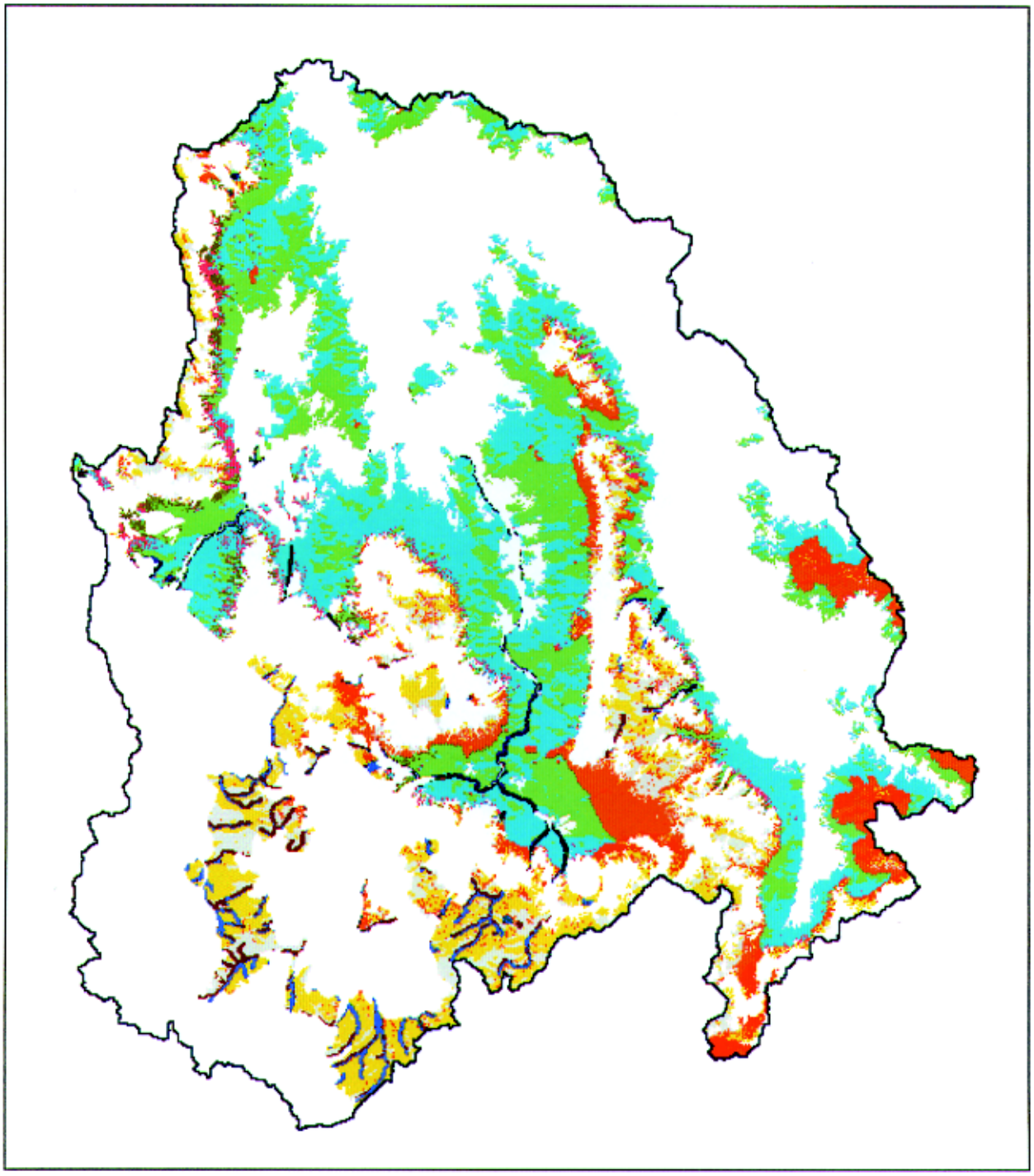

Figure 2. Environmental strata within the mapped extent of the sagebrush-grass scrub vegetation type. Each color represents a unique combination of high or low vegetation density index, standard deviation of vegetation density index, slope, elevation, and distance from stream. White areas represent the other seven vegetation types (strata not shown).

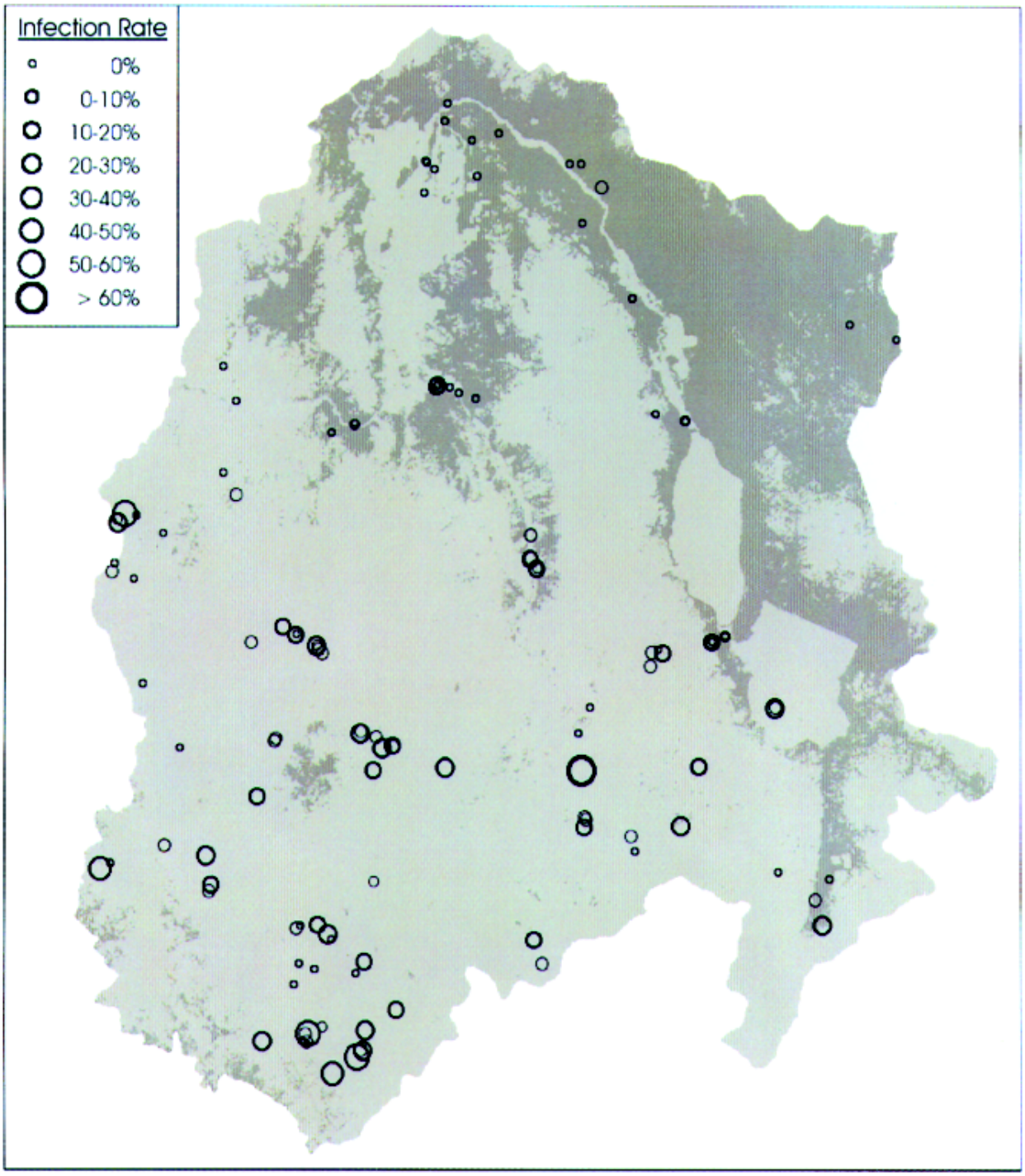

Figure 3. Seroprevalence of IgG antibody to Sin Nombre virus at sample sites in the Walker River Basin. (According to Status 1, sites with 0% prevalence were negative and all other sites were positive.)

landscape. For each prediction accuracy estimate, we calculated 95% confidence limits derived from the binomial distribution. Standard deviation for the binomial distribution is

$$\sqrt{\frac{P(1-P)}{n}}$$

where p = accuracy estimate and n = number of samples. A normal approximation of confidence limits was obtained by multiplying the standard deviation of each estimate by the t-table value associated with 95% confidence and the appropriate number of samples. These confidence intervals also allowed us to determine whether classification accuracy differed significantly between methods.

Results

Vegetation Types

The proportion of positive sites in salt desert scrub (34% of 29 sites by Status 1, 14% by Status 2) was significantly lower than in any other vegetation type (p = 0.05 criteria for significance). No significant differences were found among any of the other seven vegetation types, where positive sites were more common by both Status 1 (50% to 100%) and Status 2 (50% to 83%) (Figure 3). By assigning the predominant infection status to all sites within a given vegetation type, overall classification accuracies of 76% (Status 1) and 59% (Status 2) could be achieved (Table 1). The Status 1 criterion resulted in better classification accuracy (for negative sites and for all sites combined) than Status 2. For both Status 1 and Status 2, positive classification was more accurate (> 88%) than negative classification (50%).

DFAs for both Status 1 and Status 2 produced significant canonical correlations showing that negative sites were associated with low elevations and sparse vegetation (Table 2). These qualities most often occur in salt desert scrub (24). In contrast, positive sites were higher and generally had more dense but less uniform vegetation. Slope and distance from streams were relatively unimportant factors. For both Status 1 and Status 2, negative classification was more accurate than positive classification (Table 1). Positive classification was more accurate in Status 2 than in Status 1.

Discussion

RS and GIS data were useful indicators of the SNV infection status of deer mice in our study area. Sites with typical salt desert scrub characteristics were less likely to have infected mice than other sites. If the 25 sites where no deer mice were captured (primarily salt desert

Table 1. Classification and prediction accuracies for Sin Nombre virus infection status, by vegetation type method and canonical discriminant function analysis

Site in Walker River Basin	% classified negative	% classified positive	% overall accuracy
Vegetation type Status 1	50 ± 12[a]	88 ± 8	76 ± 10
Vegetation type Status 2	36 ± 9	92 ± 6	59 ± 12
DFA[b] Status 1	84 ± 9	69 ± 11	74 ± 10
DFA Status 2	84 ± 9	80 ± 10	82 ± 9

[a]The error terms following each estimate are 95% confidence intervals derived from the binomial distribution.
[b]DFA = discriminant function analysis.

Table 2. Sin Nombre virus infection status of sites in the Walker River Basin: canonical discriminant function analyses for Status 1 and Status 2

	Canonical correlation[a] (p-value)	Canonical loadings[b]				
		Elevation	NDVI[c]	NDVI Std[d]	Slope	Streams[e]
Status 1	0.41 (0.0003)	0.77	0.52	0.69	0.06	0.04
Status 2	0.53 (0.0001)	0.79	0.46	0.68	0.09	0.05

[a]The canonical correlation and its significance level define the overall association between infection status and the indicator variables.
[b]Canonical loadings for each indicator variable indicate their relative importance in producing a significant overall canonical correlation.
[c]NDVI = vegetation density.
[d]NDVI Std. = uniformity of vegetation density.
[e]Streams = distance to nearest mapped stream or body of water.

scrub sites) had been incorporated into our analyses as negative sites, this relationship would have been more pronounced. The relationship may be explained by the level of connectivity (i.e., biological interchange) among host populations. Salt desert scrub or similar arid habitats in the western United States are frequently dominated by heteromyid rodents (kangaroo rats, pocket mice) rather than by deer mice and other potential hosts for SNV. Although deer mice were found in salt desert scrub in the Walker River Basin and were sometimes locally abundant, their overall population density was somewhat lower than in other vegetation types, and they were more likely to be locally absent (17). We suspect that SNV infections are less likely in deer mouse populations that inhabit such regions because of their relative isolation from neighboring populations (30,31). Such fragmentation of host populations may reduce the rate of disease propagation across space and the frequency of infection recurrences within local sites. This hypothesis is supported by the clustering of negative sites in landscapes dominated by salt desert scrub (Figure 3), despite the fact that some of these sites had relatively dense deer mouse populations.

Spatial Versus Temporal Disease Patterns

Because the RS and GIS maps summarize relatively fixed spatial properties of the environment, we focused on investigating the corresponding spatial patterns of SNV infections. SNV infections also exhibit temporal dynamics (13,16-18,22,23) superimposed on the baseline spatial pattern. However, a robust temporal study would require many years of replicated, longitudinal field data, as well as real-time RS data describing temporally variable environmental characteristics (such as climatic variables) for the corresponding period. We did not incorporate weather or climate data into GIS because weather monitoring stations are widely scattered throughout most of the study area, preventing meaningful extrapolations to most of the field sites.

Sampling Design

Because characterizing large-scale spatial disease patterns requires a large sample size, we maximized the number of sites sampled rather than visiting fewer sites on multiple occasions. This cross-sectional approach captured substantial ecologic diversity and provided statistical replicates of sites with similar characteristics. The disadvantage of the approach was a degree of uncertainty in determining the actual infection status at each site. However, when generalization of results is an important goal, a large, replicated, and diverse dataset that has a modest degree of measurement error is statistically preferable to a smaller, more precisely measured but poorly replicated dataset (32).

Comparison of Methods (Table 1)

The vegetation type approach was based on possible relationships between infection status and a preexisting vegetation classification that might or might not be relevant to deer mice and SNV infections. DFA, in contrast, generated a linear function that best distinguished the properties of positive and negative sites. Our results suggest that DFA yields a better balance between classification accuracies for positive and negative status (especially for Status 2).

The vegetation type method could not classify negative status as effectively as the DFA, and balance between error rates for positive and negative classifications was poor. This could be a result of using predefined vegetation types (rather than making environmental distinctions from actual infection patterns) or inaccuracies in identifying and mapping vegetation types. Site visits suggested that the DFA identified sites with pronounced salt desert features more effectively than the vegetation map. The substantial environmental variability within the mapped extent of salt desert scrub was easily captured by the set of RS and GIS variables but was analytically "invisible" to our aggregated GAP map. Some variability might have been captured by the GAP map's 36 original vegetation subclasses, but using all these in our analysis would have presented serious statistical problems.

Other analytical approaches are possible that were not presented here. For example, decision tree analysis (33,34) offers advantages if nonlinear relationships exist; hierarchical information on the effects of each predictor variable is desired; or ease of interpretation is important (29).

Classification and Prediction Accuracy

Classification accuracy varied significantly between the Status 1 and Status 2 criteria (Table 1), with Status 2 giving better classification balance for DFA and Status 1 producing

better results for the vegetation type analysis. Unfortunately, the biological significance of these analytical differences is difficult to determine. However, the infection status of 73% of the sites was classified similarly by the two criteria. The remaining 32 sites of ambiguous infection status might represent regions where infection status changes with relatively high frequency. If so, this produces an intrinsic limitation in the capabilities of the methods we present. The choice of technique might be based on the relative risks and costs of false-negative versus false-positive predictions.

Both methods may have occasionally been unable to detect positive sites because of failure to capture positive deer mice. The likelihood of this error would be proportional to the number of resident animals not captured at a site. Our longitudinal data (17; unpub. data, Boone et al.) suggest that the 3-day sampling sessions captured most of the animals present at a site. During four 7-day trapping sessions, 86% ± 9% of animals were captured during the first 3 days of trapping. Additionally, examination of 123 3-day sessions within the context of their extended longitudinal infection timelines (17; unpub. data, Boone et al.) suggested that infection status was classified with 85% (Status 1) and 81% (Status 2) accuracy.

A cross-sectional, replicated, and randomized sampling approach should capture most sites while they exhibit their most typical infection status. However, a 'background' rate of classification errors is to be expected regardless of analytical method, given the temporally dynamic nature of SNV infections (17,18,22,23). For instance, even where infection status is predominantly positive, some sites may be sampled during atypical periods when infection is temporarily absent; the reverse could also occur. Additionally, a subset of sites might frequently change their infection status and not exhibit primary infection status. Thus it might be difficult to improve upon the highest overall classification success we achieved (with DFA and Status 2 criterion), unless temporal infection dynamics are incorporated into the predictive model. Another option would be to omit sites from analysis if they fail to meet unambiguous criteria for positive or negative status; however, this might result in the loss of biological insight.

Future Directions

We explored the ability of RS and GIS data to predict the baseline spatial patterns of SNV infections across an ecologically variable landscape. Our findings should be at least somewhat relevant to a number of other regions in the arid western United States, especially if infection dynamics are ultimately driven by host connectivity patterns. To expand these findings, we developed methods to filter environmental data to remove statistical noise and a computer simulation model to explore infection dynamics on a variety of virtual landscapes. Further work will focus on the role of landscape structure in producing spatial patterns of disease (35). For instance, deer mice in small patches of salt desert scrub within a matrix of more desirable habitat types might be more likely to be infected than mice living in large contiguous regions of salt desert scrub. Finally, it would be useful to test other types of RS and GIS data as possible indicators of SNV infections.

Further work is needed to identify possible climatic correlates of periodic outbreaks and the degree to which useful indicators of these outbreaks can be derived from RS and GIS data sources. In contrast to predictions in large-scale outbreaks, specific a priori predictions of temporal SNV infection dynamics in local sites may remain difficult. Once infections are initiated at a site (presumably by random dispersal events), changes in antibody and virus prevalence cannot be easily explained by changes in host density or environmental factors (17,18). However, it should be possible to estimate the frequency (if not the specific timing) of new infections as a function of a site's local environment. Additionally, extended longitudinal studies could identify typical infection trajectories of sites based on their environmental characteristics or demographic profiles of their host populations. When combined, these approaches should advance our ability to quantify and predict disease dynamics and human risk.

Acknowledgments

We thank Joe Blattman for field work; Tim Wade and Kathy Bishop for GIS assistance; Jack Hayes for general advice; Joan Rowe and Jeff Riolo for laboratory assistance and advice; and Ed Volterra, Benny Romero, and George Mortenson for help with arranging field work on private and other limited-access properties.

This research was funded by NIH grants 5 RO1 AI36418-04 and 1 PO1 AI39808-01, with supporting funding from the National Aeronautics and Space Administration. JDB was supported in part by NIH Postdoctoral Fellowship F32 AI09621.

Dr. Boone is a research assistant professor, Department of Microbiology, University of Nevada, Reno. His interests include disease and animal ecology and ecologic genetics.

References

1. Hugh-Jones M. Applications of remote sensing to the identification of the habitats of parasites and disease vectors. Parasitology Today 1989;5:244-51.
2. Glick G. The geographic analysis of cancer occurrence: past progress and future directions. In: Meade M, editor. Conceptual methodological issues in medical geography. Chapel Hill (NC): University of North Carolina Press; 1980. p. 170-93.
3. Beck L, Rodriguez M, Dister S, Rodriguez A, Rejmankova E, Ulloa A, et al. Remote sensing as a landscape epidemiologic tool to identify villages at high risk for malaria transmission. Am J Trop Med Hyg 1994;51:271-80.
4. Wood B, Beck L, Washino R, Palchick S, Sebesta P. Spectral and spatial characteristics of rice field mosquito habitat. International Journal of Remote Sensing 1991;12:621-6.
5. Linthicom K, Bailey C, Davies F, Tucker C. Detection of Rift Valley fever viral activity in Kenya by remote sensing imagery. Science 1987;235:1656-9.
6. Kitron U, Bouseman J, Jones C. Use of the ARC/INFO GIS to study the distribution of Lyme disease ticks in an Illinois county. Prev Vet Med 1991;11:243-8.
7. Rogers D, Randolph S. Mortality rates and population density of tsetse flies correlated with satellite imagery. Nature 1991;351:739-41.
8. Cross E, Perrine R, Sheffield C, Passaglia G. Predicting areas endemic for schistosomiasis using weather variables and a Landsat data base. Mil Med 1984;149:542-4.
9. Malone J, Zukowski S. Geographical models and control of cattle liver flukes in the southeastern USA. Parasitology Today 1992;8:266-70.
10. Childs JE, Rollin PE. Emergence of hantavirus disease in the USA and Europe. Current Opinion in Infectious Diseases 1994;7:220-4.
11. Nichol ST, Spiropoulou CF, Morzunov S, Rollin PE, Ksiazek TG, Feldmann H, et al. Genetic identification of a hantavirus associated with an outbreak of acute respiratory illness. Science 1993;262:914-7.
12. Childs JE, Ksiazek TG, Spiropoulou CF, Krebs JW, Morzunov S, Maupin GO, et al. Serologic and genetic identification of ***Peromyscus maniculatus*** as the primary rodent reservoir for a new hantavirus in the southwestern United States. J Infect Dis 1994;169:1271-80.
13. Henttonen H, Vapalahti O, Vaheri A. How many kinds of hantaviruses? Trends in Ecology and Evolution 1996;11:7-8.
14. Otteson EW, Riolo J, Rowe JE, Nichol ST, Ksiazek TG, Rollin PE, et al. Occurrence of hantavirus within the rodent population of northeastern California and Nevada. Am J Trop Med Hyg 1996;54:127-33.
15. Levis S, Rowe JE, Morzunov S, Enria DA, St. Jeor SC. New hantaviruses causing hantavirus pulmonary syndrome in central Argentina. Lancet 1997;349:998-9.
16. Mills JN, Ksiazek TG, Ellis BA, Rollin PE, Nichol ST, Yates TL, et al. Patterns of association with host and habitat: antibody reactive with Sin Nombre virus in small mammals in the major biotic communities of the southwestern United States. Am J Trop Med Hyg 1997;56:273-84.
17. Boone JD, Otteson EW, Villard P, McGwire KC, Rowe JE, St. Jeor SC. Ecology and demography of hantavirus infections in rodent populations in the Walker River Basin of Nevada and California. Am J Trop Med Hyg 1998;59:445-51.
18. Calisher CH, Sweeney W, Mills JN, Beaty BJ. Natural history of Sin Nombre virus in western Colorado. Emerg Infect Dis 1999:5:126-34.
19. McKelvey KS, Noon BR. Incorporating uncertainties in animal location and map classification into habitat relationships modeling. In: Perspectives on uncertainty in ecological data. Springer Verlag. In press, 1999.
20. Stoms DM, Davis FW, Cogan CB. Sensitivity of wildlife habitat models to uncertainties in GIS data. Photogrammetric Engineering and Remote Sensing 1992;58:843-50.
21. Mills JN, Ksiazek TG, Peters CJ, Childs JE. Long-term studies of hantavirus reservoir populations in the southwestern United States: a synthesis. Emerg Infect Dis 1999;5:135-42.
22. Engelthaler DM, Levy CE, Fink TM, Tanda D, Davis T. Short report: decrease in seroprevalence of antibodies to hantavirus in rodents from 1993-1994 hantavirus pulmonary syndrome case sites. Am J Trop Med Hyg 1998;58:737-8.
23. Abbott KD, Ksiazek TG, Mills JN. Long-term hantavirus persistence in rodent populations in central Arizona. Emerg Infect Dis 1999;5:102-12.
24. Billings WD. Vegetational zonation in the Great Basin of western North America. International Union of Biological Sciences. Series B 1951;9:101-22.
25. Scott J, Davis F, Csuti B, Noss R, Butterfield B, Groves C, et al. Gap analysis: a geographical approach to protection of biological diversity. Wildlife Monographs 1993;123:141.
26. Tucker C. Red and photographic infrared linear combinations for monitoring vegetation. Remote Sensing of Environment 1979;8:127-50.
27. Tucker C, Van Praet C, Boerwinkel E, Gaston A. Satellite remote sensing of total dry matter production in the Senegalese Sahel. Remote Sensing of Environment 1983;13:461-74.
28. Wessels K, Van Jaarsveld A, Grimbeek J, Van Der Linde M. An evaluation of the gradsect biological survey method. Biodiversity and Conservation 1998;7:1093.
29. Desert Research Institute. Modeling the spatial and temporal dynamics of hantavirus infection in host populations. Available from URL:http://dia.dri.edu/hanta/

30. Dobson AP. Introduction. In: Grenfell BT, Dobson AP, editors. Ecology of infectious diseases in natural populations. Cambridge: Cambridge University Press; 1995. p. 1-19.
31. Dobson AP, Hudson PJ. Microparasites: observed patterns. In: Grenfell BT, Dobson AP, editors. Ecology of infectious diseases in natural populations. Cambridge: Cambridge University Press; 1995. p. 52-89.
32. Hurlbert SH. Pseudoreplication and the design of ecological field experiments. Ecological Monographs 1984;54:187-211.
33. Tabachnik BG, Fidell LS. Using multivariate statistics. 3rd ed. New York: Harper Collins; 1996. p. 507-8 and 514.
34. Clark L, Pregibon D. Tree-based models. In: Chambers JM, Hastie TJ, editors. Statistical models in S. Pacific Grove (CA): Wadsworth and Brooks/ Cole; 1992. p. 377-419.
35. Schumaker NH. Using landscape indices to predict habitat connectivity. Ecology 1996;77:1218-25.

Potential Exposure to Australian Bat Lyssavirus, Queensland,1996–1999

Bradley J. McCall,* Jonathan H. Epstein,* Annette S. Neill,* Karen Heel,* Hume Field,† Janine Barrett,‡ Greg A. Smith,§ Linda A. Selvey,¶ Barry Rodwell,† and Ross Lunt#

*Brisbane Southside Public Health Unit, Cooper's Plains, Queensland, Australia; †Queensland Department of Primary Industries, Yerongpillly, Queensland, Australia; ‡The University of Queensland, St. Lucia, Australia; §Queensland Health Scientific Services, Cooper's Plains, Queensland, Australia; ¶Queensland Health; and #CSIRO Australian Animal Health Laboratory, Geelong, Victoria, Australia

Two human deaths caused by Australian bat lyssavirus (ABL) infection have been reported since 1996. Information was obtained from 205 persons (mostly adults from south Brisbane and the South Coast of Queensland), who reported potential ABL exposure to the Brisbane Southside Public Health Unit from November 1,1996, to January 31, 1999. Volunteer animal handlers accounted for 39% of potential exposures, their family members for 12%, professional animal handlers for 14%, community members who intentionally handled bats for 31%, and community members with contacts initiated by bats for 4%. The prevalence of Lyssavirus detected by fluorescent antibody test in 366 sick, injured, or orphaned bats from the area was 6%. Sequelae of exposure, including the requirement for expensive postexposure prophylaxis, may be reduced by educating bat handlers and the public of the risks involved in handling Australian bats.

Australian bat lyssavirus (ABL) was first reported in July 1996 in a black flying fox (***Pteropus alecto***) from Ballina, New South Wales (1,2). ABL has been confirmed in five species of Australian bat: four species of flying fox (suborder Megachiroptera, genus Pteropus) and one species of insectivorous bat (suborder Microchiroptera, Saccolaimus flaviventris). Two cases of human ABL infection have been reported. The first case occurred in a 39-year-old female animal handler from Rockhampton, Queensland, in November 1996, within 5 weeks of her being scratched and possibly bitten by a yellow-bellied sheath-tailed bat (***S. flaviventris***) (R. Taylor, pers. comm.). The second case occurred in a 27-year-old woman from Mackay, Queensland, in December 1998, >2 years after a bite from a flying fox. Both patients died (3,4).

Address for correspondence: Bradley J. McCall, Brisbane Southside Public Health Unit, P.O. Box 333, 39 Kessels Road, Cooper's Plains, Qld 4108, Australia; fax: 61-7-3000-9130; e-mail: mccallb@health.qld.gov.au.

ABL is a member of the family Rhabdoviridae. Although ABL possesses marked serotypic, antigenic, and molecular sequence similarities to classic rabies virus, it represents a distinct, new genotype, genotype 7 of the Lyssavirus genus (5). The clinical signs of ABL infection in the two human cases were consistent with those of classic rabies infection and included a diffuse, nonsuppurative encephalitis that led to death (3,4). Bats with ABL infection are frequently reported to have had hind limb paresis. While most infected bats are depressed when found, some exhibit uncharacteristic aggression toward humans or other bats. Frequently, a nonspecific, nonsuppurative meningoencephalitis is seen in brains of infected animals (6,7). Vaccine protection trials in mice conducted at the Centers for Disease Control and Prevention (CDC), Atlanta, Georgia, supported the decision to use human diploid cell vaccine (HDCV) for human ABL prophylaxis (7-9). Historically, Australia has been considered free of rabies and rabieslike viruses. Thus, before the first human case of ABL infection in 1996, no

measures existed to prevent rabies or rabieslike disease acquired as a result of contact with Australian domestic animals or wildlife. Since the first human ABL case, the Queensland Health Department, in accordance with the recommendations of the national Lyssavirus Expert Group, has provided postexposure prophylaxis (PEP) to persons who report potential exposure to ABL through bites, scratches, and permucosal or percutaneous exposure to bat saliva or neural tissue (9,10). Preexposure prophylaxis is recommended for persons who report frequent contact with bats.

Colonies of flying foxes are common in suburban areas of southeast Queensland. The black flying fox (***Pteropus alecto***) and the grey-headed flying fox (***P. poliocephalus***) live there throughout the year, and the little red flying fox (***P. scapulatus***) occurs seasonally. While the population of flying foxes may be decreasing in southeast Queensland, fragmentation of colonies has resulted in a wider distribution of smaller colonies (L. Hall, pers. comm.). Direct contact with bats by the general public and animal handlers is not uncommon (11). Volunteer animal handlers rehabilitate sick, injured, and orphaned bats and are frequently bitten, scratched, or exposed to bat saliva. Since November 1996, the Brisbane Southside Public Health Unit (BSPHU) and other state public health units have been involved in coordinating lyssavirus PEP. This article describes the pattern of potential human exposure to ABL reported to the Communicable Disease Control Section of BSPHU between November 1996 and January 1999 and subsequent PEP. Disease prevalence findings are presented for bats surveyed in southeast Queensland by the Animal and Plant Health Service of the Queensland Department of Primary Industries.

The Study

During the study (November 1, 1996, to January 31, 1999), the Communicable Disease Control Section of BSPHU served a population of approximately 1.1 million persons in several local government areas, south Brisbane (part of the Brisbane City Council Area), Logan, Redlands, Beaudesert, and Gold Coast (12). All persons who reported a potential ABL exposure (bat bite, scratch, percutaneous, or permucosal exposure to bat saliva or neural tissue) were asked to complete a standard questionnaire, which sought demographic information (including occupation, history of professional or volunteer bat handling, history of rabies vaccination, potential rabies exposure [bite, scratch, provoked, unprovoked], circumstances that led to the exposure, treatment received, and any laboratory investigation of the bat).

A separate questionnaire was completed for each occasion a person contacted BSPHU to report potential ABL exposure. Potential exposures were reported retrospectively, and the dates of notification and potential exposure for each case were included. All information was recorded and analyzed by using an Epi-Info 6.04b database (13). Age and gender-specific notification rates were calculated by using estimated resident population data for 1997 (12).

During the same period, healthy bats, sick and injured bats, and bats involved in a potential human exposure to ABL were tested for infection with a fluorescein-labeled antirabies monoclonal globulin (CENTOCOR) in a direct fluorescent antibody test (DFAT) on fresh brain impression smears at the Queensland Department of Primary Industries Animal Research Institute or at the CSIRO Australian Animal Health Laboratories. Material from most bats that tested positive for ABL infection and from bats associated with a potential human exposure to ABL were sent to either the Australian Animal Health Laboratory or Queensland Health Scientific Services for confirmation by DFAT, virus isolation, and polymerase chain reaction.

Results

A total of 205 notifications to BSPHU met the criteria for potential ABL exposure during the study period, an average annual notification rate of 8.1/100,000. Complete information was obtained from 202 persons. Total notifications included 86 males and 119 females (M:F ratio of 1:1.38). The age- and gender-specific average annual notification rates are presented in Figure 1. Most reported potential exposures (116 of 204) were among persons 19 to 49 years of age. The months of potential ABL exposure and notification are presented in Figure 2. Most notifications (131 of 205) were made within 2 months of each of the two fatal human cases. Nine (11%) of 80 notifications made in the 2 months following the first reported case were related to exposures that occurred >2 months before the first human case was publicized. The median interval between

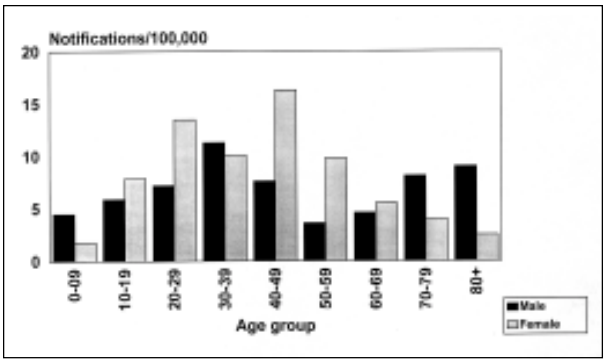

Figure 1. Age and gender-specific average annual notification rates of potential human exposure to Australian bat lyssavirus (n = 204) south Brisbane and South Coast, Queensland, 1996-1999.

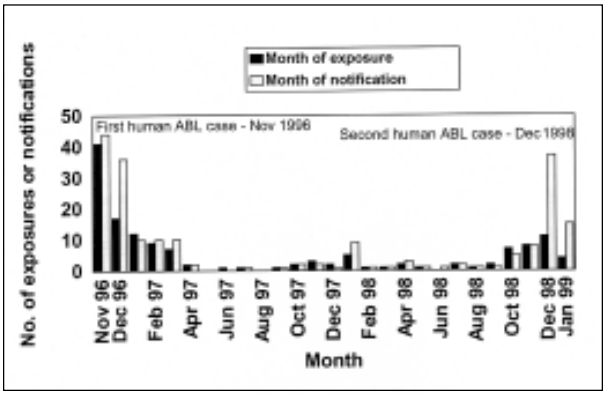

Figure 2. Dates of potential Australian bat lyssavirus exposures and notifications to the Brisbane Southside Public Health Unit, south Brisbane and South Coast, Queensland, 1996-1999.

exposure and notification of these 80 potential exposures was 17 days (0 to 1,080 days). In the 2 months following the second case, 22 (43%) of 51 notifications were related to potential exposures that had occurred before the reporting of the first human case. The median interval between exposure and notification of the 51 potential exposures was 728 days (0 to 2,907 days). A further 14 (27%) of the 51 notifications were related to potential exposures that had occurred since the first human case but had not been reported to BSPHU at the time of exposure.

Season of Exposures

Potential exposures to ABL were reported to have occurred from 1991 to 1999, most during spring and summer (September to February) (n = 151, 74%). While the occurrence of the two human ABL cases in spring and summer influenced the reporting of potential exposures at these times, this trend of increased spring-summer potential exposures persisted in the period between the two reported human ABL cases. The highest number of potential exposures (105) was reported in the year of the first human case; 99 occurred in the spring or summer of 1996-97.

Groups at Risk

Notifications were categorized according to the person's life-style and occupational potential for exposure to ABL (Table). The group at highest risk, volunteer bat handlers, reported 79 (39%) potential exposures; 8 of these handlers reported a second potential exposure during the study.

Table. Groups at risk for exposure to Australian bat lyssavirus

Groups at risk	No. of potential exposures (n=203)	Mean age and age range (yrs)	Gender (m/f)	Median interval between exposure and notification (d)	Bite/nonbite injury (n=202)	Provoked (%) (n=202)
Volunteer bat handlers	79	40.5 (16-83)	15/64	19 (0-2,105)	56/23	79/79 (100)
Household or family member of volunteer bat handlers	24	17.5 (5-51)	12/12	27 (0-1,809)	18/6	24/24 (100)
Professional animal worker	28	34 (17-69)	15/13	4 (0-1,818)	13/14	27/27 (100)
Community-intentional potential exposure	63	39 (6-85)	40/23	10 (0-2,907)	41/22	62/63 (98)
Community-unintential exposure	9	32 (16-49)	4/5	2 (0-32)	3/6	4/9 (44)

Twenty-four (12%) notifications of potential exposure were among household or family members of volunteer bat handlers. Professional animal handlers (e.g., veterinarians, wildlife biologists, park rangers) reported 28 (14%) exposures. Community members who handled bats (usually in the course of freeing them from a fence or entanglement) reported 63 (31%) potential exposures. Community members reported 9 unintentional potential exposures in which contact was initiated by the bat.

The pattern of notification varied within groups at risk during the study. The number of potential exposures reported by volunteer and professional animal handlers declined. Notifications by all groups were highest in the months after the reported fatal human cases of ABL infection. The number of potential exposures reported in the 2 months after the first human case (n = 80) was higher than after the second case (n = 51), particularly among volunteer bat handlers, who reported the highest number of potential ABL exposures in the 2 months after the first human case (43 [53%] of 80), decreasing to 12 (24%) of 51 in the 2 months after the second case. Notifications of potential exposures among community members who had intentionally handled bats rose from 11 (14%) of 80 in the 2 months after the first human ABL case to 23 (45%) of 51 in the 2 months after the second human ABL case.

Nature of Exposure

Potential exposures were classified as bite or nonbite exposures in accordance with international recommendations (14). Most potential exposures were bites (n = 132, 64%). The ratio of bite to nonbite potential exposures within groups at risk was highest among volunteer bat handlers (56:23) (Table). Potential exposures associated with unintentional contact with bats by community members were predominantly scratches (3 bite: 6 nonbite), whereas potential exposures from intentional contact with bats by all other risk groups were predominantly by bites (128 bites: 65 nonbites). Potential exposures were categorized as provoked (arising from intentional contact with a bat) or unprovoked (a contact initiated by the bat). Most potential exposures (97%) were described as provoked (Table).

Treatment

PEP was offered to all persons who reported potential ABL exposures, in accordance with international and Australian recommendations (8,14). Standard PEP for unvaccinated persons consisted of human rabies immune globulin (HRIG, 20 IU/kg) on day 0 and 5 doses of HDCV administered on days 0, 3, 7, 14, and 28. PEP for immunized persons consisted of 2 booster doses of HDCV administered on days 0 and 3. A national shortage of HRIG required modifications to the standard PEP regimen. Sixty-two potentially exposed persons received standard PEP, 100 received 5 doses of HDCV only, 16 vaccinated persons received 2 booster doses of HDCV, and 25 persons did not receive treatment when the bat tested negative. Two persons refused vaccination because of concerns about potential vaccine side effects. Sixteen persons ceased treatment when the bat tested negative.

The estimated cost of providing PEP during this study was A$137,368, which included A$30,930 for medical services funded through the Commonwealth Medicare system (calculated on the cost of six visits to a medical practitioner for each person requiring a 5-dose course of PEP and three visits for each person requiring 2 doses of PEP); A$8,200 for public health officers who interviewed potentially exposed persons; A$10,600 for laboratory testing of the bats; and A$87,638 for HDCV and HRIG. The cost of all vaccines was met by the Queensland Health Department.

ABL Test Results in Bats

All bats retrieved from a human exposure incident underwent postmortem examination and testing for ABL infection. Thirty-six bats were tested; two were positive on DFAT and polymerase chain reaction testing for Lyssavirus—a black flying fox and a little red flying fox. The tested bats included 13 black flying foxes, 11 grey-headed flying foxes, 5 little red flying foxes, and 7 insectivorous bats.

In a separate investigation, the Queensland Animal Research Institute tested bats by DFAT on brain impression smears for evidence of ABL infection since June 1996. From November 1, 1996, to January 31, 1999, some 153 healthy wild-caught flying foxes; 181 healthy wild-caught insectivorous bats; 366 sick, injured, or orphaned

flying foxes; and 39 sick or injured insectivorous bats from the area served by BSPHU and greater Brisbane were tested. Of these, 21 (6%) of the 366 sick, injured, or orphaned flying foxes tested positive for ABL infection, including the 2 involved in human exposures in the BSPHU area. All other bats tested negative.

Discussion

This is the first description of PEP provided to an Australian community after the recognition of human risk for ABL infection. The first human case triggered a large national public health campaign and considerable public awareness about the risks from bats, particularly in communities such as south Brisbane and the South Coast of Queensland, where large colonies of bats live close to human urban populations and bat/human interaction is not uncommon. Increased concern was demonstrated by the large number of notifications of potential exposure that followed reports of the two human cases (Figure 2). Most potential human exposures were among adults (ages 25 to 49). The increased proportion of women reflects the high proportion of female volunteer bat handlers in the study population.

The first 2 months of notifications represents a catch-up period in which PEP was provided to persons with exposures dating back several years. Relatively few notifications occurred after the first 2 months of the study, and it was only after the second human case, which had an assumed incubation period of approximately 2 years, that another cluster of notifications occurred (4). The median interval between potential exposure and notification increased from 17 days for those notified in the 2 months after the first human ABL case to 728 days for those notified in the 2 months after the second case. The potential exposures reported in the 2 months after the second case included 22 persons who were potentially exposed before the first case and 14 with >1 month between potential exposure and notification. The second human case with its prolonged incubation period reinforced the public perception of the severity of this disease and prompted more notifications.

Potential exposures occurred most commonly in spring and summer, coinciding with the birthing season (October to December) of the black and grey-headed flying foxes in southeastern Queensland (15). During each birthing season in southeastern Queensland, 100 to 300 neonatal and juvenile black or grey-headed flying foxes are reared by volunteer bat handlers (H. Luckhoff, pers. comm.). These orphans are commonly assumed to have been abandoned or separated from their dams. Frequently, orphans are found still clinging to the body of their dam. Further research is required to identify any association between orphaned bats and the ABL status of the dam. A case of clinical disease in an in-care juvenile black flying fox and the associated exposure of eight humans has been described (6).

Most potential exposures (107 [52%] of 205) were reported from groups who handled bats. These groups were the target of initial public health information campaigns to raise awareness of the risks for ABL infection. PEP was provided to members of these groups after the first human case, and a recommendation was issued that all workers in these fields be vaccinated with HDCV and that unvaccinated persons, including family members of volunteer bat handlers, not handle bats. Seventy-two (35%) of 205 potential exposures occurred among members of the community. Most of these (63 [88%] of 72) had rescued a trapped or fallen bat. The test results from bats indicate that sick, injured, or orphaned bats have a significantly higher crude prevalence of ABL infection ($p < 0.001$) than healthy wild-caught or captive bats. Consequently, the risk for ABL exposure among volunteer and professional bat handlers and persons who rescue bats may be relatively increased because these groups primarily handle sick, injured, or orphaned bats.

Reporting of potential exposures among groups at risk changed with time during the study. One important factor in the management of PEP was the requirement (introduced in 1997) that all bats involved in a potential human exposure be surrendered for postmortem examination and laboratory testing for ABL. Those who care for bats are often reluctant to surrender them for ABL testing. Notifications from volunteer bat handlers declined during the study period. While this may reflect a decline either in the number of bat handlers or in potential exposures among volunteer bat handlers, underreporting may be occurring in this group. Anecdotal evidence suggests that this reduction

in notifications may reflect handlers' concern for the bats. Such underreporting could be associated with future human cases. Most potential exposures resulted from intentional handling of bats. The few potential exposures from unprovoked encounters suggest that bats rarely initiate contact with humans.

The recognition of ABL infection has resulted in a large public health program to provide education, counseling, and prophylaxis to volunteer and professional bat handlers and members of the community who may be exposed to ABL. The focus of the program has been to encourage preexposure vaccination of bat handlers, prevention of potential exposures by avoidance of bat handling by nonvaccinated persons, and prompt medical care when potential exposures occur. The cost of PEP for all those potentially exposed to ABL in south Brisbane and the South Coast of Queensland during the study was considerable. Future public health interventions should continue to emphasize the risks associated with interaction with bats to reduce the requirement for PEP and the likelihood of human cases of ABL infection.

Acknowledgments

The authors thank Russell Stafford, Helen Luckhoff, Les Hall, Nicki Markus, Bruce Harrower, David Gould, the Queensland Medical Laboratory, and the medical practitioners of south Brisbane and South Coast for their assistance in aspects of patient management, laboratory investigation, vaccine delivery, and for advice throughout the study.

Mr. Epstein's work was supported by grants from the National Institutes of Health, the Hickey-Peyton International Travel Fellowship, and the Department of International Programs, Tufts University School of Veterinary Medicine.

Dr. McCall, a public health physician, has led the Communicable Disease Control team at the Brisbane Southside Public Health Unit for 5 years. His research interests include meningococcal disease, leptospirosis, and ABL.

References

1. Crerar S, Longbottom H, Rooney J, Thornber P. Human health aspects of a possible lyssavirus in a flying fox. Commun Dis Intell 1996;20:325.
2. Fraser G, Hooper P, Lunt R, Gould AR, Gleeson LJ, Hyatt AD, et al. Encephalitis caused by a lyssavirus in fruit bats in Australia. Emerg Infect Dis 1996;2:327-31.
3. Allworth A, Murray K, Morgan J. A case of encephalitis due to a lyssavirus recently identified in fruit bats. Commun Dis Intell 1996;20:504.
4. Mackenzie J. Emerging viral diseases: an Australian perspective. Emerg Infect Dis 1999;5:1-8.
5. Gould A, Hyatt A, Lunt R, Kattenbelt JA, Hengstberger S. Characterisation of a novel lyssavirus isolated from Pteropid bats in Australia. Virus Res 1998;54:165-87.
6. Field H, McCall B, Barrett J. Australian bat lyssavirus infection in a captive juvenile black flying fox. Emerg Infect Dis 1999;5:438-40.7.
7. Hooper P, Lunt R, Gould A, Samaratunga H, Hyatt AD, Gleeson LF, et al. A new lyssavirus—the first endemic rabies-related virus recognized in Australia. Bulletin Institut Pasteur 1997;95:209-18.
8. Rabies and bat lyssavirus infection. In: Watson C, editor. The Australian immunisation handbook. 6th ed. Canberra: Australian Government Publishing Service, 1997:162-8.
9. Lyssavirus Expert Group. Prevention of human lyssavirus infection. Commun Dis Intell 1996;20:505-7.
10. Lyssavirus Expert Group. Update on bat Lyssavirus. Commun Dis Intell 1996;20:535.
11. Birt P, Markus N, Collins L, Hall L. Urban flying foxes. Nature Australia 1998;Spring:55-9.
12. Australian Bureau of Statistics. 1997 estimated resident population by statistical local area. Australian Bureau of Statistics catalogue no. 3235.3. Canberra, Australia: The Organization,1997.
13. Dean AG, Dean JA, Coulombier D, Brendel KA, Smith DC, Burton AH, et al. Epi-Info, version 6.04b: a word processing, database, and statistics system for epidemiology on microcomputers (computer program). Atlanta, GA: Centers for Disease Control and Prevention, 1997.
14. Centers for Disease Control and Prevention. Rabies Prevention—United States, 1991. Recommendations of the Immunization Practices Advisory Committee. MMWR Morb Mortal Wkly Rep 1991;40:R3:1-19.
15. Hall LS. Black flying fox. In: Strachan R, editor. The mammals of Australia. Chatswood, Australia: Reed Books 1995;432-7.

Genetic Variation in *Pneumocystis carinii* Isolates from Different Geographic Regions: Implications for Transmission

Charles B. Beard,* Jane L. Carter,* Scott P. Keely,† Laurence Huang,‡ Norman J. Pieniazek,* Iaci N.S. Moura,* Jacquelin M. Roberts,* Allen W. Hightower,* Michelle S. Bens,* Amanda R. Freeman,* Sherline Lee,* James R. Stringer,† Jeffrey S. Duchin,* Carlos del Rio,§ David Rimland,§¶ Robert P. Baughman,# Deborah A. Levy,* Vance J. Dietz,* Paul Simon,* and Thomas R. Navin*

*Centers for Disease Control and Prevention, Atlanta, Georgia, USA; †University of Cincinnati College of Medicine, Cincinnati, Ohio, USA; ‡University of California, San Francisco General Hospital, San Francisco, California, USA; §Emory University School of Medicine, Division of Infectious Diseases, Atlanta, Georgia, USA; ¶Veterans' Affairs Medical Center, Atlanta, Georgia, USA; #University of Cincinnati College of Medicine, Cincinnati, Ohio, USA

To study transmission patterns of ***Pneumocystis carinii*** pneumonia (PCP) in persons with AIDS, we evaluated ***P. carinii*** isolates from patients in five U.S. cities for variation at two independent genetic loci, the mitochondrial large subunit rRNA and dihydropteroate synthase. Fourteen unique multilocus genotypes were observed in 191 isolates that were examined at both loci. Mixed infections, accounting for 17.8% of cases, were associated with primary PCP. Genotype frequency distribution patterns varied by patients' place of diagnosis but not by place of birth. Genetic variation at the two loci suggests three probable characteristics of transmission: that most cases of PCP do not result from infections acquired early in life, that infections are actively acquired from a relatively common source (humans or the environment), and that humans, while not necessarily involved in direct infection of other humans, are nevertheless important in the transmission cycle of ***P. carinii*** f. sp. ***hominis***.

Pneumocystis carinii pneumonia (PCP) in humans, caused by the opportunistic fungal pathogen ***Pneumocystis carinii*** f. sp. ***hominis***, is a frequent cause of illness in persons with AIDS. In recent years, the number of new cases of PCP has greatly diminished (1), largely as a result of highly active antiretroviral therapy and effective anti-***Pneumocystis*** chemoprophylaxis, primarily with trimethoprim-sulfamethoxazole (TMP-SMZ). However, PCP is still the most common life-threatening AIDS indicator condition in the United States in patients whose CD4+ cell count has declined to < 200 cells/µL for the first time (2). The number of persons at risk, as measured by the number of HIV-infected patients with CD4+ cell counts < 200 cells/µL, was recently estimated at around 182,000 (3).

Despite the frequency of PCP, tremendous gaps exist in understanding the basic biology and epidemiology of the causal agent. These gaps, which have been reviewed extensively (4-9), include lack of knowledge of population structure of ***P. carinii*** strains circulating among patients or in potential environmental reservoirs. The implications are important for understanding patterns of transmission and developing methods of intervention.

In the last 5 years, a substantial number of genes and gene fragments have been identified for potential use in analysis and characterization

Address for correspondence: C. B. Beard, Division of Parasitic Diseases, Centers for Disease Control and Prevention, 4770 Buford Hwy, Mail Stop F-22, Atlanta, GA 30341-3724, USA; fax: 770-488-4258; e-mail: cbb0@cdc.gov.

of ***P. carinii*** strains. These loci include the mitochondrial large subunit ribosomal RNA gene (***mtlsurRNA***) (10-12) and the internal transcribed spacers of the nuclear ribosomal RNA array (12-14). The dihydropteroate synthase (***DHPS***) gene locus, which encodes a target for the anti-***Pneumocystis*** drugs TMP-SMZ and dapsone, has also been cloned and sequenced (15). Substantial variation at this locus (16,17) suggests that the widespread use of antimicrobial chemoprophylaxis may be exerting selective pressure on ***P. carinii*** strains circulating in humans. Its polymorphism makes the locus not only potentially useful as a marker for changes in antimicrobial susceptibility levels, but also valuable for strain characterization and typing.

We examined polymorphism at two genetic loci of ***P. carinii*** isolates from persons with AIDS diagnosed in five U.S. cities. One locus, ***mtlsurRNA***, is involved in basic metabolic functions, and the other, ***DHPS***, is the target of sulfone and sulfonamide antimicrobial drugs. We examined the population structure of ***P. carinii*** strains for information that would elucidate their patterns of transmission.

Materials and Methods

Patient Samples

Specimens used in the study were obtained from March 1995 to June 1998 during routine diagnostic procedures for HIV-infected patients hospitalized with PCP in Atlanta, Cincinnati, Los Angeles, San Francisco, and Seattle. A portion of the diagnostic specimen, either induced sputum or bronchoalveolar lavage, was preserved directly with an equal volume of absolute ethanol and stored at 4°C for DNA extraction.

DNA Purification

Specimens were divided into approximately 1-mL aliquots and centrifuged at 14,000 x g for 5 to 7 minutes. The resulting cell pellet was resuspended in 1 mL of phosphate-buffered saline (0.01M, pH 7.2) containing 1 mM EDTA (PBS-EDTA), washed twice in PBS-EDTA, centrifuged, and stored at -80°C for later DNA extraction. DNA was prepared by a commercial purification procedure (Wizard Genomic DNA Purification Kit, Promega, Madison, WI) in accordance with the product recommendations for DNA purification from blood. Final pellets were resuspended in 50 µL of TE (10 mM Tris, 1 mM EDTA, pH 7.2).

Polymerase Chain Reaction (PCR) and DNA Sequencing

PCR amplification was performed at two independent genetic loci. A 360-bp fragment was amplified from the ***mtlsurRNA*** locus by using the published primers PAZ102E (5' - GAT GGC TGT TTC CAA GCC CA - 3') and PAZ102H (5' - GTG TAC GTT GCA AAG TAC TC - 3') (10). PCR conditions included a 94°C hot start for 5 minutes; followed by 35 cycles of a program consisting of 92°C for 30 seconds, 55°C for 30 seconds, and 72°C for 60 seconds; followed by a termination step at 72°C for 5 minutes. The ***DHPS*** locus was amplified by a modification of a nested PCR procedure (16,17). In the first round of this PCR, the primers ***DHPS*** F1 (5' - CCT GGT ATT AAA CCA GTT TTG CC - 3') (S.R. Meshnick, pers. comm.) and ***DHPS*** B_{45} (5' - CAA TTT AAT AAA TTT CTT TCC AAA TAG CAT C - 3') (16) were used. In the second round, the primers DHPS A_{HUM} (5' - GCG CCT ACA CAT ATT ATG GCC ATT TTA AAT C - 3') and DHPS BN (5' - GGA ACT TTC AAC TTG GCA ACC AC - 3') (16) were used. The conditions for the first round were 94°C for 5 minutes, followed by 35 cycles of 92°C for 30 seconds, 52°C for 30 seconds, 72°C for 60 seconds, and a termination step at 72°C for 5 minutes. The conditions for the second round of PCR were 94°C for 5 minutes, then 35 cycles of 92°C for 30 seconds, 55°C for 30 seconds, and 72°C for 60 seconds, followed by a termination step at 72°C for 5 minutes.

For analysis of the PCR-generated fragments, 10 µL of each 50-µL PCR amplification product was examined by horizontal gel electrophoresis on 1% agarose gels. The remaining 40 µL of successfully amplified reactions was purified by a commercial purification procedure (Wizard PCR Purification Kit, Promega, Madison, WI) and suspended in 50 µL of TE for DNA sequencing; 5 µL to 10 µL of each purified product was sequenced directly by using dye terminator chemistry (ABI Prism BigDye Terminator Cycle Sequencing Ready Reaction Kit, PE Applied Biosystems, Foster City, CA) according to the manufacturer's protocol, with the DNA oligonuceotide primers used for PCR amplification. The PCR fragments were sequenced on an ABI 377 automated DNA sequencer (PE Applied Biosystems, Foster City, CA) according to manufacturer's recommendations. The sequenced DNA fragments were analyzed by using Sequence Navigator v.1.0.1

(PE Applied Biosystems, Foster City, CA) and the GCG Wisconsin Package Version 9.1. computer program (18).

Statistical Analysis

Statistical analyses were performed with SAS software version 6.12. Logistic regression was used to examine the association between place of diagnosis and place of birth and genotype for ***mtlsurRNA*** and ***DHPS*** gene loci.

Results

Amplification with Specific Primers

PCR amplification with the selected primer sets gave consistent results in most ***P. carinii***-positive samples. The ***mtlsurRNA*** primers amplified a 360-bp fragment in 223 samples from Atlanta, Los Angeles, San Francisco, and Seattle. The ***DHPS*** primer sets amplified a 300-bp fragment in 220 of these samples. Both genetic loci were successfully amplified for 191 samples. In the Cincinnati dataset, 101 samples were amplified for the ***mtlsurRNA*** locus. The ***DHPS*** site was not examined for this group of samples. All the amplified fragments were sequenced, aligned, and examined for genetic polymorphism.

General Observations on Genotype Frequency

Four unique genotypes were observed for each of the two genetic loci examined. At the ***mtlsurRNA*** locus, all the genotypes were distinguished on the basis of polymorphism at nucleotide positions 85 and 248. Genotypes 1 (85:C; 248:C) and 2 (85:A; 248:C) were the most common (Table 1), occurring at similar frequencies and together accounting for 74.7% of the 324 samples analyzed. Genotypes 3 (85:T; 248:C) and 4 (85:C; 248:T) accounted for 9.3% and 5.9%, respectively. At the ***DHPS*** locus, genotypes 1 and 4 accounted for 80.4% of all samples (Table 2). Genotypes 2 and 3 were both relatively uncommon, seen in 5.9% and 2.3% of the samples analyzed, respectively. All the mutations seen at this locus were nonsynonymous changes resulting in amino acid substitutions; no other polymorphism was observed. Genotype 1 was the designation used to refer to the sequence defined by a threonine at position 55 and a proline at position 57. Genotype 2 referred to an alanine at 55 and a proline at 57, Genotype 3 to a threonine at position 55 and a serine at 57, and genotype 4 to an alanine at position 55 and a serine at position 57.

Table 1. Genotype analysis of ***Pneumocystis carinii*** isolates at the ***mtlsurRNA*** locus

Genotype	Nucleotide position/identity	Frequency n=324 (%)
1	85/C; 248/C	123 (38.0)
2	85/A; 248/C	119 (36.7)
3	85/T; 248/C	30 (9.3)
4	85/C; 248/T	19 (5.9)
mixed		33 (10.2)

Table 2. Genotype analysis of ***Pneumocystis carinii*** isolates at the ***DHPS*** locus

Genotype	Nucleotide (amino acid) position/identity	Frequency n=220 (%)
1	165 (55)/A (Thr) 171 (57)/C (Pro)	68 (30.9)
2	165 (55)/G (Ala) 171 (57)/C (Pro)	13 (5.9)
3	165 (55)/A (Thr) 171 (57)/T (Ser)	5 (2.3)
4	165 (55)/G (Ala) 171 (57)/T (Ser)	109 (49.5)
mixed		25 (11.4)

When the results at both genetic loci were combined, 14 unique multilocus genotypes of 16 possible combinations were observed in 191 samples for which both genes could be amplified and sequenced. The four most common multilocus genotypes accounted for 61.7% of all genotypes. The most common multilocus genotypes consisted of combinations of the most common genotypes at each individual locus. No genetic linkage of specific genotypes from the two loci was observed.

Coinfection with multiple ***P. carinii*** strains could be detected in 33 (10.2%) of 324 samples typed at the ***mtlsurRN***A locus and 25 (11.4%) of 220 typed at the ***DHPS*** locus. When the genotypes were considered together, 34 (17.8%) of 191 samples represented coinfections with multiple genotypes. When these samples were analyzed according to patient history, 21 (17.6%) of 119 samples from patients with no history of previous PCP were coinfected with multiple strains, by typing at the ***mtlsurRNA*** locus. In contrast, none of the samples from 41 patients with PCP history had multiple genotypes ($p = 0.002$, Fisher's exact test). A similar trend was observed at the ***DHPS*** locus but was not statistically significant.

Genotype Frequency Distribution Patterns by Geographic Location

Genotype frequencies in PCP isolates differed by city (Figures 1, 2). At the ***mtlsurRNA*** locus (Figure 1), the genotype distribution was significantly different (chi-square test; p = 0.001), with the ratio of genotype 1 to genotype 2 ranging from 0.7 in San Francisco to 1.8 in Cincinnati. Analysis of the ***mtlsurRNA*** genotype frequencies at each city showed that genotype distributions also differed significantly or borderline significantly, with p values from 0.001 to 0.08, with the exception of Los Angeles. Comparisons involving Los Angeles were nonsignificant, perhaps as a result of small sample size (n = 15).

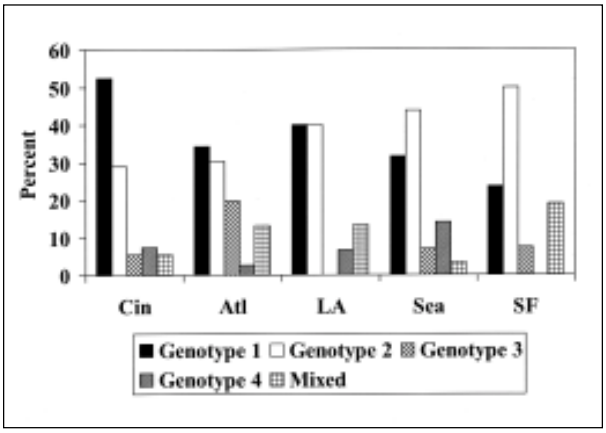

Figure 1. Distribution of ***Pneumocystis carinii mtlsurRNA*** genotypes, by city (chi-square test, p = .001)
Atlanta, n = 76; Cincinnati, n = 107; Los Angeles, n = 15; San Francisco, n = 68; Seattle, n = 57.

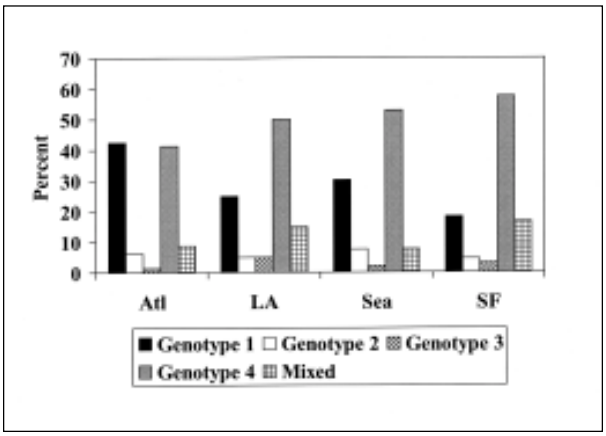

Figure 2. Distribution of ***Pneumocystis carinii DHPS*** genotypes by city (Fisher's exact test, p=.049).
Atlanta, n=80; Los Angeles, n=20; San Francisco, n=66; Seattle, n=53.

We used logistic regression to investigate whether the geographic distribution was associated more with place of birth or with place of diagnosis. We grouped places of birth and diagnosis into either "east" or "west," using the Mississippi River as the dividing line. Data from Cincinnati were not included, since place-of-birth information was not available there. None of the four ***mtlsurRNA*** genotypes was significantly associated with place of birth when the data were adjusted for place of diagnosis. However, genotypes 2 and 4 were significantly associated with place of diagnosis, when the data were adjusted for place of birth (p = 0.002, p = 0.05, respectively); the association of genotype 1 with place of diagnosis was borderline significant (p = 0.08).

The overall genotype distribution at the ***DHPS*** gene locus (Figure 2) also differed significantly (Fisher's exact test; p = 0.045) for the various cities. The ratios of genotype 4 to genotype 1 ranged from 0.97:1 in Atlanta to 3.13:1 in San Francisco. No isolates from Cincinnati were analyzed at the ***DHPS*** locus.

Logistic regression analysis of the ***DHPS*** genotypes by place of diagnosis and place of birth showed results similar to those for the ***mtlsurRNA*** genotypes. Genotypes 1 and 4 were associated with place of diagnosis (p = 0.001, p = 0.002, respectively) when data were adjusted for place of birth. In contrast, place of birth was not associated with any ***DHPS*** genotype when data were adjusted for place of diagnosis.

Discussion

P. carinii, once thought to be a protozoon but now regarded an ascomycetelike fungus (4,19,20), has been associated with human disease since the 1940s. Despite intense efforts to understand this important disease agent, lack of a suitable means of propagation has complicated study of basic biology and epidemiology. Similarly, latency and reactivation (versus recent acquisition) have not been resolved. PCR and other molecular methods have improved understanding of genetic variability and host specificity (11,12,14,20,21), as well as the cause of recurrent infections in persons with AIDS (8,22-24).

Both an indirect (environmental) source and a direct (person-to-person) source have been proposed as modes of transmission of ***P. carinii*** in humans. Three primary observations reported in this study address infection sources and transmission patterns: geographic variation in

genotype frequency distribution, which was correlated with the place of diagnosis rather than the place of birth; rate of coinfection with multiple ***P. carinii*** genotypes, which was greater in patients with primary rather than secondary PCP; and abundance of the ***DHPS*** double mutant, which accounted for 49.5% of all ***DHPS*** genotypes, strongly suggesting genetic selection.

Allelic frequency distribution patterns of ***P. carinii*** isolates were associated with place of diagnosis rather than place of birth. Place of diagnosis was determined more reliable than place of residence as the best indicator of the most likely place of exposure to ***P. carinii*** because place of residence was frequently recorded as permanent or legal residence rather than as place of residence during the 3- to 6-month period before admission. These results suggest that infection in adults is acquired later than the first few months or years of life and that any latency has natural limits. Two independent lines of study offer a context for these observations and suggest that PCP is an actively acquired infection. The first line of study comprises molecular genetic analyses of ***P. carinii*** strains from adult AIDS patients with recurrent PCP. These analyses have shown that different ***P. carinii*** genotypes are detected on subsequent PCP episodes in a substantial proportion of patients (22,23), which suggests that infections in adults are actively acquired and that subsequent infections do not necessarily represent relapses. The second line of study comprises observations of primary PCP in infants with perinatally acquired HIV infection (25) who had PCP episodes at 3 to 6 months of age; the prevalence of PCP among these infants was very similar to that among adults with AIDS. These observations suggest that ***P. carinii*** is common in the environment, consistent with the suggestion that the organism is easily acquired.

While the association with geographic distribution is consistent with recent acquisition of clinical infections, the actual source of the infection is not known. The rat ***P. carinii*** model suggests direct (animal-to-animal) transmission (5,26,27); however, if person-to-person transmission does occur, it has not been shown to be of epidemiologic significance (28,29). PCR amplification of ***P. carinii*** DNA from spore traps from various sites supports the possibility of an environmental source (30-33), but no specific plant, animal, or soil source has been identified. Identification of a specific environmental reservoir for ***P. carinii*** f. sp. ***hominis***, if one exists, could elucidate disease transmission and improve prevention efforts.

The rate of coinfection with multiple ***P. carinii*** strains by multilocus typing was 17.8% (34 of 191). Of the 191 patients for whom both genes were typed, 20 (10.5%) were coinfected at the ***mtlsurRNA*** locus and 19 (9.9%) at the ***DHPS*** locus. Five patients tested positive for multiple strains concurrently at both loci. While the sensitivity to detect coinfections was similar for both genes, concordance between the two genes was very low in detecting coinfections with multiple strains in any particular isolate—only four genotypes can be detected at each individual locus. When the loci are considered together, however, the sensitivity is greatly increased, because the number of possible genotypes increases from 4 to 16, 14 of which were observed in this study.

The 17.8% coinfection rate is within the 10% to 30% range reported by other investigators using DNA sequencing-based approaches (14,22,34). Although coinfection rates as high as 69% have been reported with single-strand conformation polymorphism analysis (35), these differences can probably be resolved by two considerations. The first is the sensitivity of the selected locus, which is a function of the genetic variability or evolutionary rate of the locus (i.e., the more variable the locus, the greater its sensitivity to detect a different genotype). In this study, ***mtlsurRNA*** and ***DHPS*** displayed a high degree of genetic conservation, with only four alleles detected at each locus, all of which have been observed (11,16,17). Because these are relatively slowly evolving genes, the sensitivity to detect coinfections with multiple strains is expected to be less than in a faster evolving locus. The second consideration is PCP prophylaxis. Correlation between primary PCP and coinfection with multiple strains suggests that patients may be exposed to multiple ***P. carinii*** strains over extended periods and harbor short-lived, latent infections. Consequently, patients who have not been treated are more likely to have been exposed (and to harbor) multiple ***P. carinii*** strains. On the other hand, patients who have been treated for PCP at least once and are taking secondary prophylaxis are less likely to become reinfected. This hypothesis is consistent with indications that ***P. carinii*** is ubiquitous in the environment

and exposure in humans is commonplace (22,23). A short latency period has been suggested (36) and is consistent both with coinfections' correlating with primary PCP and allelic frequency distributions' correlating with the place of diagnosis but not the place of birth.

The question of latency and reactivation versus recent acquisition is of great importance as it relates to prevention. If the preponderance of infections in humans results from activated latent infections, chemoprophylaxis is the only method of preventing disease. If, however, infections are actively acquired, identifying specific sources of infection would lead to other methods of prevention and reduce dependence on antimicrobial agents.

The most important clinical implication of the polymorphism observed specifically at the ***DHPS*** locus relates to the emergence of possible antimicrobial resistance; however, the observation of different ***DHPS*** alleles in ***P. carinii*** populations also has implications for transmission routes and patterns and the possibility of person-to-person transmission.

In human ***P. carinii*** isolates, four distinct genotypes have been reported at the ***DHPS*** locus (16,17). All four of these DNA base changes result in amino acid substitutions at an important structural position, in an otherwise very highly conserved gene (17,37). Genotype 1 in our study corresponds to the "wild-type" genotype, as defined by the only allele observed in ***P. carinii*** from any other mammalian species (16,17). Genotype 2 is a point mutation that results in a threonine-to-alanine substitution at amino acid position 55. Genotype 3 is also a point mutation, resulting in a proline-to-serine substitution at amino acid position 57. Genotype 4 is a double mutant, which has alanine at position 55 and serine at position 57. This particular mutation has rarely been associated with failure of both TMP-SMZ treatment (38) and prophylaxis (17). The presence of polymorphism at two different positions, both associated with amino acid substitutions, at a gene locus that otherwise lacks variability, is itself indicative of pronounced selective pressure. Such a degree of selection is not itself an indication of resistance, but certainly suggests that resistance may be emerging. Mutations in this same region of the ***DHPS*** molecule have been correlated with specific antimicrobial resistance to sulfa drugs in a number of other microorganisms, including ***Plasmodium falciparum*** (39), ***Streptococcus pneumoniae*** (40), ***Streptococcus pyogenes*** (41), ***Escherichia coli*** (42), and ***Neisseria meningitidis*** (43).

The two single mutations are uncommon by themselves (5.9% for genotype 2 and 2.3% for genotype 1), yet 50% of all isolates have the double mutant, which suggests that, alone, neither mutation is highly selected, but together they pose a very strong selective advantage. If humans are dead-end hosts for ***P. carinii***, how can such a pronounced degree of polymorphism be explained? Person-to-person transmission may be essential to allow genetic selection to occur, resulting in this polymorphism.

Geographic variation in allelic frequency detected at the ***mtlsurRNA*** locus is not unexpected, even though other studies with smaller sample sizes failed to observe differences (11). Mitochondrial DNA sequence data have been highly useful in detecting intraspecific differences between populations of diverse organisms (44,45). Perhaps more unexpected, however, was the detection of geographic variation at the ***DHPS*** locus. Unlike ***mtlsurRNA***, because it encodes a gene product that is the target of the primary anti-***P. carinii*** drug TMP-SMZ, the ***DHPS*** locus is assumed to be subject to intense selection pressure. Consequently, this selection might be expected to override any potential variation from geographic separation or geographic patterns to reflect TMP-SMZ exposure patterns. The relative frequency of the double mutant genotype was much higher in samples from the West Coast, particularly San Francisco, than in samples from Atlanta (Figure 2). The reason for this difference is not obvious because in preliminary multivariate analysis conducted with samples from Atlanta and San Francisco, when the data are controlled for sulfa exposure, place of diagnosis is still the most significant factor influencing the frequency of the double mutant genotype (data not shown). Explanations for this observation are being evaluated.

An overall frequency of approximately 50% for the ***DHPS*** double mutant genotype is somewhat higher than that reported in other recent studies (46,47). The reason for this observation is also unclear. One possible explanation is that the samples were collected more recently (March 1995 to June 1998) and therefore reflect a sulfa-induced increase in

frequency of the double mutant. Most patients were from San Francisco and Atlanta, the two populations that showed the greatest difference in genotype frequency at the ***DHPS*** locus. Sample collection in Atlanta began in 1995, but in San Francisco the earliest samples were from 1997. When we stratified the patients in Atlanta by date, 1995-96 versus 1998-99, we saw no significant difference in the frequency of mutant genotypes. Similarly, when we stratified data for San Francisco by date, 1997 versus 1998-99, we saw no differences. Consequently the frequency of the mutation did not change during this study period, nor does the variation observed according to geography appear to be confounded by the dates when specimens were collected.

Conclusions

The pattern of allelic variation differed at each of the cities where samples were obtained, and this variation correlated with the place of diagnosis but not with the place of birth. Coinfection with multiple ***P. carinii*** genotypes was associated with primary rather than secondary PCP. The position 55/57 double mutant accounted for 50% of all genotypes of the ***DHPS*** locus examined. These observations suggest the following possibilities, which contradict much of the current opinion on the epidemiology and transmission of PCP: Most cases of PCP are not a result of infections acquired very early in life; infections are actively acquired from a relatively common source (humans or the environment); and humans, while not necessarily involved in direct infection of other humans, are nevertheless important in the transmission cycle of ***P. carinii*** f. sp. ***hominis***.

Acknowledgments

The authors thank Lori Ballard and Joan Turner for technical assistance; Dan Colley, Sue Binder, and Mary Bartlett for critically reading the manuscript; Steven Meshnick for designing the specific DNA oligonucleotide primers used for PCR amplification; and Brian Holloway and the staff at the NCID Biotechnology Core Facility for preparing the primers.

Informed consent was obtained from all patients. Human experimentation guidelines of the U.S. Department of Health and Human Services and those of participating institutions were followed in the conduct of this research.

References

1. Palella FJ, Delaney KM, Moorman AC, Loveless MO, Fuhrer J, Satten GA, et al. Declining morbidity and mortality among patients with advanced human immunodeficiency virus infection. N Engl J Med 1998;338:853-60.
2. Kaplan JE, Hanson KL, Jones JL, Beard CB, Juranek DD, Dykewicz CA, et al. Opportunistic infections (OIs) as emerging infectious diseases: challenges posed by OIs in the 1990s and beyond. In: Scheld WM, Craig WA, Hughes JM, editors. Emerging infections 2. Washington: American Society for Microbiology Press; 1998. p. 257-72.
3. Centers for Disease Control and Prevention. HIV/AIDS Surveillance Rep 1997;9:17.
4. Stringer JR. The identity of ***Pneumocystis carinii***: not a single protozoan, but a diverse group of exotic fungi. Infect Agents Dis 1993;2:109-17.
5. Cushion MT. Transmission and epidemiology. In: Walzer PD, editor. ***Pneumocystis carinii*** pneumonia. New York: Marcel Dekker, Inc.; 1994. p. 123-40.
6. Wakefield AE. Re-examination of epidemiological concepts. Bailliere's Clinical infectious diseases 1995;2:431-48.
7. Beard CB, Navin TR. Molecular epidemiology of ***Pneumocystis carinii*** pneumonia. Emerg Infect Dis 1996;2:147-50.
8. Baughman RP, Keely SP, Dohn MN, Stringer JR. The use of genetic markers to characterize transmission of ***Pneumocystis carinii***. AIDS Patient Care STDS 1997;11:131-8.
9. Fishman JA. Prevention of infection due to ***Pneumocystis carinii***. Antimicrob Agents Chemother 1998;42:995-1004.
10. Wakefield AE, Pixley FJ, Banerji S, Sinclair K, Miller RF, Moxon ER, et al. Detection of ***Pneumocystis carinii*** with DNA amplification. Lancet 1990;336:451-3.
11. Wakefield AE, Fritscher CC, Malin AS, Gwanzura L, Hughes WT, Miller RF. Genetic diversity in human-derived ***Pneumocystis carinii*** isolates from four geographical locations shown by analysis of mitochondrial rRNA gene sequences. J Clin Microbiol 1994;32:2959-61.
12. Tsolaki AG, Beckers P, Wakefield AE. Pre-AIDS era isolates of ***Pneumocystis carinii*** f. sp. ***hominis***: high genotypic similarity with contemporary isolates. J Clin Microbiol 1998;36:90-3.
13. Lee CH, Lu JJ, Bartlett MS, Durkin MM, Liu T-H, Wang J, et al. Nucleotide sequence variation in ***Pneumocystis carinii*** strains that infect humans. J Clin Microbiol 1993;31:754-7.
14. Lee CH, Helweg-Larsen J, Tang X, Jin S, Li B, Bartlett MS, et al. Update on ***Pneumocystis carinii*** f. sp. ***hominis*** typing based on nucleotide sequence variations in internal transcribed spacer regions of rRNA genes. J Clin Microbiol 1998;36:734-41.
15. Volpe F, Dyer M, Scaife JG, Darby G, Stammers DK, Delves CJ. The multifunctional folic acid synthesis ***fas*** gene of ***Pneumocystis carinii*** appears to encode dihydropteroate synthase and hydroxymethyldihydropterin pyrophosphokinase. Gene 1992;112:213-8.
16. Lane BR, Ast JC, Hossler PA, Mindell DP, Bartlett MS, Smith JW, et al. Dihydropteroate synthase polymorphisms in ***Pneumocystis carinii***. J Infect Dis 1997;175:482-5.

17. Kazanjian P, Locke AB, Hossler PA et al. ***Pneumocystis carinii*** mutations associated with sulfa and sulfone prophylaxis failures in AIDS patients. AIDS 1998;12:873-8.
18. Wisconsin Package, Version 9.1 1997. Madison, WI: Genetics Computer Group.
19. Edman JC, Sogin ML. Molecular genetics of ***Pneumocystis carinii***. In: Walzer PD, editor. ***Pneumocystis carinii*** pneumonia. New York: Marcel Dekker, Inc.; 1994. p. 91-105.
20. Cailliez JC, Seguy N, Denis CM, Aliouat EM, Mazars E, Polonelli L, et al. ***Pneumocystis carinii***: an atypical fungal micro-organism. Journal of Medical & Veterinary Mycology 1996;34:227-39.
21. Mazars E, Dei-Cas E. Epidemiological and taxonomic impact of ***Pneumocystis*** biodiversity. FEMS Immunol Med Microbiol 1998;22:75-80.
22. Keely SP, Stringer JR, Baughman RP, Linke MJ, Walzer PD, Smulian AG. Genetic variation among ***Pneumocystis carinii hominis*** isolates in recurrent pneumocystosis. J Infect Dis 1995;172:595-8.
23. Keely SP, Baughman RP, Smulian AG, Dohn MN, Stringer JR. Source of ***Pneumocystis carinii*** in recurrent episodes of pneumonia in AIDS patients. AIDS 1996;10:881-8.
24. Tsolaki AG, Miller RF, Underwood AP, Banerji S, Wakefield AE. Genetic diversity at the internal transcribed spacer regions of the rRNA operon among isolates of ***Pneumocystis carinii*** from AIDS patients with recurrent pneumonia. J Infect Dis 1996;174:141-56.
25. Simonds RJ, Oxtoby MJ, Caldwell MB, Gwinn ML, Rogers MR. ***Pneumocystis carinii*** pneumonia among US children with perinatally acquired HIV infection. JAMA 1993;270:470-3.
26. Hughes WT. Natural mode of acquisition for de novo infection with ***Pneumocystis carinii***. J Infect Dis 1982;145:842-8.
27. Hughes WT. Natural habitat and mode of transmission. In: ***Pneumocystis carinii*** pneumonitis. Vol I. Boca Raton (FL): CRC Press; 1987. p. 97-105.
28. Wakefield AE. Genetic heterogeneity in ***Pneumocystis carinii***: an introduction. FEMS Immunol Med Microbiol 1998;22:5-13.
29. Helweg-Larsen J, Tsolaki AG, Miller RF, Lundgren B, Wakefield AE. Clusters of ***Pneumocystis carinii*** pneumonia: analysis of person-to-person transmission by genotyping. Q J Med 1998:91:813-20.
30. Wakefield AE. DNA sequences identical to ***Pneumocystis carinii*** f. sp. ***carinii*** and ***Pneumocystis carinii*** f. sp. ***hominis*** in samples of air spora. J Clin Microbiol 1996;34:1754-9.
31. Bartlett MS, Vermund SH, Jacobs R, Durant PJ, Shaw MM, Smith JW, et al. Detection of ***Pneumocystis carinii*** DNA in air samples: likely environmental risk to susceptible persons. J Clin Microbiol 1997;35:2511-3.
32. Casanova-Cardiel L, Leibowitz MJ. Presence of ***Pneumocystis carinii*** DNA in pond water. J Euk Microbiol 1997;44:S28.
33. Olsson M, Lidman C, Latouche S, Bjorkman A, Roux P, Linder E, et al. Identification of ***Pneumocystis carinii*** f. sp. ***hominis*** gene sequences in filtered air in hospital environments. J Clin Microbiol 1998;36:1737-40.
34. Latouche S, Ortona E, Mazars E, Margutti P, Tamburrini E, Siracusano A, et al. Biodiversity of ***Pneumocystis carinii hominis***: typing with different DNA regions. J Clin Microbiol 1997;35:383-7.
35. Hauser PM, Blanc DS, Bille J, Francioli P. Typing methods to approach ***Pneumocystis carinii*** genetic heterogeneity. FEMS Immunol Med Microbiol 1998;22:27-35.
36. Vargas SL, Hughes WT, Wakefield AE, Oz HS. Limited persistence in and subsequent elimination of ***Pneumocystis carinii*** from the lungs after ***P. carinii*** pneumonia. J Infect Dis 1995;172:506-10.
37. Achari A, Somers DO, Champness JN, Bryant PK, Rosemond J, Stammers DK. Crystal structure of the anti-bacterial sulfonamide drug target dihydropteroate synthase. Nat Struct Biol 1997;4:490-7.
38. Mei Q, Gurunathan S, Masur H, Kovacs JA. Failure of co-trimoxazole in ***Pneumocystis carinii*** infection and mutations in dihydropteroate synthase gene. Lancet 1998;351:1631-2.
39. Brooks DR, Wang P, Read M, Watkins WM, Sims PF, Hyde JE, et al. Sequence variation of the hydroxymethyldihydropterin pyrophosphokinase: dihydropteroate synthase gene in lines of the human malaria parasite, ***Plasmodium falciparum***, with differing resistance to sulfa. Eur J Biochem 1994;224:397-405.
40. Lopez P, Espinosa M, Greenberg B, Lacks SA. Sulfonamide resistance in ***Streptococcus pneumoniae***: DNA sequence of the gene encoding dihydropteroate synthase and characterization of the enzyme. J Bacteriol 1987;169:4320-6.
41. Swedberg G, Ringertz S, Skold O. Sulfonamide resistance in ***Streptococcus pyogenes*** is associated with differences in the amino acid sequence of its chromosomal dihydropteroate synthase. Antimicrob Agents Chemother 1998;42:1062-7.
42. Vedantam G, Nichols BP. Characterization of a mutationally altered dihydropteroate synthase contributing to sulfathiazole resistance in ***Escherichia coli***. Microb Drug Res 1998;4:91-7.
43. Fermer C, Kristiansen BE, Skold O, Swedberg G. Sulfonamide resistance in ***Neisseria meningitidis*** as defined by site-directed mutagenesis could have its origin in other species. J Bacteriol 1995;177:4669-75.
44. Simon C, Frati F, Beckenbach A, Crespi B, Liu H, Flook P. Evolution, weighting, and phylogenetic utility of mitochondrial gene sequences and a compilation of conserved polymerase chain reaction primers. Ann Entomol Soc Am 1994;87:651-701.
45. Hartl DL, Clark AG. Principles of population genetics. Sunderland (MA): Sinauer Associates, Inc.;1997.
46. Helweg-Larsen J, Benfield TL, Eugen-Olsen J, Lundgren JD, Lundgren B. Effects of mutations in ***Pneumocystis carinii*** dihydropteroate synthase gene on outcome of AIDS-associated ***P. carinii*** pneumonia. Lancet 1999;354:1347-51.
47. Ma L, Borio L, Masur H, Kovacs JA. ***Pneumocystis carinii*** dihydropteroate synthase but not dihydrofolate reductase gene mutations correlate with prior trimethoprim-sulfamethoxazole or dapsone use. J Infect Dis 1999;180:1969-78.

Rhinosporidium seeberi: A Human Pathogen from a Novel Group of Aquatic Protistan Parasites

David N. Fredricks,*† Jennifer A. Jolley,* Paul W. Lepp,*
Jon C. Kosek,† and David A. Relman*†
*Stanford University, Stanford, California, USA; and †Veterans Affairs,
Palo Alto Health Care System, Palo Alto, California, USA

Rhinosporidium seeberi, a microorganism that can infect the mucosal surfaces of humans and animals, has been classified as a fungus on the basis of morphologic and histochemical characteristics. Using consensus polymerase chain reaction (PCR), we amplified a portion of the ***R. seeberi*** 18S rRNA gene directly from infected tissue. Analysis of the aligned sequence and inference of phylogenetic relationships showed that ***R. seeberi*** is a protist from a novel clade of parasites that infect fish and amphibians. Fluorescence in situ hybridization and ***R. seeberi***-specific PCR showed that this unique 18S rRNA sequence is also present in other tissues infected with ***R. seeberi***. Our data support the ***R. seeberi*** phylogeny recently suggested by another group. ***R. seeberi*** is not a classic fungus, but rather the first known human pathogen from the DRIPs clade, a novel clade of aquatic protistan parasites (Ichthyosporea).

Rhinosporidiosis manifests as slow-growing, tumorlike masses, usually of the nasal mucosa or ocular conjunctivae of humans and animals. Patients with nasal involvement often have unilateral nasal obstruction or bleeding due to polyp formation. The diagnosis is established by observing the characteristic appearance of the organism in tissue biopsies (Figure 1). Treatment consists of surgical excision, but relapse occurs in approximately 10% of patients (1); antimicrobial therapy is not effective (2). Rhinosporidiosis occurs in the Americas, Europe, Africa, and Asia but is most common in the tropics, with the highest prevalence in southern India and Sri Lanka. A survey of schoolchildren from Pallam, India, found 11 cases in 781 children examined (prevalence 1.4%) (3). Autochthonous cases have been reported from the southeastern United States (4). Studies have linked infection to swimming or bathing in freshwater ponds, lakes, or rivers (2,5).

The etiologic agent of rhinosporidiosis, ***Rhinosporidium seeberi***, is an enigmatic microbe that has been difficult to classify. Recently, ***R. seeberi*** has been considered a fungus, but it was originally thought to be a protozoan parasite (2). Its morphologic characteristics resemble those of ***Coccidioides immitis***: both organisms have mature stages that consist of large, thick-walled,

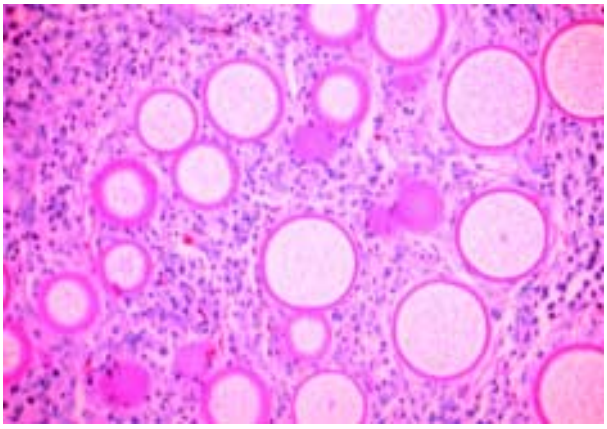

Figure 1. Histology of rhinosporidiosis. A formaldehyde-fixed section of human nasal polyp was stained with periodic acid-Schiff (PAS) and visualized by bright-field microscopy at 400X magnification. The thick walls of immature ***R. seeberi*** trophocytes stain with PAS (pink), and the spherical organisms are surrounded by inflammatory cells.

Address for correspondence: David N. Fredricks, Veterans Affairs, Palo Alto Health Care System, 154-T, 3801 Miranda Ave, Palo Alto, CA 94304, USA; fax: 650-852-3291; e-mail: fredrick@cmgm.stanford.edu.

spherical structures containing smaller daughter cells (endospores). In addition, ***R. seeberi*** is visualized with fungal stains such as methenamine silver and periodic acid-Schiff, as well as mucicarmine, which stains the fungus ***Cryptococcus neoformans***. ***R. seeberi*** has not been detected in the environment, and its natural host or reservoir is unknown. Attempts to propagate this organism on artificial media have failed, as has continuous cocultivation with human cell lines (6).

We report a molecular approach for establishing the phylogenetic relationships of ***R. seeberi*** to other eukaryotes. This approach is based on amplification of the small subunit rRNA gene sequence from infected tissue, as in the method used to identify the culture-resistant bacillus of Whipple disease (7). The sequence of the small subunit rRNA gene has proven to be a useful gauge of evolutionary relationships for many organisms from diverse taxonomic groups (8).

Materials and Methods

Specimens

We obtained a sample of frozen, minced, infected canine nasal polyp in tissue culture media that had been used for the limited propagation of ***R. seeberi*** in cell culture (6). After thawing and a 1-minute centrifugation at 500 x g, approximately 0.2 g of the tissue pellet was digested by mechanical disruption and the DNA was purified by adsorption to glass milk in the presence of a chaotropic agent, according to the manufacturer's instructions (Fast Prep, Bio 101, Vista, CA). The DNA was resuspended in 100 µL of 10 mM Tris, 1 mM EDTA buffer at pH 8.5.

Three blocks of fixed, paraffin-embedded nasal polyps from unrelated patients with histologically confirmed rhinosporidiosis were obtained. One tissue sample came from a patient born in southern Asia but living in the United States, and two samples came from patients living in Spain. Twenty-three blocks of fixed, paraffin-embedded nasal polyps from patients without rhinosporidiosis were obtained from 12 consecutive patients at the Palo Alto Veterans Affairs (VA) hospital who had undergone nasal polypectomy. Two 25-µm sections were cut from each block, and the sections were deparaffinized and digested (5). DNA from the digests was then purified by the Isoquick method (ORCA Research, Inc., Bothell, WA), and the DNA was resuspended in 25 µL of Tris/EDTA buffer. Sections from a block of fixed, paraffin-embedded human lymph node (histologically normal) were also used in some experiments as negative controls. Tissue sections of ***C. immitis*** in bone were obtained from a patient with disseminated coccidioidomycosis at the Palo Alto VA hospital and used for fluorescence in situ hybridization (FISH). Samples of Rosette agent and ***Dermocystidium salmonis*** DNA were obtained from the Bodega Marine Laboratory of the University of California, Davis.

Fungal specimens in culture were obtained from laboratories at Stanford University and the Palo Alto VA Health Care System. A cotton swab was used to transfer fungal cells from agar into a 1.5-mL microfuge tube containing 0.5 mL digestion buffer (9) and 0.1 mL glass beads. Samples were incubated at 55°C overnight, and the proteinase k was inactivated at 95°C for 10 minutes and then subjected to two freeze-thaw cycles by immersing tubes in a dry ice-isopropranol bath followed by vortex mixing.

Consensus Polymerase Chain Reaction (PCR) of the 18S rRNA Gene

Broad-range fungal PCR primers were designed from a database of >4,000 small subunit rDNA sequences, with the ARB software package (Technical University, Munich, Germany). Primers were selected that would anneal to most fungal and some protist 18S rDNA but not to 18S rDNA from the chordata (F1-fw, F2-rev, F3-rev) (Table). When the specificity of the primer pairs was tested by using human lymphocyte DNA, no amplification was observed (data not shown). The broad range of primers F1-fw/F2-rev was tested by using DNA from several diverse fungi. Amplification products of the expected size were produced by using DNA from ***Aspergillus oryzae***, ***Alternaria alternata***, ***Candida albicans***, ***Saccharomyces cerevisiae***, ***Trichyphyton rubrum***, ***Panus rudis***, ***Neurospora crassa***, ***Fusarium solani***, ***Beauveria bassiana***, ***Flammulina velutipes***, ***Gibberella zeae***, and ***Pleurotus ostreatus*** (data not shown).

PCR consisted of 40 cycles of amplification on a Perkin-Elmer GeneAmp 2400 thermal cycler. After an initial activation of ***Taq*** gold at 94°C for 10 minutes, each cycle consisted of 30 seconds of melting at 94°C, 30 seconds of annealing at 56°C, and 30 seconds of extension at 72°C. The last cycle was followed by an extension step at 72°C for 7 minutes. Amplification products were

Table. Polymerase chain reaction primers, sequencing primers, and fluorescence in situ hybridization probes

Primer/Probe	Nucleotide sequence (5'->3')	SSU rRNA Position[a]
F1-fw[b]	CAAGTCTGGTGCCAGCAGCC	554-573
F2-rev[c]	GATTTCTCGTAAGGTGCCGA	1068-1087
F3-rev	AATGCTCTATCCCCAMCACG	1531-1550
Dermo-fw	CTGCCAGTAGTCATATGCTTG	
Dermo-rev	GATCAAGTTTGATCAACTTTTCGGCA	
Rhino-fw	GGCGTGTGCGCTTAACTGTC	
Rhino-rev	TGCTGATAGAGTCATTGAAT	
Rhino FISH probe	BTGCTGATAGAGTCATTGAATTAACATCTACB	
Control FISH probe	BACGACTATCTCAGTAACTTAATTGTAGATGB	

[a]SSU rRNA position based on ***S. cerevisiae*** 18S rRNA (GenBank J01353).
[b]fw = forward primer.
[c]rev = reverse primer.

detected by electrophoresis on 2% agarose gels stained with ethidium bromide and visualized with a UV transilluminator.

On the basis of the sequences obtained by consensus PCR with primers F1-fw/F2-rev (~500 bp) and F1-fw/F3-rev (~1000 bp), primers Dermo-fw and Dermo-rev were designed (Table) and used in a PCR to amplify a more complete 18S rDNA sequence of ***R. seeberi***.

Rhinosporidium-Specific PCR

A pair of PCR primers was designed from unique regions of the ***R. seeberi*** 18S rRNA gene sequence (Rhino-fw and Rhino-rev) (Table). These primers were used in a 50-µL PCR as described, except that Ampli***Taq*** DNA polymerase (PE-ABI) was used at 1 unit per reaction, no dimethyl sulfoxide was added, 50 cycles of PCR were run with a 3-minute pre-melt at 94°C, and the annealing temperature was 55°C. To each 50-µL PCR reaction, 1 µL or 5 µL of purified DNA were added.

ß-Globin PCR

ß-globin PCR was performed on control tissues as described previously (9).

DNA Cloning, Sequencing, and Phylogenetic Analysis

Amplification products were cloned by using the Topo-TA cloning kit (Invitrogen, Carlsbad, CA), and three clones were sequenced. Each clone consisted of 1,750 bp of 18S rDNA. Priming sequences were removed for further analysis, yielding 1,699 bp of meaningful sequence. DNA sequencing was performed as described (10). A consensus sequence from the three clones was made to correct for any ***Taq*** polymerase incorporation errors. The 18S rDNA primers (Table) were used as sequencing primers.

The ***R. seeberi*** 18S rDNA sequence was aligned by using the automated aligner of the ARB software package. Ambiguously and incorrectly aligned positions were manually aligned on the basis of the conserved primary sequence and secondary structure. The phylogenetic relationship of ***R. seeberi*** to other eukaryotes was inferred from 1,350 unambiguously aligned (masked) positions with a maximum-likelihood algorithm (11,12), on the basis of a previously aligned dataset of the DRIPs clade (named after the organisms ***Dermocystidium***, the Rosette agent, ***Ichthyophonus***, and ***Psorospermium***) (13). The dataset was used to empirically determine nucleotide frequencies and instantaneous substitution rates with the restriction of a 2:1 transition to transversion ratio. The organisms used in our tree and the accession numbers for their small subunit rRNA sequences include ***Artemia salina*** (X01723), ***Xenopus laevis*** (X04025), ***Mytilus edulis*** (L24489), ***Tripedalia cystophora*** (L10829), ***Microciona prolifera*** (L10825), ***Diaphanoeca grandis*** (L10824), Rosette agent (L29455), ***R. seeberi*** (AF158369), Dermocystidium species (U21336), ***Dermocystidium salmonis*** (U21337), ***Psorospermium haeckelii*** (U33180), ***Ichthyophonus hoferi*** (D14358), ***Aspergillus fumagatus*** (M60300), ***Chytridium confervae*** (M59758), ***Mucor racemosus*** (X54863), ***Acanthamoeba castellanii*** (U07413), ***Zamia pumila*** (M20017), ***Porphyra spiralis*** (L26177), ***Lagenidium giganteum*** (X54266), ***Labyrinthuloides minuta*** (L27634), ***Perkinsus marinus*** (X75762), ***Sarcocystis muris*** (M64244). The tree

topology was confirmed by using a neighbor-joining algorithm with Jukes-Cantor corrected distance values and a maximum-parsimony algorithm (ARB). The nucleotide sequence for the partial 18S rRNA gene of ***R. seeberi*** has been deposited in GenBank (accession number AF158369).

Fluorescence in Situ Hybridization (FISH)

Tissue sections on slides were dewaxed by immersion in 99% octane (Sigma, St. Louis, MO). Samples subjected to FISH included ***R. seeberi***–infected human nasal polyps, ***C. immitis***–infected bone, a Rosette agent–infected cell line, and smears of ***C. albicans***. The ***Rhinosporidium*** probe was based on the Rhino-rev 18S rDNA primer and was biotinylated at both the 5' and 3' ends (Table). The control probe, which consisted of the complement of the ***Rhinosporidium*** probe, was also biotinylated at both ends. To each slide, 50 ng of biotinylated probe in 30 µL of hybridization buffer was added. Cover slips were placed, and the slides were incubated at 40°C overnight in a humid chamber. The hybridization buffer consisted of 10% dextran, 0.2% bovine serum albumin, and 0.01% polyadenosine, in 5X SET buffer; the 25X SET buffer consisted of 3.75M sodium chloride, 25 mM EDTA, and 0.5M Tris at pH 7.8. Cover slips were removed by immersion in 5X SET buffer at 4°C, and the slides were washed for 10 minutes per cycle, twice in 0.2X SET buffer at 25°C and once at 40°C. The slides were then subjected to tyramide signal amplification according to the manufacturer's instructions (TSA indirect, NEN Life Sciences, Boston, MA). Cy5-streptavidin (Amersham, Piscataway, NJ) at 1 mg/mL was diluted 1:500 and added to the slides for fluorescence signal detection. Tissue sections were visualized on a Bio-Rad confocal microscope at 200X magnification after the application of 15-20 µL of Vectashield mountant (Sigma) and a cover slip.

Electron Microscopy

A portion of formalin-fixed, paraffin-embedded nasal polyp from a patient with rhinosporidiosis was removed from the block, dewaxed with xylene, rehydrated with ethanol, post-stained with 1.5% osmium tetroxide, then dehydrated with ethanol, transferred to propylene oxide followed by Epon 12 resin, heat-catalyzed at 65°C, and ultrasectioned at 50 nm. The grid-mounted sections were then serially stained with lead hydroxide and uranyl acetate and examined with a Phillips 201 electron microscope at 75KV.

Results

Phylogenetic Classification of *R. seeberi* Inferred from the 18S rRNA Gene

Consensus PCR of the 18S rRNA gene with DNA from a digest of an ***R. seeberi***–infected canine nasal polyp produced amplification products of the expected size visible on gel electrophoresis (primer pairs F1-fw/F2-rev = ~500 bp and F1-fw/F3-rev = ~1000 bp) (data not shown). No amplification product was detected by using control tissue and reagents. On the basis of the initial phylogenetic assessment of these sequences, primers Dermo-fw and Dermo-rev were designed for amplification of a more complete portion of the ***R. seeberi*** 18S rRNA gene. Our phylogenetic analysis of this gene suggests that ***R. seeberi*** is a member of the DRIPs clade of aquatic protistan parasites (Figure 2). The nearest evolutionary neighbors of ***R. seeberi*** for which a sequence is available are members of the ***Dermocystidium*** genus, which infect salmon and trout.

Development and Use of a Rhinosporidium-Specific PCR Assay

A PCR assay specific for ***R. seeberi*** was developed. Primers were created by aligning 18S rDNA sequences from ***R. seeberi,*** members of the DRIPs clade, ***Saccharomyces cerevisiae***, and humans. The ***Rhinosporidium*** primers (Rhino-fw, Rhino-rev) each have three nucleotide mismatches with the sequences from the nearest phylogenetic relatives in the ***Dermocystidium*** genus and multiple other mismatches with fungal and human 18S rDNA sequences. An assay sensitivity of 1-10 gene copies was demonstrated by using a dilution series of cloned ***R. seeberi*** 18S rDNA. The specificity of the assay was assessed with DNA from human lymphocytes, ***S. cerevisiae***, ***D. salmonis***, and the Rosette agent. No amplification was detected when these DNA samples were used in the specific PCR assay, although product was amplified from these samples with either ß-globin primers (lymphocytes) or broad-range 18S rDNA primers (F1-fw/F2-rev) (Table).

The original DNA sample from the infected canine nasal polyp yielded a visible product of the expected size with the ***Rhinosporidium***-specific

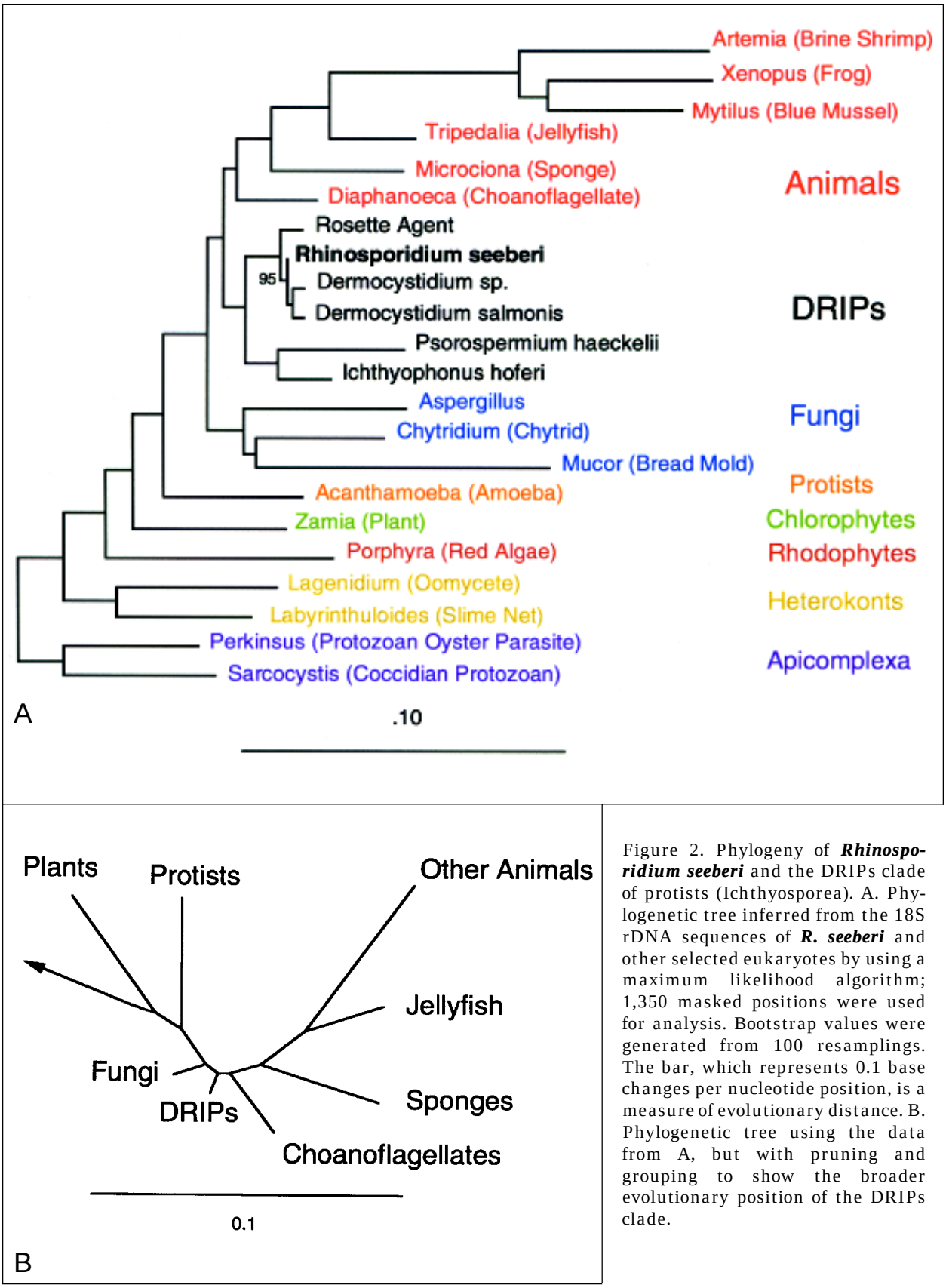

Figure 2. Phylogeny of ***Rhinosporidium seeberi*** and the DRIPs clade of protists (Ichthyosporea). A. Phylogenetic tree inferred from the 18S rDNA sequences of ***R. seeberi*** and other selected eukaryotes by using a maximum likelihood algorithm; 1,350 masked positions were used for analysis. Bootstrap values were generated from 100 resamplings. The bar, which represents 0.1 base changes per nucleotide position, is a measure of evolutionary distance. B. Phylogenetic tree using the data from A, but with pruning and grouping to show the broader evolutionary position of the DRIPs clade.

PCR assay (Figure 3). Purified DNA from the tissue blocks of human nasal polyps resected from three patients with rhinosporidiosis also yielded positive results in this PCR assay, with visible bands seen on gel electrophoresis (RS 1-3) (Figure 3). Direct sequencing of these PCR products demonstrated complete identity over the 377 bp with the cloned sequence from the canine polyp. DNA samples from 23 nasal polyp specimens resected from 12 patients without rhinosporidiosis were subjected to both ***Rhinosporidium***-specific and ß-globin PCR assays. These uninfected polyps failed to yield visible amplicons after gel electrophoresis of the ***Rhinosporidium***-specific PCR reactions (data not shown). However, all these samples yielded amplification products after ß-globin PCR, demonstrating that amplifiable DNA was present, without substantial PCR inhibition. These results confirmed that the presence of the putative ***R. seeberi*** 18S rDNA sequence correlated with the presence of disease (rhinosporidiosis).

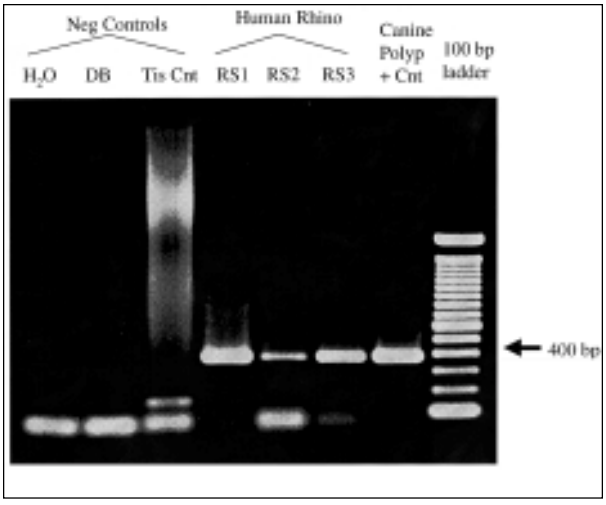

Figure 3. Agarose gel electrophoresis of ***Rhinosporidium***-specific PCR products. The specific amplification product is 377 bp. No amplification product is seen in the negative control samples consisting of water (reagent-only control), digestion buffer (DB), or lymph node tissue control (Tis Cnt). The human rhinosporidiosis samples (RS1-3) and the original canine nasal polyp show visible amplification products.

Fluorescence in Situ Hybridization

We sought to determine by using FISH if the ***R. seeberi*** 18S rDNA sequence was linked to visible pathology in tissue. The ***Rhinosporidium*** 18S rRNA probe but not the control probe bound to ***R. seeberi*** organisms in tissue, providing further evidence that the putative ***R. seeberi*** 18S rRNA sequence is present in ***R. seeberi*** organisms (Figure 4). To test the specificity of the hybridization, smears of the fungus ***C. albicans***, cells infected with the Rosette agent, and tissue sections of ***C. immitis*** were subjected to FISH. No specific hybridization to these organisms was detected by using the ***Rhinosporidium*** 18S rRNA probe compared with the control probe (data not shown).

Electron Microscopy

Transmission electron micrographs were taken of ***R. seeberi*** trophocytes in a human nasal polyp. Multiple mitochondria were visualized, showing that the cristae had tubulovesicular morphology (Figure 5), unlike the flat cristae found in fungi.

Discussion

In the 1890s, first Malbran and then Seeber (14) described an apparent sporozoan parasite in nasal polyps from patients living in Argentina. Seeber's teacher, Wernicke, named the organism ***Coccidium seeberia*** after the protozoal subdivision Coccidia and his pupil, Guillermo Seeber (2). In 1923, Ashworth described the life cycle of the organism, argued that it is a fungus, and proposed the name ***R. seeberi*** (15). Since then, the microbe has been considered a fungus by most microbiologists, although its taxonomy has been debated (1,2,16). Using a consensus PCR approach, we amplified a unique 18S rDNA sequence from a canine nasal polyp infected with ***R. seeberi***. To prove that this unique 18S rDNA sequence came from ***R. seeberi***, we sought to fulfill sequence-based guidelines for microbial disease causation, since Koch's postulates cannot be fulfilled for uncultivated microbes (17). Using a ***Rhinosporidium***-specific PCR assay, we showed that the unique rDNA sequence present in the canine polyp was also present in three human polyp samples from patients with rhinosporidiosis. We showed the

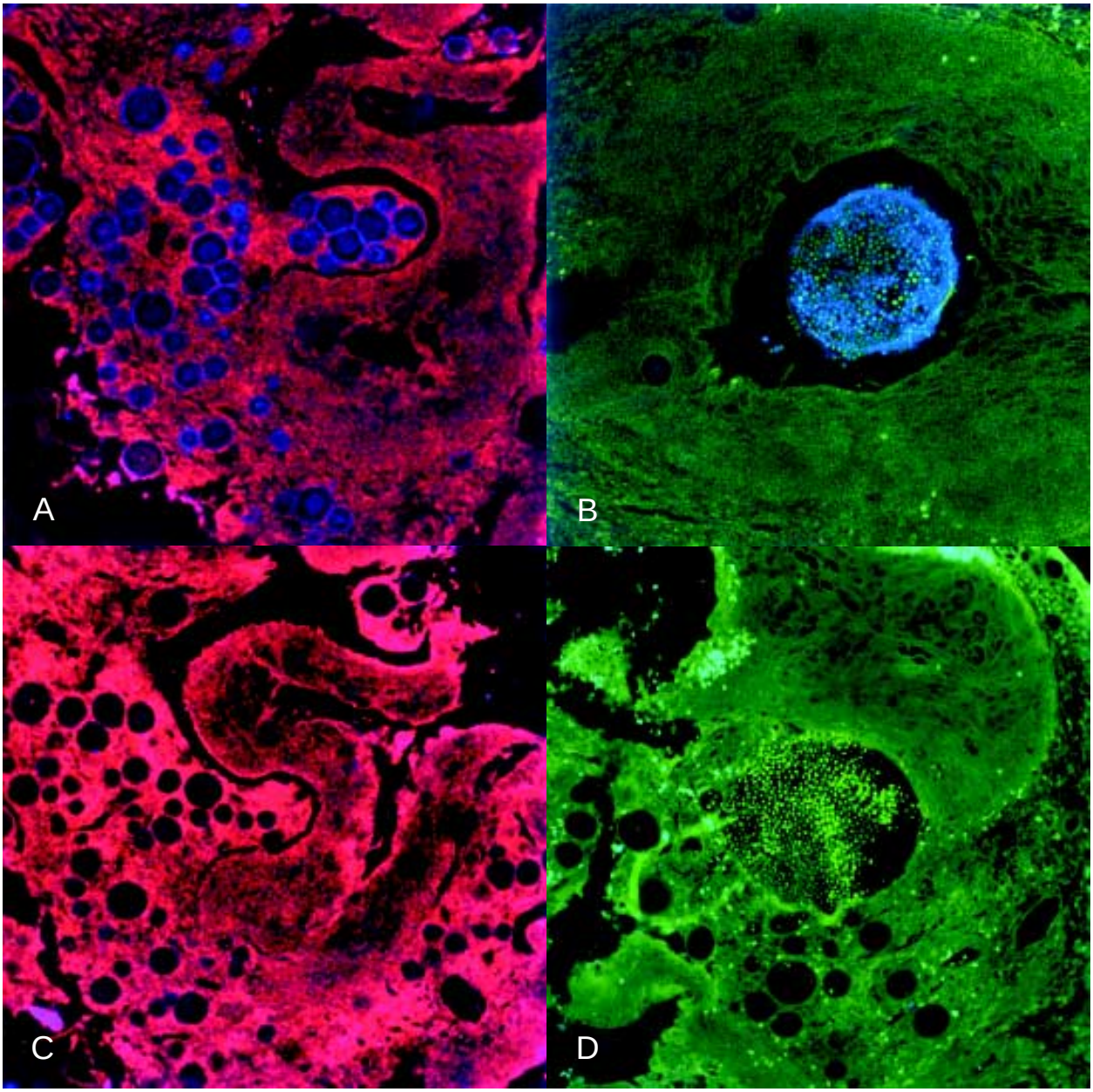

Figure 4. An oligonucleotide probe complementary to a unique region of the ***Rhinosporidium seeberi*** 18S rRNA sequence localizes to visible organisms in human nasal tissue by using fluorescence in situ hybridization. Confocal micrographs at 200X magnification. The Cy-5-labeled ***Rhinosporidium*** probe (blue) hybridizes to spherical ***R. seeberi*** trophocytes (A) and a sporangium with endospores (B). A control probe consisting of the complement of the ***Rhinosporidium*** probe labeled with Cy-5 does not hybridize to the trophocytes (C) or a sporangium with endospores (D). Images were collected in two wave-length channels: the first for Texas Red (red) or FITC (green) displays tissue architecture through autofluorescence, and the second channel for Cy-5 (blue pseudocolor) displays the probe signal.

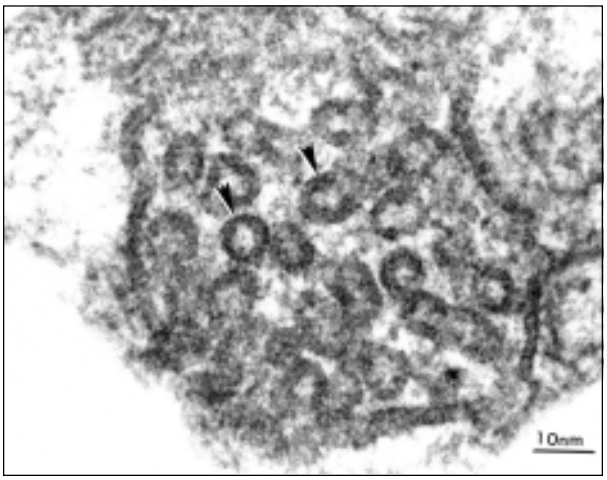

Figure 5. Transmission electron micrograph of a mitochondrion from ***Rhinosporidium seeberi.*** The cristae of this mitochondrion (arrows) have tubulovesicular morphology. Magnification 195,000X.

specificity of this association by demonstrating that this rDNA sequence was not present in control nasal polyps from 12 patients without rhinosporidiosis. We also used FISH to link the putative ***R. seeberi*** 18S rRNA sequence to organisms visible in tissue. Although the ***Rhinosporidium*** probe localized to ***R. seeberi*** organisms in tissue using FISH, the probe did not localize to two fungal organisms or another member of the DRIPs clade (Rosette agent), suggesting some specificity to the hybridization.

Sequence-based data also provide support for a causal relationship when a microbial genotype (e.g., phylogenetic placement) correctly predicts microbial phenotype and host response (17). In other words, the nature of the pathogen inferred from phylogenetic analysis of its nucleic acid sequence should be consistent with the known biologic characteristics of closely related microbes and with the nature of the disease. Therefore, the nearest phylogenetic neighbors to ***R. seeberi*** could be predicted to have similarities in morphology, tissue histology, and pathogenesis. ***D. salmonis***, the closest known relative to ***R. seeberi***, has a large spherical structure containing endospore-like daughter cells (18). Histology of infected hosts shows gill inflammation and epithelial hyperplasia. The resemblance between ***R. seeberi*** and fish pathogens has been noted before. In 1960, Satyanarayana wrote in his review of 255 cases of rhinosporidiosis (1) that since ***R. seeberi*** has a morphology similar to those of some fish parasites, it "..may also be a parasite or saprophyte of fish and that man, equines, and cattle obtain the infection through water in which fish harbouring the parasite live."

A recent independent report based on amplification of 18S rDNA from two human rhinosporidiosis tissue samples also concludes that ***R. seeberi*** is a member of the DRIPs clade of microbes (19). Our data support this conclusion and provide more evidence for a causal relationship. In addition, we describe a ***Rhinosporidium-***specific PCR assay that can be used for detecting this organism in clinical and environmental samples. Our 18S rDNA sequence differs from the sequence determined by these investigators (GenBank AF118851) at a single position out of 1,699 common bases. We excluded from analysis sequence derived from our PCR primers, as amplicons will contain the primer sequences regardless of the target sequence as long as there is partial annealing during PCR, leading to potentially spurious conclusions about sequence in these regions. The 18S rDNA sequence of ***R. seeberi*** determined by this group includes the primer sequences.

Although we describe early trophocytes with mitochondrial cristae having vesicular ultrastructure, other investigators have found sporangia with mitochondrial cristae having a flat ultrastructure (19). The different mitochondrial morphologies observed may be due to differences in developmental stage of the organism or in methods of tissue preparation for electron microscopy. Nevertheless, another member of the DRIPs clade, ***Ichthyophonus hoferi***, has vesicular mitochondrial cristae. Classic fungi (Eumycota) have flat mitochondrial cristae.

Knowledge of the molecular phylogeny of ***R. seeberi*** is more than an exercise in taxonomy. For organisms such as ***R. seeberi***, which are difficult to grow in the laboratory, phylogenetic analysis provides some insight into the characteristics of the organism that can be used to further our understanding of disease pathogenesis and epidemiology, as well as to improve diagnosis and treatment. Knowing that ***R. seeberi*** is a member of the DRIPs clade of microbes allows hypotheses to be generated about how it causes human disease by analogy, drawing on the knowledge and experience of the veterinary sciences. The separate but linked observations that rhinosporidiosis in humans is associated with exposure to water and that ***R. seeberi***

belongs to a clade of aquatic parasites lead to a testable hypothesis: the natural hosts of ***R. seeberi*** are fish or other aquatic animals, and humans acquire infection when they come into contact with water containing these fish and their parasites. Investigators should therefore look for evidence of infection in fish in ponds and rivers in disease-endemic areas. From a public health perspective, the ***R. seeberi***–specific PCR assay can be used to study environmental sources of infection (e.g., specific bodies of water) and may provide a means of preventing disease through identification of infected water.

Conversely, knowing that ***R. seeberi*** is a member of the DRIPs clade may help us understand this important, distinct group of microbes that appear to form the deepest branch in the animal lineage. ***R. seeberi*** is a member of a newly recognized group of human and animal pathogens; the name Ichthyosporea has been proposed for this expanding taxon of microbes (20). Little information is available about these organisms and how they cause disease. We hope that collaborations between researchers in human and animal medicine will correct this deficiency.

Multiple antimicrobials, including antifungal agents, have been used in the treatment of rhinosporidiosis, based on the belief that ***R. seeberi*** is a fungus. However, no antimicrobial agent is clearly effective. The medical treatment of rhinosporidiosis may be improved through screening antiparasitic drugs for an effect on disease in ***Dermocystidium***-infected fish or infected cell lines.

In conclusion, phylogenetic analysis of the ***R. seeberi*** 18S rRNA gene suggests that this culture-resistant organism is not a member of the Eumycota, but rather is the first known human pathogen from a novel clade of aquatic protistan parasites that form a branch in the evolutionary tree near the animal-fungal divergence. ***R. seeberi***-specific PCR and FISH confirm the association of this unique 18S rDNA sequence with the presence of rhinosporidiosis. This knowledge can be used to further our understanding of the natural reservoir of this organism and the risk factors, pathogenesis, and treatment of this disease. This discovery also expands our appreciation of the diversity among eukaryotic organisms that are pathogenic to humans and highlights the limitations of basing phylogenetic classification on morphology alone.

Acknowledgments

We thank Josh Fierer and Jesus Gonzales for providing human ***Rhinosporidium*** tissue blocks, Mike Levy for the canine nasal polyp used for consensus PCR, Kristin Arkush for the ***Dermocystidium salmonis*** and Rosette agent DNA, and Robin Gutell for the mask used for phylogenetic analysis of the DRIPs clade. Bob Metzenberg, Sara Fulz, Larry Mirels, and the staff of the clinical microbiology laboratories at Stanford and the Palo Alto VA hospitals supplied fungal isolates for testing broad-range 18S rDNA primers.

This study was supported by grants from the National Institutes of Health (K11-AI01360 D.N.F.) and the Donald B. and Delia B. Baxter Foundation (D.A.R).

Dr. Fredricks is a research associate in the Division of Infectious Diseases, Stanford University. He studies the use of nucleic acid sequences to detect and identify microbial pathogens, including those that are novel or uncultivated.

References

1. Satyanarayana C. Rhinosporidiosis with a record of 255 cases. Acta Oto-Laryng 1960;51:348-66.
2. Kwon-Chung KJ, Bennett JE. Rhinosporidiosis. In: Medical mycology. Philadelphia: Lea & Febiger; 1992. p. 695-706.
3. Moses JS, Shanmugham A. Epidemiological survey of rhinosporidiosis in man—a sample survey in a high school located in a hyperendemic area. Indian Vet J 1987;64:34-8.
4. Gaines JJ, Clay JR, Chandler FW, Powell ME, Sheffield PA, Keller A. Rhinosporidiosis: three domestic cases. South Med J 1996;89:65-7.
5. Kennedy FA, Buggage RR, Ajello L. Rhinosporidiosis: a description of an unprecedented outbreak in captive swans (Cygnus spp.) and a proposal for revision of the ontogenic nomenclature of ***Rhinosporidium seeberi***. J Med Vet Mycol 1995;33:157-65.
6. Levy MG, Meuten DJ, Breitschwerdt EB. Cultivation of ***Rhinosporidium seeberi*** in vitro: interaction with epithelial cells. Science 1986;234:474-6.
7. Relman DA, Schmidt TM, MacDermott RP, Falkow S. Identification of the uncultured bacillus of Whipple's disease. N Engl J Med 1992; 327:293-301.
8. Pace NR. A molecular view of microbial diversity in the biosphere. Science 1997;276:734-40.
9. Fredricks DN, Relman DA. Paraffin removal from tissue sections for digestion and PCR analysis. Biotechniques 1999;26:198-200.
10. Fredricks DN, Relman DA. Improved amplification of microbial DNA from blood cultures by removal of the PCR inhibitor sodium polyanetholesulfonate. J Clin Microbiol 1998;36:2810-6.
11. Olsen GJ, Matsuda H, Hagstrom R, Overbeek R. fastDNAmL: a tool for construction of phylogenetic trees of DNA sequences using maximum likelihood. Comput Appl Biosci 1994;10:41-8.
12. Felsenstein J. Evolutionary trees from DNA sequences: a maximum likelihood approach. J Mol Evol 1981;17:368-76.

13. Ragan MA, Goggin CL, Cawthorn RJ, Cerenius L, Jamieson AV, Plourde SM, et al. A novel clade of protistan parasites near the animal-fungal divergence. Proc Natl Acad Sci U S A 1996;93:11907-12.
14. Seeber G. Un nuevo esporozuario parasito del hombre: dos casos encontrados en polipos nasales. Thesis, Universidad Nacional de Buenos Aires, 1900.
15. Ashworth JH. On ***Rhinosporidium seeberi*** with special reference to its sporulation and affinities. Trans R Soc Edinburgh 1923;53:302-42.
16. Kwon-Chung KJ. Phylogenetic spectrum of fungi that are pathogenic to humans. Clin Infect Dis 1994;19 Suppl 1:S1-7.
17. Fredricks DN, Relman DA. Sequence-based identification of microbial pathogens: a reconsideration of Koch's postulates. Clin Microbiol Rev 1996;9:18-33.
18. Olson RE, Dungan CF, Holt RA. Water-borne transmission of ***Dermocystidium salmonis*** in the laboratory. Dis Aquat Org 1991;12:41-8.
19. Herr RA, Ajello L, Taylor JW, Arseculeratne SN, Mendoza L. Phylogenetic analysis of ***Rhinosporidium seeberi***'s 18S small-subunit ribosomal DNA groups this pathogen among members of the protoctistan Mesomycetozoa clade. J Clin Microbiol 1999;37:2750-4.
20. Cavalier-Smith T. Neomonada and the origin of animals and fungi. In: Coombs G, Vickerman K, Sleigh M, Warren A, editors. Evolutionary relationships among protozoa. London: Chapman and Hall; 1998. p. 375-407.

High Prevalence of Penicillin-Nonsusceptible *Streptococcus pneumoniae* at a Community Hospital in Oklahoma

Ronald L. Moolenaar,*‡ Ronda Pasley-Shaw,† John R. Harkess,† Anthony Lee,‡ and James M. Crutcher‡

*Centers for Disease Control and Prevention, Atlanta, Georgia, USA; †Mercy Health Center, Oklahoma City, Oklahoma, USA; and ‡Oklahoma State Department of Health, Oklahoma City, Oklahoma, USA

During 1997, Oklahoma City's Hospital A reported penicillin-nonsusceptible ***Streptococcus pneumoniae*** in almost 67% of isolates. To confirm this finding, all Hospital A ***S. pneumoniae*** isolates from October 23, 1997, through February 19, 1998, were tested for antibiotic susceptibility and repeat-tested at two other hospital laboratories. Medical records of Hospital A patients with invasive ***S. pneumoniae*** infections during 1994 through 1997 were also reviewed. These data were compared with 1998 statewide sentinel hospital surveillance data for invasive ***S. pneumoniae***. Of 48 ***S. pneumoniae*** isolates from Hospital A during October 23, 1997, through February 19, 1998, 31 (65%) were penicillin-nonsusceptible ***S. pneumoniae,*** and 23 (48%) were highly penicillin resistant. Similar prevalences were confirmed at the other hospital laboratories; however, significant interlaboratory differences were noted in the determination of third-generation cephalosporin susceptibility. During 1994 through 1997, a trend toward increasing penicillin nonsusceptibility ($p < 0.05$) was noted among ***S. pneumoniae*** isolates from nursing home patients. During 1998, 85 (30%) of 282 invasive isolates reported to the state surveillance system were penicillin-nonsusceptible ***S. pneumoniae***; 33 (12%) were highly resistant. The increase in resistance observed is notable; the interlaboratory discrepancies are unexplained. To respond, a vaccination program was implemented at Hospital A, and vaccination efforts were initiated at nursing homes.

Streptococcus pneumoniae is a major cause of bacterial pneumonia and meningitis in the United States. The spread of penicillin-nonsusceptible ***S. pneumoniae*** (PNSP) has been well documented (1-8). Within a large city, resistance patterns can vary by region (5,8). Oklahoma City has historically had a relatively high but stable prevalence of PNSP among invasive isolates; penicillin nonsusceptibility was reported in 12.2% of invasive isolates during 1984 (9). From July 1989 through June 1990, 7.6% of invasive isolates from central Oklahoma were penicillin nonsusceptible, but high penicillin resistance (1.4%) was beginning to emerge (10). In late 1997, higher than expected levels of PNSP were reported in northwest Oklahoma City at Hospital A, a 392-bed community hospital, primarily providing adult care. The hospital's inpatient census and the proportion of patients receiving Medicare had not increased since 1994; however, the microbiology laboratory had recently begun using the antimicrobial gradient strip method for measuring antibiotic susceptibility to penicillin and cephalosporins. Nonsusceptibility to penicillin among pneumococcal isolates exceeded 60%; approximately half were highly penicillin resistant. We initiated an investigation to determine whether the reported prevalence was accurate and if so, to explain it, determine a

Address for correspondence: Ronald L. Moolenaar, Centers for Disease Control and Prevention, Mailstop D18, 1600 Clifton Rd., Atlanta, GA 30333, USA; fax: 404-639-4504; e-mail: rlm8@cdc.gov.

possible trend, and compare the prevalence with that of local hospitals. Findings were used to guide local treatment and prevention measures.

The Study

Prospective Laboratory Survey

To confirm the accuracy of the preliminary antibiotic susceptibility results from Hospital A, we prospectively collected all ***S. pneumoniae*** isolates identified by Hospital A's microbiology laboratory from October 23, 1997, through February 19, 1998. An invasive isolate was defined as any positive culture for ***S. pneumoniae*** obtained from blood; cerebrospinal fluid; joint, pleural, or peritoneal fluid; or other normally sterile site. We confirmed the antibiotic susceptibility profiles of each of these isolates by retesting them at another community facility, Hospital B. To determine antibiotic susceptibility, both hospitals used oxacillin disk screening followed by the antimicrobial gradient disk (E-test). The penicillin susceptibility of the invasive isolates was also confirmed using broth dilution at the laboratory of Children's Hospital of Oklahoma, which serves as the regional pediatric referral hospital in Oklahoma.

For this report, the term ***penicillin nonsusceptible*** (PNSP)is used to describe any ***S. pneumoniae*** organism with reduced susceptibility to penicillin. We used the National Committee for Clinical Laboratory Standards' cut points to identify antibiotic susceptibility and determine whether nonsusceptible organisms had intermediate or high resistance (for penicillin, < 0.06 µg/mL was considered susceptible; 0.10-1.00 µg/mL was intermediate, and > 2.00 µg/mL was resistant) (11).

Hospitals A and B used the E-test to evaluate the susceptibility of each isolate to third-generation cephalosporins, but Hospital A used cefotaxime as the test antibiotic whereas Hospital B used ceftriaxone. Both hospitals also tested isolates for susceptibility to trimethoprim sulfamethoxazole (TMP-S).

The serotypes of 16 of the ***S. pneumoniae*** isolates (the first 13 invasive isolates collected and 3 additional noninvasive isolates) from Hospital A were determined by the Division of Bacterial and Mycotic Diseases Laboratory, Centers for Disease Control and Prevention (CDC). The susceptibility profiles and serotypes of these isolates were compared with those obtained from a 1996 nursing home outbreak of invasive multidrug-resistant ***S. pneumoniae*** in a geographically distant region of Oklahoma (12).

Hospital A Retrospective Cohort Study

To describe the epidemiology of ***S. pneumoniae*** at Hospital A during 1994 through 1997, we retrospectively identified all patients with invasive isolates by reviewing records of the hospital's microbiology laboratory. After linking these with patient medical records, we extracted information on demographics, medical history, clinical course, and results of antibiotic susceptibility testing of the isolates for each patient. Trends over time were determined by the chi-square for trend test, and potential predictor factors for acquiring nonsusceptible organisms—such as hospitalization within the past year at Hospital A, nursing home residence, and various demographic factors—were evaluated (Epi-Info version 6.04b, CDC).

1998 Oklahoma Sentinel Hospital Surveillance

During this investigation, a sentinel hospital surveillance system was started for invasive ***S. pneumoniae*** in Oklahoma. We compared the prevalence of PNSP at Hospital A with data from the 26 sentinel hospitals that participated in this surveillance system in 1998. Ten were among the acute-care hospitals studied in central Oklahoma during 1989 to 1990 (10); the others were scattered throughout the state. Some hospitals used bacterial broth dilution or antimicrobial gradient strips for penicillin susceptibility testing; others used bacterial disk diffusion or an antimicrobial panel. The sentinel hospitals accounted for approximately 58% of all medical and surgical hospital beds in the state.

Results

Prospective Laboratory Survey

From October 23, 1997, through February 19, 1998, Hospital A's microbiology laboratory identified ***S. pneumoniae*** isolates from 48 patients. Of these, 17 (35%) were invasive: 2 were from cerebrospinal fluid, and 15 were from blood. The remaining 31 (65%) were noninvasive; 22 isolates were from sputum and 9 from nose, sinus, tonsils, or bronchial washings. The median patient age was 60 years; only 5 (10%) were <18 years of age. Of patients, 26 (54%) were male. Twenty (80%) of the 25 for whom race was known

were white, 4 (16%) were black, and l (4%) was Asian. Twenty-nine (60%) of the patients resided in Oklahoma County; the rest were from seven other Oklahoma counties. The isolates were tested at hospitals A and B for susceptibility to several different antibiotics.

Hospital A reported that 31 (65%) of the 48 ***S. pneumoniae*** isolates were not susceptible to penicillin; 8 (17%)had intermediate resistance and 23 (48%) had high penicillin resistance. Twenty-three (48%) isolates were nonsusceptible to cefotaxime, and 13 (27%) were highly cefotaxime resistant. Of 47 isolates tested, 29 (62%) were nonsusceptible to TMP-S; 23 (49%) were highly resistant (Table 1). All isolates were susceptible to vancomycin.

When these isolates were tested for penicillin susceptibility at Hospital B, a similar prevalence of PNSP was reported (62%), though fewer were highly resistant (29%). However, when testing for susceptibility to a third-generation cephalosporin was performed at Hospital B, only 11 (23%) of 48 isolates were reported as nonsusceptible to ceftriaxone, compared with the 23 (48%) nonsusceptible to cefotaxime at Hospital B (Table 1). For all 15 isolates for which cefotaxime susceptibility results at Hospital A differed from ceftriaxone susceptibility results at Hospital B, the difference was in the direction of higher resistance to cefotaxime than to ceftriaxone (sign test, $p < 0.001$).

When penicillin susceptibilities of the 17 invasive isolates tested with the E-test by both hospitals were compared with the susceptibilities determined at Children's Hospital of Oklahoma using broth dilution, the results were again similar. For 11 (65%) of the invasive isolates, all three test results were interpreted as the same. When discordance was noted, the differences were minor (i.e., susceptible was interpreted as intermediate [or vice versa], or intermediate was interpreted as resistant [or vice versa]). No major differences occurred in interpretation of penicillin susceptibility (susceptible to resistant or resistant to susceptible) (Table 2).

Among the 16 serotyped isolates, 10 serotypes were identified: 4, 6A, 9V (3 isolates), 12F, 18C, 19A (2 isolates), 22F, 23F (4 isolates), 33F, and 35B. Only two (12.5%)(6A and 35B) would not have been covered by pneumococcal vaccine. Among the 23F isolates, two were invasive, and two were not. One of the invasive

Table 1. Antibiotic-susceptibility test results[a] for 48 isolates of ***Streptococcus pneumoniae*** from Hospital A, Oklahoma, October 23, 1997, through February 19, 1998, and retest results from Hospital B

	Hospital A No. (%)	Hospital B No. (%)
Oxacillin disk		
Sensitive	16/47 (34)	17/46 (37)
Resistant	31/47 (66)	29/46 (63)
Penicillin		
Sensitive	17/48 (35)	18/48 (38)
Intermediate	8/48 (17)	16/48 (33)
Resistant	23/48 (48)	14/48 (29)
Ceftriaxone		
Sensitive	not performed	37/48 (77)
Intermediate		7/48 (15)
Resistant		4/48 (8)
Cefotaxime		
Sensitive	25/48 (52)	not performed
Intermediate	10/48 (21)	
Resistant	13/48 (27)	
Trimethoprim-sulfamethoxazole		
Sensitive	18/47 (38)	16/47 (34)
Intermediate	6/47 (13)	2/47 (4)
Resistant	23/47 (49)	29/47 (62)

[a]By E-test and oxacillin disc.

Table 2. Penicillin-susceptibility test results from three laboratories for 17 invasive isolates of ***Streptococcus pneumoniae***, Hospital A, Oklahoma, November 1997 through February 1998

	E-test		Broth dilution
Source	Hospital A	Hospital B	Children's Hospital of Oklahoma
Blood	I	S	S
Blood	R	I	R
Blood	R	R	R
Blood	R	I	I
Blood	S	S	S
Blood	I	I	I
Blood	R	R	I
Blood	S	S	S
Blood	R	I	I
Blood	S	S	S
CSF	S	S	S
Blood	S	S	S
Blood	I	I	I
CSF	R	R	I
Blood	R	R	R
Blood	R	R	R
Blood	S	S	S
I or R %	65%	59%	59%

I, having intermediate resistance; R, highly resistant; S, susceptible to the antibiotic.
CSF = cerebrospinal fluid

23F isolates was highly sensitive to everything tested; the other three were highly resistant to several antibiotics and had similar susceptibility profiles to the 23F isolates identified in the nursing home outbreak months earlier (12).

Hospital A Retrospective Cohort Study

Review of the epidemiology of ***S. pneumoniae*** infection at Hospital A during 1994 through 1997 revealed 71 case-patients with invasive infections. Forty-three (61%) were female, 62 (87%) were white, and 7 (10%) were black. The median age was 64 (range: 1 to 94), and 21 (30%) patients died. Twenty-three (32%) had been hospitalized at Hospital A during the previous 6 months. Nineteen (27%) were residents of a nursing home, 51 (72%) acquired infection in the community, and one (1%) acquired infection while hospitalized for another illness. Five (7%) had asplenia. Sixty-five (92%) isolates were from blood; four (6%) from the joint, pleural, or peritoneal fluid; and one (1%) each from cerebrospinal fluid and an aortic graft. Fifty-six (79%) infected patients resided in Oklahoma City or its vicinity.

Fifty-eight (82%) patients with invasive ***S. pneumoniae*** infections during this period fit the Advisory Committee on Immunization Practices' (ACIP) criteria for pneumococcal vaccine (13). Of the 21 deaths, 20 (95%) would have met the criteria. Only one patient's record, however, showed receipt of pneumococcal vaccine. This patient had had a splenectomy and did not survive the infection.

For the 71 case-patients, 27 (38%) isolates were PNSP, and 13 (18%) were highly resistant. Fifteen (21%) were nonsusceptible to cefotaxime, and one (1%) was highly resistant. All isolates tested were sensitive to vancomycin and clindamycin. Forty-two (59%) patients with invasive pneumococcal disease initially received ceftriaxone, and 3 (4%) received vancomycin; 20 (28%) received vancomycin at some point during their hospital stay. Case-patients with PNSP infections were not more likely to die than patients with penicillin-susceptible infections.

Over the 4-year period of the study, a trend toward increased nonsusceptibility to penicillin was noted at Hospital A (1 of 9, 8 of 24, 7 of 20, 11 of 18; $p = 0.02$). The same trend was noted for cefotaxime nonsusceptibility (0 of 9, 3 of 24, 5 of 20, 9 of 18; $p = 0.008$). A significant trend toward increased penicillin nonsusceptibility was noted in nursing home patients (0 of 2, 2 of 6, 4 of 7, 4 of 4; $p < 0.05$) but not in non-nursing home residents (2 of 7, 7 of 18, 4 of 13, 7 of 14; $p > 0.05$). Nursing home residents were more likely than non-nursing home residents to have a nonsusceptible strain of ***S. pneumoniae,*** but this finding was not significant (10 of 18 vs. 20 of 53, risk ratio [RR] = 1.5; 95% confidence interval [CI] = 0.9 – 2.5; $p > 0.05$). Similarly, patients who had been hospitalized at Hospital A in the previous 6 months were more likely to have PNSP infections than those who had not been hospitalized there, but again the association was not significant (18 of 33 vs. 12 of 38, RR = 1.7; 95% CI = 1.0-3.0; $p = 0.09$).

1998 Oklahoma Sentinel Surveillance

Surveillance data were available from 26 sentinel hospital laboratories in Oklahoma during 1998, including Hospital A's. Seventeen laboratories used the E-test, four used broth dilution, three used disk diffusion (Kirby Bauer), and two used an antimicrobial panel (Microscan) for susceptibility testing. Of 282 invasive isolates tested, 197 (70%) were penicillin susceptible; 52 (18%) had intermediate resistance, and 33 (12%) were highly penicillin resistant. Of the 26 sentinel hospitals, 13 had at least 10 invasive isolates of ***S. pneumoniae*** during 1998. The prevalence of PNSP ranged from 10% to 45% in these 13 hospitals.

Discussion

The high prevalence of PNSP invasive isolates observed among vaccine-eligible, elderly adults from Hospital A in Oklahoma City is similar to that recently reported as the highest of a range of proportions from CDC's Emerging Infections Program's Active Bacterial Core Surveillance for 1997 (8). Penicillin nonsusceptibility varied among Oklahoma sentinel hospitals, but overall it has increased markedly since studies were conducted in Oklahoma in the 1980s (9,10).

The increase in penicillin nonsusceptibility at Hospital A appears to be the result of a trend over the past 4 years. While we found no evidence of an increase in the number of patients with invasive ***S. pneumoniae*** coming from nursing homes, we did note an increasing prevalence of PNSP among such patients.

The community in which Hospital A is located is fairly affluent. Resistance levels can vary within a city, and more affluent or suburban

communities may have higher rates of antibiotic resistance among ***S. pneumoniae*** isolates (5), perhaps attributable to more frequent use of antibiotics. Some resistant isolates were similar to those detected in a recent nursing home outbreak involving a single clone of a highly resistant organism (12). Contribution of an outbreak clone to the high prevalence observed here is possible; however, our evidence suggests that several resistant serotypes contributed to the observed increase. Although the reason for the PNSP increase at Hospital A is unclear, local antibiotic prescribing practices and one or more highly resistant clones circulating in the community or nursing homes may have been involved.

This investigation had at least three limitations. First, the number of invasive isolates for the retrospective study was small, and specific risk factors for acquiring PNSP at Hospital A were not identified. Thus, no single factor explains the high rates observed. Other studies have suggested that age (< 6, or > 65), race, recent antibiotic use, socioeconomic status, and geographic factors may be associated with resistance (2,5). Second, because of the small number of isolates collected prospectively beginning in October 1997, we could not confirm or explain the significant difference in third-generation cephalosporin susceptibility reported by hospitals A and B. Although these facilities used two different test antibiotics (cefotaxime and ceftriaxone) to determine susceptibility, the genetic mechanism responsible for cephalosporin resistance would have been expected to have made the same organisms equally susceptible to either antibiotic. If confirmed, this finding is relevant in clinical settings where cefotaxime is used to test for susceptibility and ceftriaxone is used for treatment because ***S. pneumoniae*** may not have equal susceptibility to both antibiotics. Although we found reliability among the three laboratories for determining penicillin susceptibility, consistent with reports in the microbiology literature (14,15), the lack of interlaboratory reliability in differentiating between high and intermediate penicillin resistance was also unexplained. Finally, we did not assess whether treatment failure contributed to illness and death. Although case-patients with PNSP infections were not more likely to die than patients with penicillin-susceptible infections, the impact of underlying illnesses and the virulence of the infecting strain on the outcome is not known.

For Hospital A and the state of Oklahoma, our findings have implications for disease treatment and prevention. Surveillance, increased use of the pneumococcal vaccine, and judicious use of antimicrobial drugs are important components of the effort to limit the spread of resistant ***S. pneumoniae*** (3,13,16). For determining community-specific prevalence of PNSP infections, use of hospital antibiograms has been shown to be comparable to active surveillance with centralized testing (17). However, our investigation suggested that when different third-generation cephalosporin test antibiotics are used and when determining high versus intermediate penicillin nonsusceptibility, significant differences can occur between hospital laboratories in the determination of susceptibility. Such differences, whatever their explanation, have important clinical implications for the optimal use of antibiotics (e.g., vancomycin, ceftriaxone, and fluoroquinolones). Accurate laboratory information is needed at the local level to optimize use of antibiotics and minimize the development of antibiotic resistance. Accurate surveillance information is needed at the state level to compare regional prevalences. Further study with more isolates is needed to identify ways to improve the accuracy of this surveillance system.

This investigation documented that many cases of invasive pneumococcal disease could have been prevented by improved immunization practices: 82% of Hospital A case-patients during 1994 to 1997 were eligible for vaccine by ACIP criteria, but only one had record of receiving it. Although hospital records may not have reflected true vaccination status, 1997 data from the Behavioral Risk Factor Surveillance System showed that 40% of Oklahoma residents > 65 reported having received the pneumonia vaccine, which is less than the national goal of >60% (18). Targeting vaccination programs at nursing homes may be particularly effective. Oklahoma has recently required that all nursing homes offer pneumococcal vaccination to their residents and provide documentation of vaccination status.

In addition, Hospital A instituted a hospital-based pneumococcal immunization program with standing orders to vaccinate inpatients aged 65 years who are eligible for the vaccine based on ACIP criteria (13). Because nearly one out of

three of the patients with invasive pneumococcal disease admitted to Hospital A during 1994 to 1997 had been hospitalized there in the previous 6 months, an inpatient screening and vaccination program could have prevented a substantial number of cases. Hospital-based programs have been shown to be effective in vaccinating high-risk adults in other settings (19-21), and the use of standing orders to vaccinate eligible adults with pneumococcal vaccine has been recommended by the Task Force on Community Preventive Services (22). Adult vaccination programs in nontraditional settings (e.g., pharmacies, churches, and the workplace) might further raise vaccination coverage in this area (23).

Finally, efforts to promote judicious use of antibiotics are needed to minimize the spread of antibiotic-resistant ***S. pneumoniae***. Several studies have demonstrated that antimicrobial drug use is associated with resistance in ***S. pneumoniae*** (24-26). A combination of interventions involving education of both physicians and patients has been successful in reducing antibiotic use (27) and would likely reduce the trend of increasing resistance in Oklahoma.

Acknowledgments

The authors thank June Ketchum, Dennis Zinn, Everett Dodd, Keeta Gilmore, Denise Robison, and Carolyn Bradley for susceptibility testing of isolates; the surveillance coordinators at the 26 sentinel hospitals for providing data on invasive ***S. pneumoniae;*** John Elliott and Jay Butler for assistance with serotyping isolates and interpreting the results; and Andy Pelletier and Cyndy Whitney for insightful comments.

Dr. Moolenaar is a CDC medical epidemiologist. He was serving as Deputy State Epidemiologist in Oklahoma at the time of this study.

References

1. Breiman RF, Butler JC, Tenover FC, Elliott JA, Facklam RR. Emergence of drug-resistant pneumococcal infections in the United States. JAMA 1994;271:1831-5.
2. Butler JC, Hoffman J, Cetron MS, Elliott JA, Facklam RR, Breiman RF, et al. The continued emergence of drug-resistant ***Streptococcus pneumoniae*** in the United States: an update from the Centers for Disease Control and Prevention's pneumococcal sentinel surveillance system. J Infect Dis 1996;174:986-93.
3. Centers for Disease Control and Prevention. Defining the public health impact of drug-resistant ***Streptococcus pneumoniae***: report of a working group. MMWR Morb Mortal Wkly Rep 1996;45(RR-1):1-20.
4. Pastor P, Medley F, Murphy TV. Invasive pneumococcal disease in Dallas County, Texas: results from population-based surveillance in 1995. Clin Infect Dis 1998;26:590-5.
5. Hoffman J, Cetron MS, Farley MM, Baughman WS, Facklam RR, Elliott JA, et al. The prevalence of drug-resistant ***Streptococcus pneumoniae*** in Atlanta. N Engl J Med 1995;333:481-6.
6. Heffernan R, Henning K, Labowitz A, Hjelte A, Layton M. Laboratory survey of drug-resistant ***Streptococcus pneumoniae*** in New York City, 1993-1995. Emerg Infect Dis 1998;4:113-6.
7. Butler JC, Cetron MS. Pneumococcal drug resistance: the new "special enemy of old age." Clin Infect Dis 1999;28:730-5.
8. Centers for Disease Control and Prevention. Geographic variation in penicillin resistance in ***Streptococcus pneumoniae***—selected sites, United States, 1997. MMWR Morb Mortal Wkly Rep 1999:48;656-61.
9. Istre GR, Tarpay M, Anderson M, Pryor A, Welch D, the Pneumococcus Study Group. Invasive disease due to ***Streptococcus pneumoniae*** in an area with a high rate of relative penicillin resistance. J Infect Dis 1987;156:732-5.
10. Haglund LA, Istre GR, Pickett DA, Welch DF, Fine DP, and the Pneumococcus Study Group. Invasive pneumococcal disease in central Oklahoma: emergence of high-level penicillin resistance and multiple antibiotic resistance. J Infect Dis 1993;168:1532-6.
11. National Committee for Clinical Laboratory Standards. Performance standards for antimicrobial susceptibility testing (5th informational supplement). NCCLS document no. M100-S5. Villanova, PA: The Committee, 1994.
12. Nuorti JP, Butler JC, Crutcher JM, Guevara R, Welch D, Holder I, et al. An outbreak of multidrug-resistant pneumococcal pneumonia and bacteremia among unvaccinated nursing home residents. N Engl J Med 1998;338:1861-8.
13. Centers for Disease Control and Prevention. Prevention of pneumococcal disease: recommendations of the Advisory Committee on Immunization Practices (ACIP). MMWR Morb Mortal Wkly Rep 1997:46(RR-8):1-24.
14. Macias EA, Mason EO Jr, Ocera HY, La Rocco MT. Comparison of E test with standard broth microdilution for determining antibiotic susceptibilities of penicillin-resistant strains of ***Streptococcus pneumoniae***. J Clin Microbiol 1994;32:430-2.
15. Tenover FC, Baker CN, Swenson JM. Evaluation of commercial methods for determining antimicrobial susceptibility of ***Streptococcus pneumoniae***. J Clin Microbiol 1996;34:10-4.
16. Jernigan DB, Cetron MS, Breiman RF. Minimizing the impact of drug-resistant ***Streptococcus pneumoniae*** (DRSP): a strategy from the DRSP Working Group. JAMA 1996;275:206-9.
17. Chin AE, Hedberg K, Cieslak PR, Cassidy M, Stefonek KR, Fleming DB. Tracking drug-resistant ***Streptococcus pneumoniae*** in Oregon: an alternative surveillance method. Emerg Infect Dis 1999;5:688-93.
18. Centers for Disease Control and Prevention. Influenza and pneumococcal vaccination levels among adults aged greater than or equal to 65 years—United States. MMWR Morb Mortal Wkly Rep 1998:47;797-802.

19. Klein RS, Adachi N. An effective hospital-based pneumococcal immunization program. Arch Intern Med 1986;146:327-9.
20. Vondracek TG, Pham TP, Huycke MM. A hospital-based pharmacy intervention program for pneumococcal vaccination. Arch Intern Med 1998;158:1543-7.
21. Gyorkos TW, Tannenbaum TN, Abrahamowicz M. Evaluation of the effectiveness of immunization delivery methods. Can J Public Health 1994;85(Suppl):S14-30.
22. Centers for Disease Control and Prevention. Vaccine-preventable diseases: improving vaccination coverage in children, adolescents and adults. A report on recommendations of the Task Force on Community Preventive Services. MMWR Morb Mortal Wkly Rep 1999;48(RR-8):1-15.
23. Centers for Disease Control and Prevention. Adult immunization programs in nontraditional settings: quality standards and guidance for program evaluation—a report of the National Vaccine Advisory Committee and use of standing orders programs to increase adult vaccination rates: recommendations of the Advisory Committee on Immunization Practices. MMWR Morb Mortal Wkly Rep 2000;49(RR-1):1-13.
24. Bedos JP, Chevret S, Chastang C, Geslin P, Regnier B, and the French Cooperative Pneumococcus Study Group. Epidemiological features of and risk factors for infection by ***Streptococcus pneumoniae*** strains with diminished susceptibility to penicillin: findings of a French survey. Clin Infect Dis 1996;22:63-72.
25. Nava JM, Bella F, Garau J, Lite J, Morera MA, Marti C, et al. Predictive factors for invasive disease due to penicillin-resistant ***Streptococcus pneumoniae***: a population based study. Clin Infect Dis 1994;19:884-90.
26. Frick PA, Black DJ, Duchin JS, Delaganis S, Mckee WM, Fritsche TR. Prevalence of antimicrobial drug-resistant ***Streptococcus pneumoniae*** in Washington state. West J Med 1998;169:364-9.
27. Gonzales R, Steiner JF, Lum A, Barret PH. Decreasing antibiotic use in ambulatory practice: impact of a multidimensional intervention on the treatment of uncomplicated acute bronchitis in adults. JAMA 1999;281:1512-9.

Rickettsia mongolotimonae: A Rare Pathogen in France

Pierre-Edouard Fournier,* Hervé Tissot-Dupont,*† Hervé Gallais,† and Didier Raoult*
*Faculté de Médecine, Université de la Méditerranée, Marseille, France; and †Hôpital de la Conception, Marseille, France

We report a second case of laboratory-confirmed infection caused by ***Rickettsia mongolotimonae*** in Marseille, France. This rickettsiosis may represent a new clinical entity; moreover, its geographic distribution may be broader than previously documented. This pathogen should be systematically considered in the differential diagnosis of atypical rickettsioses, especially rashless fevers with lymphangitis and lymphadenopathy, in southern France and perhaps elsewhere.

Rickettsia mongolotimonae (1) was first obtained as isolate HA-91 from ***Hyalomma asiaticum***, a tick collected in Inner Mongolia in 1991 (2). The first evidence of ***R. mongolotimonae*** pathogenicity in humans was obtained in our laboratory in 1996 in a woman who had an atypical tick-transmitted disease. This second case of ***R. mongolotimonae*** infection was unexpected, especially because the symptoms in the second case differed from those of the first case and of other rickettsioses cases.

On May 19, 1998, a 49-year-old HIV-positive man was admitted to a hospital in Marseille, France, with fever and myalgias for 5 days. The patient, who had been HIV positive since 1988, was being treated with a combination of zidovudine, lamivudine, and nevirapine. With this therapy, he had been asymptomatic for 5 years. His CD4+ lymphocyte count was 503/µL, and his plasma viral level was 5,916 copies per ml (3.77 log). He was a gardener who lived in a rural area 40 km from Marseille and had contact with animals, including cats, rabbits, squirrels, and birds. On May 8, 1998, he worked in his garden but did not notice any tick bites. On examination the day of admission, he had an eschar (tache noire) surrounded by an inflammatory halo on his left leg. He had a fever of 39°C, chills, headache, and myalgias. A lymphangitis expanded from the inoculation eschar to the left groin, where a painful satellite lymphadenopathy was observed (Figure). Clinical examination was otherwise normal. Laboratory results were unremarkable.

Figure. Lymphangitis expanding from the inoculation eschar on the left leg to an enlarged, painful lymph node on the left groin of a patient with ***Rickettsia mongolotimonae*** infection.

Address for correspondence: Didier Raoult, Unité des Rickettsies, CNRS, Faculté de Médecine, Université de la Méditerranée, 27 Boulevard Jean Moulin, 13385 Marseille cedex 05, France; fax: 33-04-91-83-0390; e-mail: Didier.Raoult@medecine.univ-mrs.fr.

An acute-phase serum sample drawn that day was sent to our laboratory, along with a biopsy of the eschar. Although the patient had no rash, Mediterranean spotted fever was suspected. After 15 days of treatment with 200 mg per day of doxycycline, the symptoms resolved. A second serum sample was collected on May 26.

Microimmunofluorescence testing was performed (3). Although the first serologic test was negative, the second serum sample had low titers to ***R. mongolotimonae*** and ***R. conorii*** (1:16 for immunoglobulin [Ig] G and 1:16 for IgM). The eschar sample was spread onto human embryonic lung fibroblasts by the centrifugation shell-vial technique (4). After 7 days incubation at 32°C, a Gimenez staining of methanol-fixed human embryonic lung fibroblasts cells showed ***Rickettsia***-like bacilli. DNA was extracted from the ground eschar biopsy and from 200 µL of shell-vial supernatant, by using a QIAmp Tissue kit (QIAGEN GmbH, Hilden, Germany) according to the manufacturer's instructions. These extracts were used as templates with primers complementary to portions of the coding sequences of the rOmpA, citrate synthase, and 16S rRNA encoding genes in three polymerase chain reaction (PCR) assays (5). The base sequences of the obtained PCR products were determined (5). All sequences shared 100% similarity with ***R. mongolotimonae*** when compared with GenBank data.

Eight new rickettsioses, three of which were described in Europe, have been identified in the past 13 years, including Japanese spotted fever due to ***R. japonica;*** Astrakhan fever due to Astrakhan fever rickettsia; Flinder's Island spotted fever due to ***R. honei***; cat flea typhus due to ***R. felis***; African tick-bite fever due to ***R. africae***; and the proposed rickettsioses due to ***R. mongolotimonae*** (1), ***R. slovaca*** (6), and ***R. helvetica*** (7). ***R. conorii***, responsible for Mediterranean spotted fever, has long been considered the only tick-transmitted European rickettsia in the Mediterranean Sea area. However, the results of this and previous studies (1,6) indicate that both ***R. mongolotimonae*** and ***R. slovaca*** are agents of human rickettsioses in France.

In the only reported case of ***R. mongolotimonae*** infection in France, migratory birds carrying ticks were hypothesized to be responsible for transmitting the infection, as ***R. mongolotimonae*** had been isolated only from ticks from China (1). On the basis of this hypothesis, the initial case was thought to be a unique imported infection. However, the occurrence of a second case in the same area suggests that the disease may be more common than expected around Marseille. ***R. mongolotimonae*** was initially isolated from ***Hyalomma asiaticum*** ticks in China, but its reservoir in our area is unknown. However, the fact that the patient worked in a garden near cypress trees where numerous birds nested suggests that migratory birds should be considered a possible source. We were unable to detect this bacterium by using ***omp***A PCR-amplification and culture in 540 ***Rhipicephalus*** ticks from the Marseille area; these ticks are prevalent in southern France (8,9). An active search for the vector of ***R. mongolotimonae***, which may be a rare tick species in Southern France, should be conducted.

The symptoms of both patients occurred in spring, which is unusual for Mediterranean spotted fever (1). The symptoms of the first patient were like those of Mediterranean spotted fever, except that the rash was discrete. The second patient had no rash but had lymphangitis, expanding from the inoculation eschar to the groin, and a painful lymphadenopathy. These differences in clinical symptoms may be explained by the HIV-positive status of this patient. Two cases are inadequate to describe a disease; however, our preliminary data suggest that ***R. mongolotimonae*** infections may have a discrete rash or no rash, along with lymphangitis and satellite lymphadenopathy.

This second case of ***R. mongolotimonae*** infection is important for several reasons. First, this rickettsiosis may represent a new clinical entity. Second, the geographic distribution of the illness may be broader than previously documented. ***R. mongolotimonae*** should be systematically considered in the differential diagnosis of atypical rickettsioses in southern France, especially fevers without rash but with lymphangitis and lymphadenopathy, in southern France and perhaps elsewhere.

Dr. Fournier is a physician in the French reference center for the diagnosis and study of rickettsial diseases. His research interests include the clinical and epidemiologic features of the rickettsioses.

References

1. Raoult D, Brouqui P, Roux V. A new spotted-fever-group rickettsiosis. Lancet 1996;348:412.

2. Yu X, Fan M, Xu G, Liu Q, Raoult D. Genotypic and antigenic identification of two new strains of spotted fever group rickettsiae isolated from China. J Clin Microbiol 1993;31:83-8.
3. Teysseire N, Raoult D. Comparison of Western immunoblotting and microimmunofluorescence for diagnosis of Mediterranean spotted fever. J Clin Microbiol 1992;30:455-60.
4. Marrero M, Raoult D. Centrifugation-shell vial technique for rapid detection of Mediterranean spotted fever rickettsia in blood culture. Am J Trop Med Hyg 1989;40:197-9.
5. Roux V, Fournier PE, Raoult D. Differentiation of spotted fever group rickettsiae by sequencing and analysis of restriction fragment length polymorphism of PCR amplified DNA of the gene encoding the protein rOmpA. J Clin Microbiol 1996;34:2058-65.
6. Raoult D, Berbis P, Roux V, Xu W, Maurin M. A new tick-transmitted disease due to ***Rickettsia slovaca***. Lancet 1997;350:112-3.
7. Nilsson K, Lindquist O, Pahlson C. Association of ***Rickettsia helvetica*** with chronic perimyocarditis in sudden cardiac death. Lancet 1999;354:1169-73.
8. Peter O, Raoult D, Gilot B. Isolation by a sensitive centrifugation cell culture system of 52 strains of spotted fever group rickettsiae from ticks collected in France. J Clin Microbiol 1990;28:1597-9.
9. Drancourt M, Kelly PJ, Regnery RL, Raoult D. Identification of spotted fever group rickettsiae using polymerase chain reaction and restriction-endonuclease length polymorphism analysis. Acta Virol 1992;36:1-6.

Costs and Benefits of a Subtype-Specific Surveillance System for Identifying *Escherichia coli* O157:H7 Outbreaks

Elamin H. Elbasha,* Thomas D. Fitzsimmons,*† and Martin I. Meltzer*
*Centers for Disease Control and Prevention, Atlanta, Georgia, USA; and †Colorado Department of Public Health and Environment, Denver, Colorado, USA

We assessed the societal costs and benefits of a subtype-specific surveillance system for identifying outbreak-associated ***Escherichia coli*** O157:H7 infections. Using data from Colorado, we estimated that if it averted five cases annually, the system would recover all its costs.

Escherichia coli O157:H7 infections pose a serious public health threat (1-4). Surveillance, rapid reporting of cases, and prompt epidemiologic investigations are essential elements of timely public health response (2,5). Surveillance that uses molecular subtyping methods has at least two advantages over traditional surveillance systems (6). First, it is sensitive enough to identify outbreaks not detected by traditional surveillance or can detect them earlier. Second, it is specific enough to differentiate sporadic cases from outbreak-related cases and distinguish between single and multiple outbreaks.

A subtype-specific surveillance system consists of 1) mandatory submission of ***E. coli*** O157:H7 isolates for subtyping; 2) a centrally located laboratory equipped to perform subtyping by pulsed-field gel electrophoresis; 3) active links between local and state health officials; and 4) epidemiologic capacity to investigate the possibility of an outbreak once identical strains are identified.

In August 1997, the Colorado Department of Public Health and Environment, using subtype-specific surveillance, identified an outbreak associated with eating hamburgers from beef processed in a plant in Nebraska and distributed nationally. After the outbreak was traced to the contaminated beef, the company recalled 25 million pounds of ground beef, the largest meat recall recorded (7).

We used cost-benefit analysis to assess the economic feasibility (from a societal perspective) of using a system similar to the one in Colorado for identifying ***E. coli*** O157:H7 outbreaks.

The Study

A system is cost-beneficial if the discounted benefits it generates are at least as great as the discounted costs of installing and operating the system. The life span of the subtype-specific surveillance system in Colorado is 5 years, yielding benefits over the lifetime of people affected by it. Data on the costs of the system were obtained from the Colorado Department of Public Health and Environment (Table 1). The system was not set up only to subtype for ***E. coli*** O157:H7 but also to identify outbreaks of other organisms (e.g., ***Salmonella typhi***); only ***E. coli***-related costs were considered here. The sensitivity of the results was examined with all the costs of the system attributed to ***E. coli*** O157:H7 subtyping.

In estimating the costs of outbreak investigations, we assumed that, as a result of the system, two epidemiologic investigations would be carried out each year, with an average cost of $9,600 per outbreak (Table 1). The costs associated with recalling any outbreak-related

Address for correspondence: Elamin H. Elbasha, Centers for Disease Control and Prevention, 4770 Buford Highway, Mail Stop K73, Atlanta, GA 30341, USA; fax: 770-488-8464; e-mail: ebe4@cdc.gov.

Table 1. Costs of installing and operating the subtype-specific surveillance system, Colorado, 1996

Labor and equipment costs	Total costs	*Escherichia coli*-related costs[a]
Equipment	$40,000	$16,000
Laboratory scientist (per year)[b]	$10,000	$4,000
Analyzing the isolates (per year)[c]	$12,000	$12,000
Investigating an outbreak[d,e]	$9,600	$9,600
Present value of outbreak costs (in 5 years)[f]	$90,568	$90,568
Annual operating costs[g]	$41,200	$35,200

[a]From the proportion of ***E. coli*** isolates among the total number of isolates expected to be subtyped each year, we extrapolated that 40% of the equipment and labor costs were ***E. coli***-related.
[b]The salary and fringe benefits of a full-time laboratory analyst.
[c]Analyzing 300 isolates at a cost of $40 per isolate.
[d]This cost included, but was not limited to, the value of time (15 days) spent investigating an outbreak, answering telephone calls, conducting meetings, improving and transferring pulsed-field gel electrophoresis image files to various groups, creating databases, requesting information, responding to media calls, and handling legal issues. We assumed that, as a result of the system, two outbreaks would be investigated each year (6).
[e]The costs of additional labor and the epidemiologic investigation of an outbreak were estimated at $5,000 and $4,600, respectively.
[f]At a discount rate of 3%.
[g]Laboratory scientist ($10,000) + analyzing the isolates ($12,000) + investigating two outbreaks (2 x $9,600 = $19,200)

product were not included. Data (e.g., percentage of contaminated beef) that would allow us to attribute economic value to the amount of the product recalled were not available. In the sensitivity analysis, costs were increased by 100% to account for such missing data.

The benefits of the surveillance system are the economic savings accrued from ***E. coli*** O157:H7 cases averted. Determining the number of cases averted as a result of using the system is difficult. One way of determining this number is by estimating the attack rate and multiplying that number by the amount of beef recalled (8).

However, for the outbreak in Colorado, data for estimating specific attack rates were lacking. Instead, we estimated two threshold numbers of cases that must be averted for the costs to be equal to the benefits of the system. The first threshold number was calculated by assuming the system averts a constant number of cases every year. The second number was calculated under the assumption that the system averts only a given number of cases in the first year and no cases in subsequent years. If the estimated threshold is below a reasonable number, the system is cost beneficial. A reasonable number is calculated by consulting the literature and expert opinion.

The average cost of an ***E. coli*** O157:H7 infection was estimated by using an infection outcome tree (4) (Figure). A person infected with ***E. coli*** O157:H7 can be in only one disease severity category (Figure; Table 2). The far-left branch of the tree is designated as severity category no. 9. The probability is 0.2% (10% hospitalization x 50% hemolytic uremic syndrome [HUS] x 4% death) that an infected person will be hospitalized for hemorrhagic colitis, come down with HUS, and die after 1 year. From the time of infection until the time of death, the societal costs for this patient are $991,221 (medical costs $39,204 + productivity losses $3,041 + lost lifetime earnings $948,976).

Data on the probability of being in any of these categories were obtained from Roberts et al. (3). The economic costs associated with each category were based on the methods and assumptions of Buzby et al. (4), with modifications (Table 2). Productivity losses were estimated by multiplying the average wage in 1996 by the number of days missed from work. The average wage rate was estimated by using the average daily earnings of a nonagricultural nonsupervisory employee, assuming that fringe benefits are 39% of total wages or salaries and a labor participation rate of 84% (4). We estimated the costs of a death by using only the lost lifetime earnings, as estimated by Haddix et al. (9) and updated by the rates of change in wages. Because we did not assess pain and suffering from the disease or loss of human life, our estimates of benefits should be considered conservatively low.

All costs and benefits were adjusted to 1996 dollars according to the consumer price index or its components (various issues of the Statistical Abstract). All future costs and benefits were

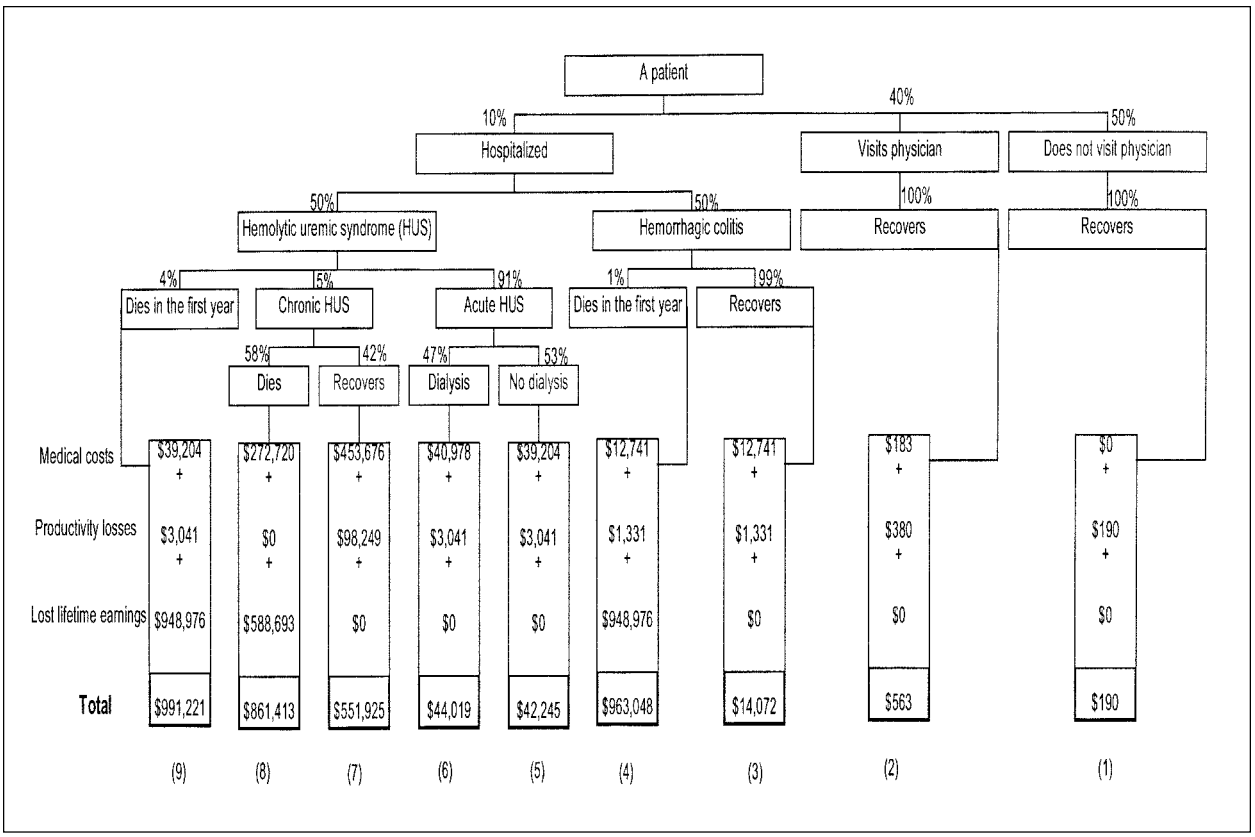

Figure. ***Escherichia coli*** O157:H7 infection outcome tree. Severity categories (1)-(9) are described in Table 2.

Table 2. Assumptions about disease severity following an ***Escherichia coli*** O157:H7 infection[a]

Severity category	Assumptions
No. 1	Patient does not seek medical care, recovers, and misses 2 days of work
No. 2	Patient seeks medical care for hemorrhagic colitis, has one laboratory test, recovers, and misses 4 days of work
No. 3	Patient is hospitalized for hemorrhagic colitis for 6.5 days and recovers after missing 14 days of work
No. 4	Patient is hospitalized for hemorrhagic colitis for 6.5 days, misses 14 days of work, and dies in the first year
No. 5	Patient is hospitalized for acute HUS[b] for 5 days in ICU[c] and 10 days in a regular room, and recovers after missing 32 days of work
No. 6	Patient is hospitalized for acute HUS[b] for 5 days in ICU[c] and 10 days in a regular room, requires dialysis for 12 days, and recovers after missing 32 days of work
No. 7	Patient is hospitalized for hemorrhagic colitis; comes down with chronic HUS[b]; may require dialysis, transplants, or drug therapy; cannot work for an extended period; and recovers
No. 8	Patient is hospitalized for hemorrhagic colitis; comes down with chronic HUS[b]; may require dialysis, transplants, or drug therapy; cannot work for an extended period; and dies
No. 9	Patient is hospitalized for acute HUS[b] for 5 days in ICU[c] and 10 days in a regular room and dies after missing 32 days of work

[a]Adapted from Buzby et al. (4). A patient is defined as a person infected with ***E. coli*** O157:H7 who has at least a gastrointestinal illness for more than 1 day.
[b]HUS, hemolytic uremic syndrome.
[c]ICU, intensive care unit.

discounted at 3%. Other rates were used in the sensitivity analysis.

The discounted average cost of an ***E. coli*** O157:H7 infection was $7,788 (Table 3). The main component of the cost of a case was the expected cost of sequelae and death. The undiscounted cost of a case was $15,927. The discounted cost of installing and operating the surveillance system over a period of 5 years was $182,042 (Table 3). Included in this category were the costs of investigating outbreaks ($90,568 in 5 years), of the subtyping equipment ($16,000), and of analyzing the isolates ($60,000 in 5 years) (Table 1). At a 3% discount, five cases per year (or 14 cases in the first year only) must be averted for the costs of the system to be equal to its benefits (Table 3). Without discounting, the threshold number dropped to 2.4 cases per year (Table 3).

Sensitivity Analysis

The estimated costs of a case were sensitive to the estimates of the probability of death after infection. If the probability of death is raised to 2.3% (4), the cost of a case increases to $25,997, and the threshold number of cases averted for the system to be economically feasible decreases to 1.5 per year for 5 years, or 4.3 cases in the first year and none in the following years (Table 3).

If all the costs of subtyping (including subtyping for other organisms) were included in the analysis, the system would recover its costs after averting 6.4 infections annually, or 20.9 cases in the first year only, with no cases detected in subsequent years. If the costs of the system doubled or the benefits of a case averted decreased by 50%, the threshold number would increase to 9.9 cases per year, or 28.4 cases in the first year only (Table 3). Doubling the number of outbreaks or considering only direct medical costs would raise the threshold numbers to 7.4 and 11.4 cases per year, respectively.

Conclusions

If 15 cases were averted by the recall of the 25 million pounds of potentially contaminated beef, the Colorado system would have recovered all costs for the 5 years of start-up and operation by detecting a single outbreak (Table 3). In comparison, the outbreak-related 1993 recall of 255,000 regular (0.1-lb) hamburgers in Washington State was estimated to have prevented 800 cases (8).

The discounted average cost of an ***E. coli*** O157:H7 infection of $7,788 (Table 3) was a relatively conservative estimate compared with that of $38,000 (in 1995 dollars) by Buzby et al. (4). The major differences are the probability of death and the economic value of life used in the estimation (11).

If other benefits of the system (e.g., obviating the need to investigate sporadic cases) are included, the system becomes even more cost

Table 3. Discounted costs of an ***Escherichia coli*** O157:H7 infection, discounted costs of the surveillance system, and threshold number of cases, 1996

Components affecting costs	Discount rate[a] 3%	0%	5%
Discounted average cost of an ***E. coli*** O157:H7 infection	$7,788	$15,927	$5,847
Discounted costs of installing and operating the system	$182,042	$192,000	$176,018
Baseline (best estimate)			
Cases that need to be averted every year for 5 years[b]	5.0	2.4	6.6
Cases that need to be averted in the first year alone[c]	14.2	7.2	18.5
One-way sensitivity analysis			
Increasing labor and equipment costs from $20,000 to $50,000			
Cases that need to be averted every year for 5 years[b]	6.4	3.1	8.6
Cases that need to be averted in the first year alone[c]	20.9	10.6	27.2
Decreasing the costs of an infection from $7,788 to $3,894			
Cases that need to be averted every year for 5 years[b]	9.9	4.8	13.2
Cases that need to be averted in the first year alone[c]	28.4	14.5	36.9
Increasing the probability of death from 0.4% to 2.3%			
Cases that need to be averted every year for 5 years[b]	1.5	0.5	2.6
Cases that need to be averted in the first year alone[c]	4.3	1.5	7.3

[a]The most frequently assumed discount rate is 5%. However, 3% is the recommended rate. No discounting is suggested for testing the sensitivity of the results (10).

[b]Threshold number of cases averted every year for 5 years above which the system is cost-beneficial.

[c]Threshold number of cases averted in the first year above which the system is cost-beneficial, assuming the system does not avert any cases in subsequent years and continues to incur costs.

beneficial. Unproductive extensive traceback investigations of sporadic ***E. coli*** O157:H7 infections have been conducted (12). Investigating such sporadic cases can be very costly (Table 1), and a subtype-specific system can reduce such costs.

According to the National Electronic Telecommunications System for Surveillance, 90 cases of ***E. coli*** O157:H7 were reported in Colorado in 1998 (13), an annual incidence rate of 2.3 per 100,000 population. In comparison, the national incidence rate calculated from these data was 1.2 per 100,000 population (3,161 cases).

This study was limited by lack of data that would have enabled us to estimate attack rates from the outbreak, cases averted by the meat recall, and the benefit to society (money saved) by establishing the system. Despite its limitations, this study has important implications for public health policy. From a societal perspective, a surveillance system does not need to prevent a large number of cases to yield return on the resources invested in it.

Acknowledgments

The authors thank Patrick McConnon, Paul Mead, Peter Drotman, and Pam Shillam for helpful discussions.

This research is supported in part by CDC and Oak Ridge Institute of Science and Education through an interagency agreement between the US Department of Energy and CDC.

Dr. Elbasha is a health economist in the Prevention Effectiveness Branch, Division of Prevention Research and Analytic Methods, Epidemiology Program Office, CDC. His research interests include assessment of the burden of diseases, the cost-effectiveness and cost-benefits of various public health interventions, analysis of economic policies that impact public health, and integration of economic analysis and methods into epidemiologic models and data.

References

1. Griffin PM, Tauxe RV. The epidemiology of infections caused by ***Escherichia coli*** O157:H7, other enterohemorrhagic ***E. coli***, and the associated hemolytic uremic syndrome. Epidemiol Rev 1991;13:60-98.
2. American Gastroenterological Association. Consensus statement: ***Escherichia coli*** O157:H7 infections: an emerging national health crisis, July 11-13, 1994. Gastroenterology 1995;108:1923-34.
3. Roberts T, Buzby J, Lin J, Mead P, Nunnery P, Tarr PI. Economic aspects of ***E. coli*** O157:H7: disease outcome trees, risk, uncertainty, and social cost of disease estimates. In: Prediction, detection, and management of tomorrow's epidemics. Greenwood B, De Cock K, eds. John Wiley & Sons, Chichester, UK. pp 156-72.
4. Buzby JC, Roberts T, Lin JC-T, MacDonald JM. Bacterial foodborne disease: medical costs and productivity losses. Washington: U.S. Department of Agriculture, Economic Research Service. AER No. 741. August 1996.
5. Centers for Disease Control and Prevention. Preliminary report: foodborne outbreak of ***Escherichia coli*** O157:H7 infections from hamburgers—western United States, 1993. MMWR Morb Mortal Wkly Rep 1993;42:85-6.
6. Bender JB, Hedberg CW, Besser JM, Boxrud DJ, MacDonald KL, Osterholm MT. Surveillance for ***Escherichia coli*** O157:H7 infections in Minnesota by molecular subtyping. N Engl J Med 1997;337:388-94.
7. Kolata G. Detective work and science reveal a new lethal bacteria. New York Times. 1998 Jan 6;147:A1, A14.
8. Bell BP, Goldoft M, Griffin PM, Davis MA, Gordon DC, Tarr PI, et al. A multiple outbreak of ***Escherichia coli*** O157:H7-associated bloody diarrhea and hemolytic uremic syndrome from hamburgers: the Washington State experience. JAMA 1994;272:1349-53.
9. Haddix AC, Teutsch SM, Shaffer PA, Dunet DO, editors. A guide to decision analysis and economic evaluation. New York: Oxford University Press; 1996.
10. Gold MR, Siegel JE, Russell LB, Weinstein MC, editors. Cost-effectiveness in health and medicine. New York: Oxford University Press; 1996.
11. Landefeld JS, Seskin EP. The economic value of life: linking theory to practice. Am J Public Health 1982;6:555-66.
12. Centers for Disease Control and Prevention. Enhanced detection of sporadic ***Escherichia coli*** O157:H7 infections—New Jersey, July, 1994. MMWR Morb Mortal Wkly Rep 1993;44:417-8.
13. Centers for Disease Control and Prevention. Summary of notifiable diseases, United States, 1998. MMWR Morb Mortal Wkly Rep 1999;47:1-93.

Dengue Epidemic in Belém, Pará, Brazil, 1996–97

Amélia P.A. Travassos da Rosa, Pedro F.C. Vasconcelos, Elizabeth S. Travassos da Rosa, Sueli G. Rodrigues, Bernard Mondet, Ana C.R. Cruz, Maria R. Sousa, and Jorge F.S. Travassos da Rosa
Instituto Evandro Chagas, Belém, Pará, Brazil

We describe clinical and epidemiologic findings during the first epidemic of dengue fever in Belém, Pará State, Brazil, in 1996-97. Of 40,237 serum samples, 17,440 (43%) were positive for dengue by virus isolation or serologic testing. No hemorrhagic cases or deaths were reported.

Dengue fever (DF) and dengue hemorrhagic fever (DHF) are caused by infection with one of the four serotypes of dengue virus (DEN-1, DEN-2, DEN-3, and DEN-4), transmitted by ***Aedes aegypti*** mosquitoes. In Brazil, DF epidemics reported in the 1980s and 1990s involved more than a million cases. However, only 671 DHF cases were diagnosed, with 26 deaths (1).

Ae. aegypti was reintroduced in Pará State in 1992, and the first dengue cases were reported in 1995 in the southeast region (Redenção and Rondon do Pará). In October 1996, eight cases of febrile denguelike illness were reported in Belém (population 1,300,000), a city in the Brazilian Amazon region at the confluence of the Amazon River and the Atlantic Ocean. In early November, DEN-1 virus was isolated and identified (2-4). DEN-2 virus was identified in October 1997, and since then, both serotypes have been responsible for illness in Belém. This was the first time dengue virus transmission occurred in Belém during the last 70 years and the third time the disease occurred in the Brazilian Amazon region. Previous outbreaks had been reported in 1981-82 in Boa Vista, Roraima (5), and in 1991 in Araguaina, Tocantins State (6).

We describe cases of denguelike illness diagnosed at Instituto Evandro Chagas. A case of dengue was defined as illness with the following symptoms: acute onset of high fever, headache, myalgia, arthralgia, dizziness, and other symptoms and signs suggestive of denguelike illness in a patient with a positive IgM by IgM-capture enzyme-linked immunosorbent assay (MAC ELISA), virus isolation or serologic conversion in paired serum samples, and an increase of at least fourfold in titer in the convalescent-phase serum sample (7-9).

Address for correspondence: Pedro Fernando da Costa Vasconcelos, Instituto Evandro Chagas, Av. Almirante Barroso 492, 66090-000, Belém, Pará, Brazil; fax: 55-91-226-1284; e-mail: pedrovasconcelos@iec.pa.gov.br.

The Study

From January to December 1997, 40,237 serum samples were drawn from febrile patients in Belém, 20,038 (49.8%) of whom were male. The patients were all residents of the municipalities of Belém (31,506 samples) and Ananindeua (8,731 samples). Most were ambulatory patients seen in the Arbovirus Department, Evandro Chagas Institute; some patients were referred by public health centers, private physicians, and clinics. At the Institute, all patients were examined clinically and had blood samples drawn. A questionnaire was administered that included information about clinical symptoms and signs and demographic data. Patients who had been ill <10 days and whose serologic tests were negative for dengue were requested to provide a second blood sample 7 to 14 days later. For patients who had at least one hemorrhage and either dehydration or hemoconcentration, a leukogram, platelet count, and hematocrit were performed.

Serum samples were tested for dengue antibodies by MAC ELISA (4) and hemagglutination-inhibition test (2). The antigens for both tests were prepared by using infected mouse

brain extracted by the sucrose acetone method. The criteria used for establishing primary and secondary infection were those recommended by the World Health Organization (7,8).

To isolate dengue virus, 0.1-ml aliquots of whole blood from patients with clinical symptoms lasting <5 days and negative serologic results were injected into cultures of C6/36 cells (10). The cultures were visually examined daily, and cells were tested on days 7 and 14 by immunofluorescence (3).

Isolated virus strains were initially screened by direct immunofluorescence against a flavivirus standard hyperimmune fluid prepared at the Institute. Strains that reacted were identified to serotype by using an indirect immunofluorescence test with monoclonal antibodies against the four dengue viruses provided by the Centers for Disease Control and Prevention.

The epidemic distribution was accompanied early in 1997 by a seasonal increase in rainfall typical of the Brazilian Amazon. However, the highest dengue positivity rates were reported in the dry months of September to December. Coincidentally, DEN-2 virus was isolated in October. At first, cases were reported only in Belém and Ananindeua, but in December 1997, at least 15 other municipalities reported transmission cycles involving either DEN-1 or DEN-2 or both.

Of all sera collected, 17,525 (43.5%) were positive by serologic testing or DEN virus isolation: 13,805 (78.8%) from Belém and 3,720 (21.2%) cases from Ananindeua (Figure). Both primary and secondary serologic responses were found. Among the positive samples, 9,469 (54.25%) were among female and 7,971 (45.75%) among male patients ($p < 0.0001$); 45.95% of the patients were 25 to 44 years of age (Table 1). Paired serum samples were obtained from 3,558 patients, 2,997 (84.2%) of whom had serologic conversions.

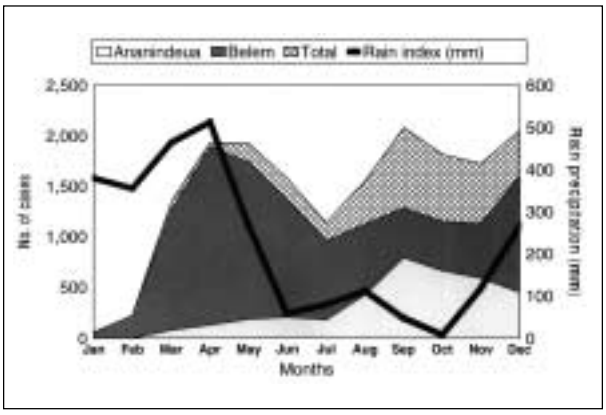

Figure. Monthly distribution of rain precipitation (line) and dengue fever cases as seen at Instituto Evandro Chagas, Pará, Brazil. Source for rain precipitation, Instituto Nacional de Meteorologia, Brazil.

No DHF cases were reported, in spite of the fact that since October 1997 DEN-2 had been isolated from 24 patients with previous DEN-1 infection (Table 2). Clinical symptoms were more severe in older children and adults than in young children, but no differences were observed between the clinical symptoms of patients with DEN-1 and DEN-2 infection.

Table 1. Distribution of patients with serologic tests positive for dengue

	Male			Female			Total	
Age	No.	Pos	%	No.	Pos	%	Pos	%
<4	186	60	0.76	325	76	0.8	136	0.78
5–9	308	89	1.12	425	186	1.96	275	1.58
10–14	1,033	444	5.56	816	356	3.76	800	4.59
15–24	4,080	1,596	20	3,765	1,643	17.35	3,239	18.56
25–34	5,083	2,184	27.37	4,375	2,127	22.47	4,311	24.7
35–44	3,919	1,684	21.1	4,638	2,023	21.37	3,707	21.25
45–54	3,319	1,016	12.73	3,572	1,558	16.46	2,574	14.75
>55	2,110	898	11.36	2,283	1,500	15.83	2,398	13.79
Total	20,038	7,971	100	20,199	9,469	100	17,440	100

Table 2. Strains of dengue virus isolated from patients from Belém and Ananindeua, Instituto Evandro Chagas, October 1996 to August 1998

	DEN-1	DEN-2	Total
1996	31	-	31
1997	751	48	799
1998[a]	58	60	118
Total	840	108	948

[a]Through August.

Conclusions

During 1953 and 1954, Causey and Theiler (11) used seroneutralization in mice to survey several municipalities of the Amazon region; they found 9.8% and 2.2% of serum samples positive for dengue virus serotypes DEN-1 and DEN-2, respectively, among residents > 50 years of age. These results suggest that dengue viruses were circulating in Belém and other municipalities of the Amazon Valley early in the 20th century.

The dengue epidemic in Belém was unusual in that a "lag phase" (12) lasted for at least 4 months before extensive transmission began. In spite of laboratory diagnosis of cases from the beginning of the outbreak and the reporting of these results to health authorities, control measures were unsuccessful. Consequently, explosive transmission began in March 1997 and is still occurring (1998-99).

In the last 4 years, the Brazilian Ministry of Health (13) has reported an increase in dengue cases from approximately 56,000 in 1994 to >530,000 in 1998. High indexes of ***Ae. aegypti*** infestation exist in all important urban centers of Brazil, reflecting a poor health education program. The fact that more cases occurred in female than in male patients ($p < 0.0001$) suggests that women are at increased risk for dengue infection because of high peridomestic exposure.

Dengue transmission has been reported in 22 of the 27 Brazilian states, and the mosquito vector is present in all states; therefore, the situation in Brazil may be rapidly approaching hyperendemicity, with the cocirculation of two serotypes (DEN-1 since 1986 and DEN-2 since 1990). The risk for DHF will increase if a new serotype (DEN-3 or DEN-4) is introduced. Endemicity is the most constant factor associated with the evolution of epidemic DHF in a geographic area (14). Although few cases have been reported until recently, DHF may become an important cause of hospitalization and death in the Americas, including Brazil.

Acknowledgments

The authors thank Marcio R.T. Nunes, Gisele C.A. Barra, Denise I. Cerqueira, Nelma Mesquita, Andes K. Mahagama, Eliana Pinto, and Mioni T.F. Magalhães, and the Instituto Nacional de Meteorologia (Ministry of Agriculture) for data on precipitation and Robert Tesh for review of the manuscript.

This study was supported by the Fundação Nacional de Saúde (FNS)/IEC.

Dr. Travassos da Rosa was chief of the Arbovirus Department at Instituto Evandro Chagas and Director of the WHO Collaborating Center of Arbovirus there from 1979 to 1998. Since 1998, she has been a visiting scientist in the Department of Pathology, Center for Tropical Diseases, University of Texas Medical Branch in Galveston. Her research interests focus on the serology and taxonomy of arboviruses and hantaviruses.

References

1. Pinheiro FP, Nelson M. Re-emergence of dengue and dengue haemorrhagic fever in the Americas. Dengue Bulletin, World Health Organization (New Delhi) 1997:21:16-24.
2. Shope RE. The use of a microhemagglutination-inhibition test to follow antibody response after arthropod-borne virus infection in a community of forest animals. Anais de Microbiologia (Rio de Janeiro) 1963;11(parte A):167-71.
3. Tesh RB. A method for the isolation and identification of dengue viruses, using mosquito cell cultures. Am J Trop Med Hyg 1979:28:1053-9.
4. Kuno G, Gomez I, Gubler DJ. Detecting artificial antidengue IgM immune complexes using an enzyme-linked immunosorbent assay. Am J Trop Med Hyg 1987:36:153-9.
5. Osanai CH, Travassos da Rosa APA, Tang AT, Amaral RS, Passos AC, Tauil PL. Surto de dengue em Boa Vista, Roraima. Rev Inst Med Trop Sao Paulo 1983:25:53-4.
6. Vasconcelos PFC, Travassos da Rosa ES, Travassos da Rosa JFS Freitas RB, Dégallier N, Rodrigues SG, et al. Epidemia de febre clássica de dengue causada pelo sorotipo 2 em Araguaína, Tocantins, Brasil. Rev Inst Med Trop Sao Paulo 1993:35:141-8.
7. World Health Organization. Dengue haemorrhagic fever: diagnosis, treatment and control. Geneva: The Organization; 1986. p. 58+.
8. World Health Organization. Dengue haemorrhagic fever: diagnosis, treatment and control. 2nd ed. Geneva: The Organization; 1997. p. 84+.
9. Gubler DJ. Dengue and dengue hemorrhagic fever. Clin Microbiol Rev 1998;11:480-96.

10. Beaty BJ, Calisher CH, Shope RE. Arboviruses. In: Schmidt NJ, Emmons E, editors. Diagnostic procedures for viral, rickettsial and chlamydial infections, 6th ed. Washington: American Public Health Association; 1989: p. 797-855.
11. Causey OR, Theiler M. Virus antibody survey on sera of residents of the Amazon Valley in Brazil. Am J Trop Med Hyg 1958:7:36-41.
12. Gubler DJ. Vigilancia activa del dengue y de la dengue hemorragica del dengue. Boletin de la Oficina Sanitaria Panamericana 1989:107:22-30.
13. Fundação Nacional de Saúde. Casos de dengue e febre amarela no Brasil. Brasília: Ministério da Saúde; 1999.
14. Gubler DJ. Epidemic dengue/dengue haemorrhagic fever: a global public health problem in the 21st Century. Dengue Bulletin, World Health Organization (New Delhi) 1997:21:1-15.

Mycobacterium tuberculosis Beijing Genotype Emerging in Vietnam

Dang Duc Anh,* Martien W. Borgdorff,† L.N. Van,‡ N.T.N. Lan,§ Tamara van Gorkom,¶ Kristin Kremer,¶ and Dick van Soolingen¶

*National Institute of Hygiene and Epidemiology, Hanoi, Vietnam; †Royal Netherlands Tuberculosis Association, The Hague, The Netherlands; ‡National Institute of Tuberculosis and Respiratory Diseases, Hanoi, Vietnam; §Tuberculosis and Lung Diseases Center, Ho Chi Minh City, Vietnam; and ¶National Institute of Public Health and the Environment, Bilthoven, The Netherlands

To assess whether the ***Mycobacterium tuberculosis*** Beijing genotype is emerging in Vietnam, we analyzed 563 isolates from new cases by spoligotyping and examined the association between the genotype and age, resistance, and BCG vaccination status. Three hundred one (54%) patients were infected with Beijing genotype strains. The genotype was associated with younger age (and hence with active transmission) and with isoniazid and streptomycin resistance, but not with BCG vaccination.

A high degree of diversity of ***Mycobacterium tuberculosis*** has been shown with restriction fragment length polymorphism (RFLP) typing using IS***6110*** as a probe, particularly in countries like the Netherlands, where many tuberculosis (TB) cases occur among immigrants (1). However, in the Beijing region of China, a particular genotype was found in >80% of the TB patients and was thus designated the Beijing genotype (2). In other parts of China and in Asian countries such as Mongolia, Thailand, and Korea, 40% to 50% of the tested ***M. tuberculosis*** isolates represented this genotype (2). Although Beijing genotype strains carry a large number of IS***6110*** insertion elements, the IS***6110*** RFLP patterns are highly similar (2). Moreover, the spoligopatterns of Beijing genotype strains are identical and distinct from those of other ***M. tuberculosis*** strains (1), which suggests that strains of the Beijing genotype have emerged recently from a single ancestor.

Reasons for the predominance of a narrow range of genotypes may include limited contact with other populations or a selective advantage of certain strains due to reduced sensitivity to vaccine-induced immunity. For instance, wide-scale application of vaccines against whooping cough (***Bordetella pertussis***) has led to shifts in the populations of circulating pathogens (3). BCG vaccination, which has been applied widely in China since the early 1950s, may have led to a similar shift in the population of ***M. tuberculosis***. Alternatively, a selective advantage may be provided by reduced sensitivity to anti-TB drugs. The Beijing genotype was associated with recent transmission of drug-resistant strains in Cuba, Germany, Russia, and Estonia (4-7). The largest known epidemic of multidrug-resistant TB in North America was caused by the "W" strain, a variant of the Beijing genotype (8).

Vietnam is one of 22 countries in which 80% of the world's new TB cases occur (9). Among these 22 countries, Vietnam has one of the most successful directly observed therapy short-course programs, with a cure rate of approximately 90% and a case-detection rate estimated at 67% in 1996 and at >70% since then (National Tuberculosis Programme, unpub. data). BCG coverage has been high (>80%) during the past decade, and the level of primary multidrug resistance was recently estimated at 2.3% (9,10). We investigated the spread of ***M. tuberculosis*** Beijing genotype strains in Vietnam and whether the spread is associated with BCG vaccination status or drug resistance.

Address for correspondence: D. van Soolingen, Diagnostic Laboratory for Infectious Diseases and Perinatal Screening, National Institute of Public Health and the Environment, P.O. Box 1, 3720 BA Bilthoven, The Netherlands; fax: 31-30-2744418; e-mail: d.van.soolingen@rivm.nl.

In total, 822 isolates were obtained from TB patients whose age and BCG status were known. Of these, 563 had newly diagnosed disease (Table 1). The isolates were collected in 1998 and the first quarter of 1999 at the Tuberculosis and Lung Diseases Centre in Ho Chi Minh City and the National Institute of Tuberculosis and Respiratory Diseases in Hanoi, respectively. The isolates were analyzed by spoligotyping (11). In spoligotyping, the genomic direct repeat (DR) region of ***M. tuberculosis*** complex bacteria is amplified by polymerase chain reaction (PCR) and the presence of 43 spacer sequences between the DRs is examined in a reversed line-blot assay (2,11). In previous studies, this method has proven highly reliable for distinguishing Beijing genotype strains (2). Among the 563 spoligopatterns analyzed, two predominant genotypes were recognized (Figure), of which the Beijing type was the most frequent (n = 301; 53%). The second most frequent genotype was not found in the database of spoligopatterns of 2,500 ***M. tuberculosis*** isolates from countries all over the world, held at the National Institute of Public Health and the Environment in Bilthoven and designated Vietnam genotype (n = 152; 27%) (Figure). The remaining 110 isolates exhibited 18 different spoligopatterns.

The Beijing genotype was strongly associated with younger age (X^2_{trend}; p <0.001), but not with BCG status, after the data were adjusted for age (Table 1). As levels of drug resistance varied between Hanoi and Ho Chi Minh City and the number of samples from Hanoi was small, the association of the Beijing genotype and drug resistance was restricted to Ho Chi Minh City (Table 2). Drug resistance was found more commonly in the Beijing than in other genotypes (Table 2). The association with drug resistance was significant for isoniazid (OR 1.7; 95% CI 1.1-2.6) and streptomycin (odds ratio [OR] 3.1; 95% confidence interval [CI] 2.0-4.6) resistance.

TB occurs partly as primary disease (typically defined as occurring within 5 years of infection) and partly as endogenous reactivation or exogenous reinfection (occurring >5 years

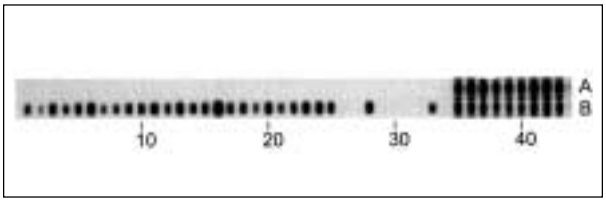

Figure. Representative spoligotype patterns of the Beijing (A) and the Vietnam (B) genotypes. Numbers indicate the spacer oligonucleotide sequences, present on the reversed line blot, which are derived from reference ***Mycobacterium tuberculosis*** strain H37Rv and ***M. bovis*** BCG vaccine strain P3.

Table 1. Beijing genotype of ***Mycobacterium tuberculosis*** in 563 new tuberculosis cases, by age and BCG status, in Hanoi and Ho Chi Minh City, Vietnam, 1998

		Beijing genotype		OR[a] (95% CI[b])	
	No.	No.	(%)	Crude	Adjusted[c]
Province					
Hanoi	64	37	(58)	1 (p>0.05)	
Ho Chi Minh City	499	264	(53)	0.8 (0.5-1.4)	
Age group					
<25	76	54	(71)	1 (p<0.001)	1
25-34	173	102	(59)	0.6 (0.3-1.0)	0.6 (0.3-1.1)
35-44	164	83	(51)	0.4 (0.2-0.7)	0.4 (0.2-0.8)
45-54	74	31	(42)	0.3 (0.1-0.6)	0.3 (0.2-0.6)
55-64	39	16	(41)	0.3 (0.1-0.6)	0.3 (0.1-0.7)
65+	37	15	(41)	0.3 (0.1-0.6)	0.3 (0.1-0.7)
BCG scar					
Yes	285	167	(59)	1(p<0.05)	1
No	278	134	(48)	0.7 (0.5-0.9)	0.9 (0.6-1.3)
Total	563	301	(54)		

[a]OR, odds ratio.
[b]CI, confidence interval.
[c]Adjusted for age and BCG vaccination.

Table 2. Risk factors for drug resistance in 499 new tuberculosis cases in Ho Chi Minh City

		Resistance (%)					OR[a] (95% CI[b])	
	No.	INH	SM	RIF	EMB	MDR	INH	SM
Genotype								
Beijing	264	28	42	3	3	3	1.7 (1.1-2.6)	3.1 (2.0-4.6)
Other	235	19	19	2	1	2	1 ($p<0.05$)	1 ($p<0.001$)
Age group								
<25	66	17	36	3	0	3	1 ($p>0.05$)	1 ($p>0.05$)
25-34	165	27	32	3	2	3	1.8 (0.9-3.8)	0.8 (0.4-1.5)
35-44	147	25	33	1	1	1	1.7 (0.8-3.5)	0.8 (0.5-1.6)
45-54	59	19	25	3	5	3	1.1 (0.5-2.9)	0.6 (0.3-1.3)
55-64	30	23	23	3	3	3	1.5 (0.5-4.4)	0.5 (0.2-1.4)
65+	32	31	31	0	0	0	2.3 (0.8-6.1)	0.8 (0.3-2.0)
BCG scar								
Yes	259	22	31	3	2	3	1 ($p>0.05$)	1 ($p>0.05$)
No	402	73	22	2	2	2	1.3 (0.9-2.0)	1.1 (0.7-1.6)
Total	499	24	31	2	2	2		

[a]OR, odds ratio.
[b]CI, confidence interval.
INH, isoniazide; SM, streptomycin; RIF, rifampin; EMB, ethambutol; MDR, multidrug resistant

after infection). With increasing age, a decreasing proportion of cases is due to primary TB. Thus, the association of the Beijing genotype and young age suggests a recent spread of the Beijing genotype in Vietnam. The study of Qian et al., in which spoligotyping was performed on paraffin-embedded material, indicated that the Beijing genotype was presumably already prevalent in the Beijing region 30 to 40 years ago (12).

In Vietnam, the Beijing genotype occurs more commonly in those with a BCG scar than in those without it. However, this is likely to represent a cohort effect of BCG vaccination, rather than reduced sensitivity to vaccine-induced immunity of Beijing genotype strains. Because of increasing BCG vaccination coverage in Vietnam over the past 2 decades, young people are more likely to be vaccinated than older people. Within age groups, occurrence of the Beijing genotype is not associated with BCG vaccination status.

Its striking association with anti-TB drug resistance may explain the Beijing genotype's predominance in recently infected patients. Anti-TB drugs are widely used in Vietnam, and anti-TB drug resistance would thus provide a selective advantage. In vitro experiments should determine whether Beijing genotype strains have an increased intrinsic resistance to anti-TB drugs or an enhanced capacity to gain resistance against these drugs.

Dr. Anh is head of the Department of Bacteriology, National Institute of Hygiene and Epidemiology, Hanoi, Vietnam. Areas of interest include molecular epidemiology of mycobacterial infection and epidemiologic surveillance of bacterial meningitis in children.

References

1. Van Soolingen D, Borgdorff MW, de Haas PEW, Kremer K, Veen J, Sebek MGG, et al. Molecular epidemiology of tuberculosis in The Netherlands: a nationwide study during 1993 through 1997. J Infect Dis 1999;180:726-36.
2. Van Soolingen D, Qian L, de Haas PEW, Douglas JT, Traore H, Portaels F. Predominance of a single genotype of ***Mycobacterium tuberculosis*** in countries of East Asia. J Clin Microbiol 1995;33:3234-8.
3. Van Loo IHM, van der Heide HGJ, Nagelkerke NJD, Mooi FR. Temporal trends in the population structure of ***Bordetella pertussis*** during 1949-1996 in a highly vaccinated population. J Infect Dis 1999;179:915-23.
4. Diaz R, Kremer K, de Haas PEW, Gomez RI, Marrero A, Valdivia JA. Molecular epidemiology of tuberculosis in Cuba outside of Havana, July 1994-June 1995: utility of spoligotyping versus IS***6110*** restriction fragment length polymorphism. Int J Tuberc Lung Dis 1998;2:743-50.
5. Niemann S, Rüsch-Gergdes S, Richter E. IS***6110*** fingerprinting of drug-resistant ***Mycobacterium tuberculosis*** strains isolated in Germany during 1995. J Clin Microbiol 1997;35:3016-20.
6. Martilla HJ, Soini H, Eerola E, Vyshnevskaya E, Vyshnevskiy BI, Otten TF. A Ser315Thr substitution in ***katG*** is predominant in genetically heterogeneous multidrug-resistant ***Mycobacterium tuberculosis*** isolates originating from the St. Petersburg area in Russia. Antimicrobiol Agents Chemother 1998;42:2443-5.

7. Ghebremichael S, Kruuner A, Levina K, Kallenius G, Hoffner SE. Molecular epidemiology of multi-drug resistant (MDR) tuberculosis in Estonia. Abstracts of the 19th Annual Congress of the European Society of Mycobacteriology. 1998; IV: 334.
8. Bifani PJ, Plikaytis BB, Kapur V, Stockbauer K, Pan X, Lutfey ML. Origin and interstate spread of a New York City multidrug-resistant ***Mycobacterium tuberculosis*** clone family. JAMA 1996;275:452-7.
9. Netto EM, Dye C, Raviglione MC. Progress in global tuberculosis control 1995-1996, with emphasis on 22 high-incidence countries. Int J Tuberc Lung Dis 1999;3:310-20.
10. World Health Organization/International Union Against Tuberculosis and Lung Disease global project on anti-tuberculosis drug resistance surveillance, 1994-1997. Anti-tuberculosis drug resistance in the world. Geneva: The Organization; 1997.
11. Kamerbeek J, Schouls LM, Kolk A, Van Agterveld M, van Soolingen D, Kuijper S. Simultaneous detection and strain differentiation of ***Mycobacterium tuberculosis*** for diagnosis and epidemiology. J Clin Microbiol 1997;35:907-14.
12. Qian LS, Van-Embden JDA, Van der Zanden AGM, Weltevreden EF, Duanmu H, Douglas JT. Retrospective analysis of the Beijing family of ***Mycobacterium tuberculosis*** in preserved lung tissues. J Clin Microbiol 1999;37:471-4.

Bartonella spp. Isolated from Wild and Domestic Ruminants in North America[1]

Chao-chin Chang,* Bruno B. Chomel,* Rickie W. Kasten,* Remy Heller,† Katherine M. Kocan,‡ Hiroshi Ueno,§ Kazuhiro Yamamoto,* Vernon C. Bleich,¶ Becky M. Pierce,¶ Ben J. Gonzales,¶ Pamela K. Swift,¶ Walter M. Boyce,* Spencer S. Jang,* Henri-Jean Boulouis,# and Yves Piémont†

*School of Veterinary Medicine, University of California, Davis, California, USA; †Institut de Bactériologie, Université Louis Pasteur, Strasbourg, France; ‡College of Veterinary Medicine, Oklahoma State University, Stillwater, Oklahoma, USA; §School of Veterinary Medicine, Rakuno-Gakuen University, Ebetsu, Hokkaido, Japan; ¶California Department of Fish and Game, Bishop, Rancho Cordova, California, USA; #Ecole Nationale Vétérinaire d'Alfort, 94704 Maisons-Alfort, France

Bartonella species were isolated from 49% of 128 cattle from California and Oklahoma, 90% of 42 mule deer from California, and 15% of 100 elk from California and Oregon. Isolates from all 63 cattle, 14 deer, and 1 elk had the same polymerase chain reaction/restriction fragment length polymorphism profiles. Our findings indicate potential for inter- and intraspecies transmission among ruminants, as well as risk that these ***Bartonella*** spp. could act as zoonotic agents.

Bartonella species have been identified as important zoonotic agents (1,2). Cats are the main reservoir of ***Bartonella henselae***, the agent that causes cat scratch disease in humans (1). Long-term bacteremia in cats and flea transmission from cat to cat, as confirmed by experimental infection, support a vectorborne transmission (3). Some human cases of cat scratch disease were not associated with any known exposure to cats (4), suggesting that other animal species may serve as reservoirs of ***Bartonella***. Recently, new ***Bartonella*** species have been isolated from a wide range of mammals, including rodents (5-10), lagomorphs (11), carnivores (12-14), and cervids (14,15). Similarly, 90% of 42 mule deer (***Odocoileus hemionus***) from California were bacteremic with ***Bartonella*** isolates that were similar to isolates from roe deer in France (15) by polymerase chain reaction/restriction fragment length polymorphism (PCR/RFLP) of the 16S rRNA and citrate synthase genes (14). Modes of transmission in these ruminants need to be established. Tick transmission has been suspected but not yet proven for dogs infected with ***B. vinsonii*** subsp. ***berkhoffii*** (16). Since fleas are less likely than ticks to infest cattle (17), ticks may play an important role in the transmission of ***Bartonella*** species from wild ruminants.

Our objectives were to determine if elk (***Cervus elaphus***), bighorn sheep (***Ovis canadensis***), and domestic cattle (***Bos taurus***) are infected with ***Bartonella*** and to determine the molecular relationships between ***Bartonella*** isolated from cattle and wild ruminants. We performed a cross-sectional study to compare the prevalence of ***Bartonella*** infection in a beef cattle herd in the California Sierra Nevada foothills and a dairy herd from the California Central Valley.

The Study

In February 1997, 42 samples from free-ranging mule deer were obtained from the Round Valley population, Mono and Inyo counties, California. In November 1997, 84 samples were

Address for correspondence: Bruno B. Chomel, Department of Population Health and Reproduction, School of Veterinary Medicine, University of California, Davis, CA 95616, USA; fax: 530-752-2377; e-mail: bbchomel@ucdavis.edu.

[1]An earlier version of this paper was presented at the Second International Conference on Emerging Zoonoses, Strasbourg, France, November 5–9, 1998.

collected from bighorn sheep herds in California and New Mexico. During January and February 1998, 100 blood samples were collected from elk in California and Oregon. One hundred twenty-eight cattle samples were collected: 12 from Oklahoma beef cattle in April 1998 and 116 from two California herds from May to July 1998. Fifty-three samples were collected from a >4,000-head beef cattle herd in the Sierra Nevada foothills and 63 samples from a >1,500-head dairy herd in the Central Valley. These 116 cattle were all > 2 years of age. Blood samples collected into lysis-centrifugation tubes were plated within 48 hours. Blood samples collected into EDTA tubes were frozen at -70° until plated. Wildlife and domestic herds were selected on the basis of ongoing surveys by the California and Oregon Departments of Fish and Game and researchers at the Universities of California and Oklahoma.[2]

Blood samples were cultured on heart infusion agar containing 5% rabbit blood and incubated in 5% CO_2 at 35°C for at least 4 weeks (18). Gram staining and biochemical tests were performed on representative isolates, which were defined as isolates with a unique PCR/RFLP profile for each of the three ruminant species. Nine representative isolates were identified, including one cattle strain (pattern I), five deer strains (patterns I, II, IV, V, and VI), and three elk strains (patterns I, II, and III). Standard methods were used to test for various preformed enzymes and carbohydrate use. Preformed bacterial enzyme activity was tested by Microscan Rapid Anaerobe Panel (Dade International Inc., West Sacramento, CA) (19).

An approximately 400-bp fragment of the citrate synthase gene was amplified as described (20). The amplified product was digested with ***Taq***I and ***Hha***I and ***Mse***I restriction endonucleases and visualized by gel electrophoresis. Banding patterns were compared with ***B. henselae*** (strain U-4; University of California, Davis, CA).

Cellular fatty acid composition was analyzed for representative cattle, deer, and elk isolates. Isolates were grown on rabbit blood agar at 35°C for 5 days. Fatty acid methyl ester derivatives were separated on a Hewlett-Packard series II 5890 gas chromatograph.

The PCR products used for DNA sequencing were purified with Microcon centrifugal filter devices (Millipore Corp., Bedford, MA) and sequenced with a fluorescent-based automated sequencing system. Primer BhCS.1137n (5'-AATGCAAAAAGAACAGTAAACA-3') (20) was used for partial sequencing of the 400-bp product of the citrate synthase gene. Nine representative strains from ruminants and one ***B. henselae*** strain (strain U-4, University of California, Davis) were sequenced. The GAP program of GCG software (Wisconsin Sequence Analysis Package, Genetics Computer Group, version 10) was used for alignments and comparisons of sequences, based on the 276 bp of the citrate synthase gene.

Using Epi Info version 6.03, we performed a chi-square test to assess association between prevalence of bacteremia of ***Bartonella*** infection and herd location. The ***Bartonella*** infection prevalence ratio (PR) was calculated to show the proportionate increase of infection prevalence due to difference in herd location.

Results

Bartonella spp. were isolated from 5 (42%) of 12 Oklahoma cattle, 58 (50%) of 116 California cattle, 38 (90%) of 42 California mule deer, 15 (15%) of 100 elk, and none of 84 bighorn sheep. In the California beef cattle herd, 25 (96%) of 26 bulls and 22 (81%) of 27 cows were ***Bartonella*** bacteremic; in the dairy herd, 11 (17%) of 63 cows were bacteremic. ***Bartonella*** bacteremia prevalence in the Sierra Nevada foothills beef cattle herd was therefore significantly higher than in the Central Valley dairy cattle herd (PR = 5.1; 95% confidence interval [CI] = 2.9-8.8). Prevalence of ***Bartonella*** bacteremic cows in the foothills herd was also significantly higher (81% vs. 17%) than in the Central Valley dairy cattle herd (PR = 4.7; 95% CI = 2.7-8.2). For elk, bacteremia prevalence differed significantly (p = 0.0002) between California (0 of 47) and Oregon (15 [28%] of 53). No ***Bartonella***-bacteremic elk were found in the two California herds, but 11 (38%) of 29 elk from southwestern Oregon and 4 (17%) of 24 elk from northwestern Oregon were bacteremic.

The organisms isolated were short, slender gram-negative rods. By measuring preformed

[2]Collection sites for bighorn sheep were the Peninsular Ranges in California and the San Francisco River, Turkey Creek, and Red Rock in New Mexico. For elk, collection sites were the San Luis National Wildlife Refuge in Merced County and the Tupman Tule Elk State Reserve in Kern County (California); the Roseburg, Drain, and Demet herds, Douglas County (southwestern Oregon); and the Jewell Wildlife Area, Clatsop County (northwestern Oregon).

enzymes (Rapid Anaerobe Panel), the tested strains were found to be biochemically inert except for the production of peptidases, characteristic of the ***Bartonella*** profile (10077640).

Several strain profiles were observed by PCR/RFLP of the citrate synthase gene, using ***Taq***I and ***Hha***I and ***Mse***I endonucleases for deer (five profiles) and elk (three profiles) isolates (Figure). Conversely, all 63 cattle isolates had the same PCR/RFLP profile (Figure) with the same restriction enzymes. Overall, six different PCR/RFLP profiles were obtained from ***Bartonella*** isolated from cattle, deer, and elk. ***Bartonella*** isolated from cattle (63 of 63 tested; lanes 2, 12, and 22), mule deer (14 of 38 tested; lanes 3, 13, and 23), and an elk from southwestern Oregon (1 of 11 tested; lanes 10, 20, and 30) yielded the same PCR/RFLP profile (pattern I) with the three enzymes used. A second profile (pattern II) was obtained for ***Bartonella*** isolated from elk captured in northwestern Oregon (4 of 4 tested; lanes 8, 18, and 28) and from mule deer (5 of 38 tested; lanes 4, 14, and 24). A third profile (pattern III) was obtained for 10 of the 11 ***Bartonella*** isolated from elk captured in southwestern Oregon (lanes 9, 19, and 29). The other three profiles (patterns IV, V, and VI) were obtained for ***Bartonella*** isolated from mule deer ([pattern IV: 12 of 38 tested; lanes 6, 16, and 26]; [pattern V: 5 of 38 tested; lanes 5, 15, and 25]; and [pattern VI: 2 of 38 tested; lanes 7, 17, and 27]).

The cellular fatty acid composition was characteristic of the ***Bartonella*** genus for all isolates. The main fatty acids observed for the cattle, deer, and elk strains were octadecanoic acid ($C_{18:1}$, 45%-66%), octadecanoic acid ($C_{18:0}$, 12%-23%), and hexadecanoic acid ($C_{16:0}$, 13%-20%).

After pairwise comparisons, the partial sequencing analysis (276 bp) of the citrate synthase gene for the nine representative ruminant strains showed a high percentage of DNA similarity, from 93.12% to 100% (Table 1). The strains cattle-1, deer-1, and elk-1 belonging to the PCR/RFLP pattern I had 95.65% to 99.64% DNA similarity. The strains deer-2 and elk-2 with PCR/RFLP pattern II had 100% DNA similarity. The strain deer-1 with PCR/RFLP pattern I was closely related (98.91% DNA identity) to the strain deer-2 with PCR/RFLP pattern II. For strains deer-4 and deer-5, corresponding to PCR/RFLP patterns IV and V (similar digestion profiles with ***HhaI*** and ***MseI*** endonucleases and different profiles from ***TaqI*** endonuclease), a 98.55% DNA similarity was observed. Partial sequence analysis (276 bp) of the citrate synthase gene showed that all strains from ruminants were closely related to ***B. weissii***, a ***Bartonella*** species isolated from domestic cats (Table 2).

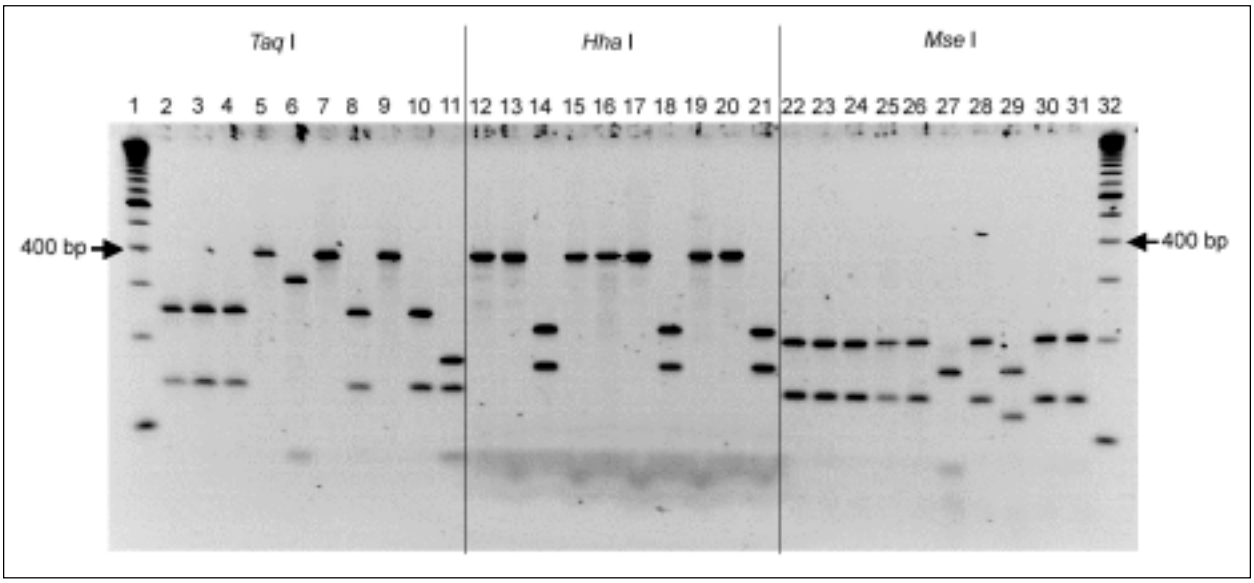

Figure. Polymerase chain reaction/restriction fragment length polymorphism of the citrate synthase gene of isolates from cattle, deer, and elk, with ***Taq***I, ***Hha***I, and ***Mse***I endonucleases. Lanes 1 and 32, standard 100-bp molecular ladder; lanes 2, 12, and 22, cattle isolate; lanes 3 to 7, 13 to 17, and 23 to 27, deer isolates; lanes 8 to 10, 18 to 20, and 28 to 30, elk isolates; lanes 11, 21, and 31, ***B. henselae*** strain.

Table 1. DNA similarity values and GenBank accession numbers based on 276 bp of the citrate synthase gene of the nine representative ruminant strains

Organism/ accession no.	% Similarity by strain								
	Cattle-1	Deer-1	Deer-2	Deer-4	Deer-5	Deer-6	Elk-1	Elk-2	Elk-3
Cattle-1 AF228768	100.00	95.65	96.01	94.57	94.57	94.57	99.64	96.01	94.57
Deer-1 AF228769	-	100.00	98.91	93.84	93.84	93.12	95.65	98.91	93.84
Deer-2 AF228771	-	-	100.00	94.20	94.20	93.48	96.01	100.00	94.20
Deer-4 AF228774	-	-	-	100.00	98.55	94.93	94.57	94.20	94.57
Deer-5 AF228775	-	-	-	-	100.00	94.20	94.57	94.20	94.57
Deer-6 AF228776	-	-	-	-	-	100.00	94.20	93.48	96.01
Elk-1 AF228770	-	-	-	-	-	-	100.00	96.01	94.57
Elk-2 AF228772	-	-	-	-	-	-	-	100.00	94.20
Elk-3 AF228773	-	-	-	-	-	-	-	-	100.00

Table 2. DNA similarity values based on 276 bp of the citrate synthase gene of the nine ruminant strains compared with those of the ***Bartonella*** strains in GenBank

Organism/accession no.	% Similarity by strain								
	Cattle-1	Deer-1	Deer-2	Deer-4	Deer-5	Deer-6	Elk-1	Elk-2	Elk-3
B. bacilliformis U28076	86.59	87.68	87.32	84.78	85.51	84.78	86.59	87.32	87.68
B. grahamii Z70016	90.22	90.22	90.58	91.67	90.22	90.58	90.58	90.58	89.49
B. taylorii Z70013	88.41	87.32	86.96	87.68	87.68	87.68	88.04	86.96	88.04
B. tribocorum AJ005494	89.86	89.13	89.49	90.58	89.13	88.41	89.49	89.49	88.04
B. doshiae Z70017	88.41	86.59	86.96	86.96	86.23	87.68	88.04	86.96	85.87
B. vinsonii subsp. ***vinsonii*** U28074	88.69	89.05	87.96	88.69	88.69	89.42	88.32	87.96	87.96
B. vinsonii subsp. ***berkhoffii*** U28075	89.86	89.49	89.13	87.68	87.68	88.41	89.49	89.13	86.96
B. vinsonii subsp. ***arupensis*** U77057	90.22	89.13	89.13	90.94	90.94	90.22	89.86	89.13	88.77
B. weissii AF071190	99.64	95.65	96.01	94.57	94.57	94.20	100.00	96.01	94.57
B. clarridgeiae U84386	90.58	89.49	89.86	88.77	88.04	88.77	90.22	89.86	89.49
B. henselae strain U-4	90.58	88.41	89.49	88.77	88.77	87.32	90.22	89.49	87.68
B. henselae strain Houston-1 L38987	90.58	88.41	89.49	88.77	88.77	87.32	90.22	89.49	87.68
B. koehlerae AF176091	89.13	88.41	88.77	89.49	88.77	87.32	88.77	88.77	87.32
B. quintana Z70014	90.22	88.04	88.41	87.68	86.96	88.41	89.86	88.41	88.77
B. elizabethae Z70009	88.41	88.04	88.41	90.22	88.77	89.49	88.04	88.41	88.04
Strain C7-rat Z70020	88.41	88.04	88.41	90.22	88.77	89.49	88.04	88.41	88.04
Strain C5-rat Z70018	88.77	88.77	89.13	90.22	88.77	87.32	88.77	89.13	87.68
Strain C4-phy Z70019	87.32	86.23	86.96	86.96	86.96	86.59	86.96	86.96	85.15
Strain C1-phy Z70022	86.59	85.51	86.23	86.23	86.23	85.87	86.23	86.23	84.42
Strain R-phy2 Z70011	87.32	86.23	86.96	86.96	86.96	86.59	86.96	86.96	85.15
Strain R-phy1 Z70010	88.04	87.68	88.04	87.32	87.32	87.32	87.68	88.04	85.87
Strain N40 Z70012	90.22	88.77	89.13	88.77	87.32	87.32	89.86	89.13	86.96
Strain A1 U84372	88.77	87.68	88.77	88.04	87.32	88.04	88.41	88.77	86.23
Strain A2 U84373	88.41	87.32	88.41	87.68	87.68	87.68	88.04	88.41	86.23
Strain A3 U84374	88.77	88.04	88.77	88.04	88.04	88.04	88.41	88.77	86.23
Strain B1 U84375	88.49	89.13	88.77	88.77	88.77	89.49	89.13	88.77	88.04
Strain B2 U84376	89.86	89.49	89.13	88.41	88.41	89.13	89.49	89.13	87.68
Strain C1 U84377	88.77	89.13	88.77	87.68	86.96	88.41	88.41	88.77	86.59
Strain C2 U84378	88.77	89.13	88.77	87.68	86.96	88.41	88.41	88.77	86.59
Strain D1 U84379	89.86	88.77	88.77	90.58	90.58	89.86	89.49	88.77	88.41
Strain D2 U84380	90.22	89.13	89.13	90.94	90.94	90.22	89.86	89.13	88.41
Strain D3 U84381	90.58	89.86	89.49	90.58	90.58	90.58	90.22	89.49	88.77
Strain D4 U84382	90.22	89.13	89.13	90.94	90.94	90.22	89.86	89.13	88.77
Strain D5 U84383	89.49	89.13	88.41	90.22	90.22	89.49	89.13	88.41	88.04
Strain D6 U84384	90.58	89.86	89.49	90.58	90.58	90.58	90.22	89.49	88.77
Strain D7 U84385	90.22	89.13	89.13	90.94	90.94	90.22	89.86	89.13	88.41

Conclusion

This is the first published report of isolation of ***Bartonella*** spp. from free-ranging wild ruminants and domestic ruminants in North America. Our results suggest that deer, elk, and domestic cattle are possible reservoirs of ***Bartonella*** spp. Selected bighorn sheep populations from California and New Mexico appeared to be free of ***Bartonella***. The first report of infection of cattle with a ***Bartonella*** organism was made in 1934 by Donatien and Lestoquard, who proposed the name ***B. bovis*** or ***Haemobartonella bovis*** (21). In 1942, Lotze and Yiengst also described ***Bartonella***-like structures in American cattle (22); however, their identifications of ***Bartonella***-like structures were based only on the morphologic aspects of these organisms in red blood cells also infected with ***Theileria*** or ***Anaplasma***, two well-known tickborne infections.

Partial sequencing analysis of the citrate synthase gene of the ruminant strains showed that they were all closely related to each other and to a feline strain, ***B. weissii***. Further studies by DNA-DNA hybridization may determine if these strains are specific to ruminants but closely related to ***B. weissii***, or if they are in fact ***B. weissii***. If the ruminant strains are identical to ***B. weissii***, the high prevalence (89%) of ***Bartonella*** bacteremia observed in beef cattle may indicate that ruminants are the main reservoirs of ***B. weissii***, which is not commonly isolated from cats.

The prevalence of ***Bartonella*** bacteremia was high in beef cattle and mule deer, possibly related to exposure to potential vectors. Since fleas are rarely observed on cattle and tick infestation is common in both cattle and deer, ticks are a possible source of infection for ruminants (17). Furthermore, ***Bartonella*** DNA has recently been demonstrated in a high percentage of ticks infesting roe deer in Europe (23,24). The herd of beef cattle from the Sierra Nevada foothills, where tick infestation is common, has permanent access to open pastures. In contrast, the dairy cattle herd from the Central Valley has little or no access to pastures and tick infestations are not commonly observed (R. BonDurant, pers. comm.). Therefore, geographic differences in the prevalence of ***Bartonella*** infection in California cattle herds warrant further investigation for possible tick transmission of ***Bartonella*** spp. among these animals.

PCR/RFLP analysis of the citrate synthase gene has been widely used for identification of ***Bartonella*** organisms to the species level (25-27). We identified one PCR/RFLP profile for all the cattle isolates, but several profiles for deer and elk. This diversity by geographic location is of epidemiologic interest and warrants further investigation. Only one elk from southwestern Oregon had a strain with a similar PCR/RFLP profile to that of domestic cattle, suggesting that wild ruminants could be infected with ***Bartonella*** species that are not commonly shared with cattle.

Our findings also suggest that transmission of ***Bartonella*** may occur among cattle and wildlife, especially mule deer, which are more abundant in the western USA than elk and are more likely to be sympatric with cattle. Collection and analysis of ticks on wild animals and cattle and from the environment will be necessary to determine if ticks can be infected with ***Bartonella*** species. Whether ***Bartonella*** isolated from these ruminants are human pathogens is still unclear. The recent report of a cattle rancher who was infected with a new ***B. vinsonii*** subspecies (28) warrants further investigation to establish if these ***Bartonella*** species could be zoonotic and whether humans could potentially be infected by tick bites during work or recreation.

Dr. Chang is pursuing his Ph.D. in epidemiology at the University of California, Davis, under the direction of Bruno B. Chomel. His research interests include epidemiology of zoonoses, especially the molecular epidemiology of ***Bartonella*** infections and potential vectors for ***Bartonella*** spp. transmission.

Dr. Chang's research was funded by a grant from the Center for Companion Animal Health, University of California, Davis, California, USA.

References

1. Bass JW, Vincent JM, Person DA. The expanding spectrum of ***Bartonella*** infections. II. Cat scratch disease. Pediatr Infect Dis J 1997;16:163-79.
2. Chomel BB. Cat-scratch disease and bacillary angiomatosis. Rev Sci Tech 1996;15:1061-73.
3. Chomel BB, Kasten RW, Floyd-Hawkins KA, Chi B, Yamamoto K, Roberts-Wilson J, et al. Experimental transmission of ***Bartonella henselae*** by the cat flea. J Clin Microbiol 1996;34:1952-6.
4. Margileth AM. Cat-scratch disease. A therapeutic dilemma. Vet Clin North Am Small Anim Pract 1987;17:91-103.

5. Birtles RJ, Fichet-Calvet E, Raoult D, Ashford RW. Detection and genotypic differentiation of ***Bartonella*** species infecting a Tunisian ***Psammomys obesus*** population. 13th Sesqui-annual meeting of the American Society of Rickettsiology; 1997 Sep 21-24; Seven Springs Mountain Resort, Champion, Pennsylvania. [Abstract 34].
6. Ellis BA, Regnery RL, Beati L, Bacellar F, Rood M, Glass GG, et al. Rats of the genus ***Rattus*** are reservoir hosts for pathogenic ***Bartonella*** species: an Old World origin for a New World disease? J Infect Dis 1999;180:220-4.
7. Heller R, Kubina M, Delacour G, Mahoudeau I, Lamarque F, Artois M, et al. Prevalence of ***Bartonella*** spp. in blood of wild small rodents. Abstracts of the General Meeting of the American Society for Microbiology, 1997;97:115.
8. Heller R, Riegel P, Hansmann Y, Delacour G, Bermond D, Dehio C, et al. ***Bartonella tribocorum*** sp. nov., a new ***Bartonella*** species isolated from the blood of wild rats. Int J Syst Bacteriol 1998;48:1333-9.
9. Hofmeister EK, Kolbert CP, Abdulkarim AS, Magera JMH, Hopkins MK, Uhl JR, Ambyaye A, Telford III SR, Cockerill III FR, Persing DH. Cosegregation of a novel ***Bartonella*** species with ***Borrelia burgdorferi*** and ***Babesia microti*** in ***Peromyscus leucopus.*** J Infect Dis 1998;177:409-16.
10. Kosoy MY, Regnery RL, Tzianabos T, Marston EL, Jones DC, Green D, et al. Distribution, diversity, and host specificity of ***Bartonella*** in rodents from the southeastern United States. Am J Trop Med Hyg 1997;57:578-88.
11. Heller R, Kubina M, Mariet P, Riegel P, Delacour G, Dehio C, Lamarque F, Kasten R, Boulouis HJ, Monteil H. ***Bartonella alsatica*** sp. nov., a new ***Bartonella*** species isolated from the blood of wild rabbits. Int J Syst Bacteriol 1999;49:283-8.
12. Kordick DL, Swaminathan B, Greene CE, Wilson KH, Whitney AM, O'Connor S, et al. ***Bartonella vinsonii*** subsp. ***berkhoffii*** subsp. nov., isolated from dogs; ***Bartonella vinsonii*** subsp. ***vinsonii***; and emended description of ***Bartonella vinsonii***. Int J Syst Bacteriol 1996;46:704-9.
13. Kelly PJ, Rooney JJA, Marston EL, Jones DC, Regnery RL. ***Bartonella henselae*** isolated from cats in Zimbabwe [letter]. Lancet 1998;351:1706.
14. Chomel BB, Kasten RW, Chang CC, Yamamoto K, Heller R, Maruyama S, et al. Isolation of ***Bartonella*** spp. from California wildlife. International Conference on Emerging Infectious Diseases; 1998 Mar 8-11; Atlanta, Georgia. p. 21.10.
15. Heller R, Kubina M, Delacour G, Lamarque F, Van Laere G, Kasten R, et al. Isolation of ***Bartonella*** spp. from wildlife in France. International Conference on Emerging Infectious Diseases; 1998 Mar 8-11; Atlanta, Georgia. p. 21.18.
16. Pappalardo BL, Correa MT, York CC, Peat CY, Breitschwerdt EB. Epidemiologic evaluation of the risk factors associated with exposure and seroreactivity to ***Bartonella vinsonii*** in dogs. Am J Vet Res 1997;58:467-71.
17. Wall R, Shearer D. Veterinary entomology. 1st ed. London: Chapman and Hall; 1997. p. 338.
18. Chomel BB, Abbott RC, Kasten RW, Flowd-Hawkins KA, Kass PH, Glaser CA, et al. ***Bartonella henselae*** prevalence in domestic cats in California: risk factors and association between bacteremia and antibody titers. J Clin Microbiol 1995;33:2445-50.
19. Welch DF, Hensel DM, Pickett DA, San Joaquin VH, Robinson A, Slater LN. Bacteremia due to ***Rochalimaea henselae*** in a child: practical identification of isolates in the clinical laboratory. J Clin Microbiol 1993;31:2381-6.
20. Norman AF, Regnery R, Jameson P, Greene C, Krause DC. Differentiation of ***Bartonella***-like isolates at the species level by PCR-restriction fragment length polymorphism in the citrate synthase gene. J Clin Microbiol 1995;33:1797-803.
21. Donatien A, Lestoquard F. Sur une ***Bartonella*** nouvelle du boeuf, ***Bartonella bovis*** n. sp. Bull Soc Pathol Exot 1934;7:652-4.
22. Lotze JC, Yiengst MJ. Studies on the nature of ***Anaplasma***. Am J Vet Res 1942;3:312-20.
23. Bergmans AMC. Cat scratch disease: Studies on diagnosis and identification of reservoirs and vectors. Ph.D. Thesis, Utrecht University, The Netherlands, 1996; 152pp.
24. Schouls LM, Van de Pol I, Rijpkema SG, Schot CS. Detection and identification of ***Ehrlichia***, ***Borrelia burgdorferi*** sensu lato, and ***Bartonella*** species in Dutch ***Ixodes ricinus*** ticks. J Clin Microbiol 1999;37:2215-22.
25. Koehler JE, Quinn FD, Berger TG, LeBoit PE, Tappero JW. Isolation of ***Rochalimaea*** species from cutaneous and osseous lesions of bacillary angiomatosis. N Engl J Med 1992;327:1625-31.
26. Regnery RL, Andersen BE, Clarridge JE III, Rodriguez-Barradas MC, Jones DC, Carr JH. Characterization of a novel ***Rochalimaea*** species, ***R. henselae*** sp. nov., isolated from blood of a febrile, human immunodeficiency virus-positive patient. J Clin Microbiol 1992;30:265-74.
27. Dolan MJ, Wong MT, Regnery RL, Jorgensen JH, Garcia M, Peters J, et al. Syndrome of ***Rochalimaea henselae*** adenitis suggesting cat scratch disease. Ann Intern Med 1993;118:331-6.
28. Welch DF, Carroll KC, Hofmeister EK, Persing DH, Robison DA, Steigerwalt AG, et al. Isolation of a new subspecies, ***Bartonella vinsonii*** subsp. ***arupensis***, from a cattle rancher: identity with isolates found in conjunction with ***Borrelia burgdorferi*** and ***Babesia microti*** among naturally infected mice. J Clin Microbiol 1999;37:2598-601.

Carbapenem-Resistant *Pseudomonas aeruginosa* with Acquired *bla*$_{VIM}$ Metallo-ß-Lactamase Determinants, Italy

To the Editor: Acquired metallo-ß-lactamase determinants in ***Pseudomonas aeruginosa*** and other major bacterial pathogens are of concern for development of antimicrobial drug resistance. The carbapenemase and extended-spectrum cephalosporinase activity of metallo-ß-lactamases, as well as their resistance to ß-lactamase inhibitors, may severely limit the antimicrobial agents active against bacterial strains that produce such enzymes (1,2). Antimicrobial chemotherapy may become ineffective against ***P. aeruginosa*** strains with a multidrug-resistant phenotype that have acquired a metallo-ß-lactamase determinant.

We recently described a new acquired metallo-ß-lactamase determinant, ***bla***$_{VIM}$, in a carbapenem-resistant ***P. aeruginosa*** clinical isolate (VR-143/97) from the University Hospital of Verona, Italy (3). This isolate was the index strain of an outbreak of ***bla***$_{VIM}$-positive ***P. aeruginosa***, which was caused both by strains that were clonally related to VR-143/97 and by clonally unrelated strains (4). ***bla***$_{VIM}$ is the second known metallo-ß-lactamase determinant that can spread among ***P. aeruginosa***; the first was ***bla***$_{IMP}$, which was detected in the early 1990s in nosocomial isolates of various ***Enterobacteriaceae***, ***P. aeruginosa,*** and other nonfastidious gram-negative nonfermenters from the Far East (1,2,5-7) and, recently, in an ***Acinetobacter baumannii*** clinical isolate from Italy (8). Although completely unrelated at the sequence level, ***bla***$_{VIM}$ resembles ***bla***$_{IMP}$ in being carried on an integron-borne mobile gene cassette and in encoding an enzyme (VIM-1) with broad substrate specificity (3). Because of these properties, ***bla***$_{VIM}$ has the potential to become a dangerous resistance determinant.

An analysis of carbapenem-resistant ***P. aeruginosa*** from Italian hospitals since 1998 showed production of metallo-ß-lactamase, assayed as described (3), in five isolates from three hospitals in Italy. Two isolates (PPV-97 and PPV-108) were from the University Hospital of Pavia (PPV-97 was isolated in September 1998 from the urine of an inpatient in the neurosurgery department, and PPV-108 was isolated in November 1998 from a decubitus ulcer of an inpatient in the vascular surgery department); two (TS-832035 and TS-832347) were isolated in February 1999 from the University Hospital of Trieste (both from the blood of inpatients, in the intensive care unit and in the internal medicine department, respectively); and one (SAP-01/99) was isolated in September 1999 from the Rome University Hospital "Policlinico Umberto I" (from the blood of an inpatient in the vascular surgery department). Except for those from Pavia Hospital, where the two departments share the same surgical unit, no epidemiologic relationship could be established among any of them or with those previously isolated in Verona (3,4).

The five isolates were highly resistant to carbapenems (MICs for imipenem and meropenem were >64 µg/mL) and to carbenicillin, ticarcillin, ticarcillin/clavulanate, piperacillin, piperacillin/tazobactam, mezlocillin, ciprofloxacin, gentamicin, tobramycin, and netilmicin. All five were also resistant to ceftazidime and cefepime, except for SAP-01/99, which had intermediate resistance to the above drugs. Some isolates retained susceptibility to aztreonam (PPV-97, TS-832035, and SAP-01/99) or amikacin (PPV-108, TS-832035, and TS-832347).

In a colony-blot hybridization assay (3), all the above isolates were recognized by a ***bla***$_{VIM}$-specific probe consisting of an amplicon that contained the entire ***bla***$_{VIM}$ coding sequence (3). None were recognized by a probe specific for ***bla***$_{IMP}$ and consisting of a 0.5-kb ***Hin***dIII fragment from the ***bla***$_{IMP}$ gene (8).

Our results indicate that circulation of carbapenem-resistant ***P. aeruginosa*** carrying ***bla***$_{VIM}$ metallo-ß-lactamase determinants, originally detected in one Italian hospital (3-4), could soon become widespread. The detection in different hospitals of ***bla***$_{VIM}$-positive isolates that apparently were epidemiologically unrelated suggests that the environmental reservoir of ***bla***$_{VIM}$-containing strains is relatively broad and that this novel determinant has potential relevance for the emerging phenomenon of carbapenem resistance in ***P. aeruginosa***. Since we did not sequence the ***bla***$_{VIM}$-related genes carried by the various isolates, we do not yet know whether they differ from that cloned from ***P. aeruginosa*** VR-143/97 (3). The five isolates described in this report are being characterized to ascertain their clonal relatedness and identify the sequences of their ***bla***$_{VIM}$-related determinants. The recent appearance of this and other acquired metallo-ß-lactamases among ***P. aeruginosa***

and other gram-negative pathogens in Europe (8-10) underlines the need for systematic surveillance to monitor the spread of similar resistance determinants.

This work was supported by grants no. FMRX-CT98-0232 from the European TMR Research Network on metallo-ß-lactamases and no. 9906404271 from MURST ex-40%.

Gian Maria Rossolini,* Maria Letizia Riccio,* Giuseppe Cornaglia,† Laura Pagani,‡ Cristina Lagatolla,§ Laura Selan,¶ and Roberta Fontana†

* Università di Siena, Siena, Italy; †Università di Verona, Verona, Italy; ‡Università di Pavia, Pavia, Italy; §Università di Trieste, Trieste, Italy; and ¶Università "La Sapienza," Rome, Italy

References

1. Livermore DM. Acquired carbapenemases. J Antimicrob Chemother 1997;39:673-6.
2. Rasmussen BA, Bush K. Carbapenem-hydrolyzing ß-lactamases. Antimicrob Agents Chemother 1997;41:223-32.
3. Lauretti L, Riccio ML, Mazzariol A, Cornaglia G, Amicosante G, Fontana R, et al. Cloning and characterization of ***bla***$_{VIM}$, a new integron-borne metallo-ß-lactamase gene from a ***Pseudomonas aeruginosa*** clinical isolate. Antimicrob Agents Chemother 1999;43:1584-90.
4. Mazzariol A, Cornaglia G, Piccoli P, Lauretti L, Riccio ML, Rossolini GM, et al. Carbapenem-hydrolyzing ß-lactamases in ***Pseudomonas aeruginosa***. Eur J Clin Microbiol Infect Dis 1999;18:455-6.
5. Senda K, Arakawa Y, Nakashima K, Ito H, Ichiyama S, Shimokata K, et al. Multifocal outbreaks of metallo-ß-lactamase-producing ***Pseudomonas aeruginosa*** resistant to broad-spectrum ß-lactams, including carbapenems. Antimicrob Agents Chemother 1996;40:349-53.
6. Lee K, Chong Y, Shin HB, Yong D. Rapid increase of imipenem-hydrolyzing ***Pseudomonas aeruginosa*** in a Korean hospital. In: Program and Abstracts of the 38th Interscience Conference on Antimicrobial Agents and Chemotherapy. Washington: American Society for Microbiology; 1998. [Abstract E85].
7. Koh TH, Babini GS, Woodford N, Sng LH, Hall LM, Livermore DM. Carbapenem-hydrolysing IMP-1 ß-lactamase in ***Klebsiella pneumoniae*** from Singapore. Lancet 1999;353:2162.
8. Cornaglia G, Riccio ML, Mazzariol A, Lauretti L, Fontana R, Rossolini GM. Appearance of IMP-1 metallo-ß-lactamase in Europe. Lancet 1999;353:899-900.
9. Woodford N, Palepou M-FI, Babini GS, Bates J, Livermore DM. Carbapenemase-producing ***Pseudomonas aeruginosa*** in the UK. Lancet 1998;352:546-7.
10. Cardoso O, Sousa JC, Leitão R, Peixe L. Carbapenem-hydrolysing ß-lactamase from clinical isolates of ***Pseudomonas aeruginosa*** in Portugal. J Antimicrob Chemother 1999;44:135.

Malaria and Global Warming in Perspective?

To the Editor: I read with great interest the article "From Shakespeare to Defoe: malaria in England in the Little Ice Age" (1). Unfortunately, the article is not as balanced as a presentation last year by Paul Reiter, which clearly illustrated that, although climate is important in the transmission of malaria, the influence of other factors (e.g., access to medical care and improved housing) is likely to be of more importance in Europe.

Malaria indeed was quite common in Europe, even in the Roman Empire and in Medieval Europe, and until a few decades ago, it was still present in parts of Europe, Australia, and North America. In fact, the failure of the 1806 British invasion of Zeeland in the Netherlands may be attributable to infection of the British forces with malaria. However, the authors referenced by Reiter have never made the claim that in the coming years warmer "temperatures will result in malaria transmission in Europe and North America." On the contrary, the reports of the Intergovernmental Panel on Climate Change Reiter quotes conclude that "Although climate change could increase the potential transmission of malaria [in Europe and North America], existing public health resources—disease surveillance, surface water management, and treatment of cases—would make reemergent malaria unlikely" (2,3).

Reiter's argument that some scientists attribute the recent observed increase in malaria risk to climate trends is also not accurate. While acknowledging the sensitivity of the malaria mosquito and parasite to climate, these researchers examine insect and incidence data to explore multiple factors underlying malaria emergence. Another group of scientists uses mathematical simulation models to estimate changes in malaria risk over the next few decades. These models, which are heuristic tools not meant to predict future worlds, assess how potential risk for malaria may by affected by changes in climate (4). The goals of both types of research are to improve knowledge of the complex malaria transmission cycle, define epidemic-prone areas, identify the reasons for increased malaria risk, and develop solutions to protect vulnerable communities.

Dr. Reiter acknowledges the sensitivity of malaria to climatic influences, and I am sure that he agrees that change in climate will affect risk for transmission—he may be skeptical as to whether global warming will ever become a fact, but that is another question. While Reiter's paper offers an interesting perspective on the history of malaria in Europe, it provides no illuminating information on the influence of climate change on human health.

Pim Martens
Maastricht University, Maastricht, the Netherlands

References

1. Reiter P. From Shakespeare to Defoe: malaria in England in the Little Ice Age. Emerg Infect Dis 2000;6:1-11.
2. Intergovernmental Panel on Climate Change. The regional impacts of climate change: an assessment of vulnerability. Working Group II. Intergovernmental Panel on Climate Change. New York: Cambridge University Press; 1998. Chapters 5, 8.
3. Intergovernmental Panel on Climate Change. Climate change 1995: impacts, adaptations and mitigation of climate change: scientific-technical analyses. Working Group II, Intergovernmental Panel on Climate Change. New York: Cambridge University Press; 1996. Chapter 18.
4. Martens P. Health and climate change: modelling the impacts of global warming and ozone depletion. London: Earthscan Publications Ltd.; 1998.

For P. Reiter's response, please see
http://www.cdc.gov/ncidod/EID/vol6no4/reiter.htm

Serologic Evidence of Human Monocytic and Granulocytic Ehrlichiosis in Israel

To the Editor: We read with great attention the article by Dr. Keysary et al., who reported the first evidence of human monocytic and granulocytic ehrlichiosis in Israel (1); however, we disagree with their conclusions.

Ehrlichiae comprise a large group of intracellular organisms pathogenic for animals and occasionally for humans. Because these organisms are closely related, serologic cross-reactions occur within and between groups, leading to mistakes in identification. For example, ***Ehrlichia chaffeensis*** was misdiagnosed as ***E. canis*** in humans (2) and human granulocytic ehrlichiosis as human monocytic ehrlichiosis in areas where the vector was not present (3). Because of such cross-reactions, serology alone is not sufficient to establish the existence of a new ehrlichial disease.

With the exception of ***Rhipicephalus sanguineus***, the brown dog tick, which is distributed worldwide, tick species of medical importance are very geographically specific. For example, the ***Ixodes*** and ***Dermacentor*** spp. found in Europe are not those found in the United States. Consequently, tick-transmitted organisms and diseases are also very specific geographically. For example, ***Borrelia*** spp. found in the Old World are not found in America (except for ***B. burgdorferi stricto sensu,*** which is found in both Europe and America). ***R. rickettsii***, transmitted by ***Dermacentor andersoni*** and ***D. variablilis,*** is reported in the United States but not in Europe, where the vectors are not present.

American monocytic ehrlichiosis is caused by ***E. chaffeensis***, which is transmitted by the tick ***Amblyomma americanum,*** found only in America. The main reservoir is the deer ***Odocoileus virginanus*** (4).

It is very unlikely that a tick-borne disease occurred in a country where neither the vector nor the reservoir of the bacterium exists. All attempts to demonstrate the presence of ***E. chaffeensis*** in the Old World, including Africa, have failed. Indeed, there is no convincing evidence of the existence of ***E. chaffeensis*** outside America.

Philippe Brouqui* and J. Steven Dumler†
Unité des Rickettsies, Faculté de Médecine, Marseille, France; and Johns Hopkins University School of Hygiene & Public Health, Baltimore, Maryland, USA

References

1. Keysary A, Amram L, Keren G, Sthoeger Z, Potasman I, Jacob A, et al. Serologic evidence of human monocytic and granulocytic ehrlichiosis in Israel. Emerg Infect Dis 1999;5:775-8.
2. Maeda K, Markowitz N, Hawley RC, Ristic M, Cox D, McDade JE. Human infection with ***Ehrlichia canis***, a leukocytic rickettsia. N Engl J Med 1987;316:853-6.
3. Brouqui P, Raoult D. Human ehrlichiosis. N Engl J Med 1994;330:1760-1.
4. Dumler JS, Bakken JS. Ehrlichial diseases of humans: emerging tick-borne infections. Clin Infect Dis 1995;20:1102-10.

Serologic Evidence of Human Monocytic and Granulocytic Ehrlichiosis in Israel

To the Editor: Our article on ehrlichiosis in Israel is one of several reporting serologic evidence of ehrlichiosis outside North America (1-4). Serologic tests were performed for immunoglobulin (IgG) antibodies to ***Ehrlichia chaffeensis***, ***E. canis,*** and human granulocytic ehrlichiosis (HGE) agent to prevent misinterpretation due to cross-reaction. The conclusions meet the criteria published by the American Society for Rickettsiology, in which a confirmed diagnosis of human monocytic ehrlichiosis (HME) is based on a "single serum titer of 256" in a patient with clinically compatible disease (5).

The argument that the same epidemiologic circumstances that exist in the United States have to be prevalent in Israel for the disease to be present is not compelling. Reporting serologic evidence of ehrlichiosis in Israel alerts physicians to the possibility of HME and HGE when they see patients with symptoms compatible with these diseases. We agree that isolation and molecular identification of both agents are essential to confirming the presence of these diseases in Israel.

Avi Keysary and Trevor Waner
Israel Institute for Biological Research,
Ness Ziona, Israel

References

1. Keysary A, Amram L, Keren G, Sthoeger A, Potasman I, Jacob A, et al. Serologic evidence of human monocytic and granulocytic ehrlichiosis in Israel. Emerg Infect Dis 1999;5:775-8.
2. Morais JD, Dawson JE, Greene C, Filipe AR, Galhardas LC, Bacellar F. First European case of ehrlichiosis. Lancet 1991;338:833-4.
3. Bakken JS, Krueth J, Tilden RL, Dumler JS, Kristiansen BE. Serological evidence of human granulocytic ehrlichiosis in Norway. Eur J Microbiol Infect Dis 1996;15:829-32.
4. Christova IS, Dumler JS. Human granulocytic ehrlichiosis in Bulgaria. Am J Trop Med Hyg 1999;60:58-61.
5. Walker DH. Consensus workshop on diagnosis of human ehrlichiosis. Bulletin of the American Society for Rickettsiology 1999;2:1-8.

Upcoming Events

Parasite Genomes—Thematic Issue Now Available

The International Journal for Parasitology, Volume 30/4 (April 2000), announces the publication of a thematic issue on Parasite Genomes, guest-edited by Paul Brindley at Tulane University, New Orleans, USA.

Experts in the field have contributed articles on medically and economically important parasites, both helminths and protozoans. Topics include "The African trypanosome genome," by Najib M. El-Sayed, Priti Hegde, John Quackenbush, Sara E. Melville, and John E. Donelson; "Genes and genomes of ***Necator americanus*** and related hookworms," by Mark L. Blaxter; "The conserved genome organisation of non-***falciparum*** malaria species: the need to know more," by Leonard H.M. van Linn, Chris J. Janse, and Andrew P. Waters; "Mitochondrial genome diversity in parasites," by Jean E. Feagin; and "The ***Giardia lamblia*** genome," by Rodney D. Adam.

Free access to the full text of the 20 articles can be found at http://www.elsevier.nl/locate/ijpara.

5th International Conference on Legionella
Ulm, Germany
September 26–29, 2000

The 5th International Conference on Legionella will be held in Ulm, Germany, September 26-29, 2000. Topics include pathogenesis, immunology, ecology, clinical microbiology, epidemiology, surveillance, and prevention. Proceedings will be published by the American Society for Microbiology.

For more information, contact Jens Thomsen, Department of Medicine, Microbiology and Hygiene, University of Ulm, 89081 Ulm, Germany; telephone: 49-731-50-24603; fax: 49-731-50-24619; e-mail: jens.thomsen@medizin.uni-ulm.de; http://www.uni-ulm.de/legionella/.

Third Internet Conference on Salivarian Trypanosomes and Trypanosomatids
October 2–18, 2000

The third Internet Conference on Salivarian Trypanosomes and Trypanosomatids will take place October 2–18, 2000, at http://www.dbbm.fiocruz.br/trypnews/events/ticstt.html or http://pubweb.nwu.edu/~kmt564/TICSTT.html. Through featured presentations, posters, and discussion boards, the conference will cover all aspects of trypanosome research, including biology and ultrastructure, biochemistry and drug development, immunology and pathology, molecular biology, epidemiology, vectors, and control. Proceedings will be published in the International Journal for Parasitology.

For presentations (6 megabyte limit), the deadlines are September 1 for HTML format and August 15 for other formats. For posters (1.5 megabyte limit), the deadline is August 15; only HTML format will be accepted. Instructions for authors are available on-line at the above URL. For more information, contact Alberto Davila, Instituto Oswaldo Cruz, Rio de Janeiro, Brazil; e-mail: davila@gene.dbbm.fiocruz.br; or Kevin Tyler, Northwestern University, Chicago; e-mail: k-tyler@nwu.edu.

Nosocomial Infections Conference
Institut Pasteur, Paris, France
November 15–18, 2000

The rapid proliferation of nosocomial infections, mostly in intensive care and surgical units, is related to increases in surgical interventions, multidrug-resistant microorganisms, and the number of immunocompromised patients at high risk. Prophylaxis and treatment may be delayed because of poor diagnosis, biofilm formation on implants, and the emergence of new pathogens from bacterial genetic exchange and in vivo mutagenesis.

Topics to be discussed during the Nosocomial Infections Conference include surveillance, new methods for rapid microorganism identification and typing, identification of genes linked to antibiotic resistance, molecular studies of pathogenicity, and biofilm formation.

The Institut Pasteur Euroconferences are intended to facilitate communication between academicians and industry. Committee members for the Nosocomial Infections Conference are Patrice Courvalin, Jean-Christophe Lucet, Philippe Sansonetti, and Cécile Wandersman.

For more information, contact Ludovic Drye, Conference Coordinator, Institut Pasteur EuroConferences, 28 rue du Docteur Roux, 75724 Paris Cedex 15, France; telephone: 331-406-13374; fax: 331-406-13405; e-mail: ldrye@pasteur.fr; conference web site: http://www.pasteur.fr/applications/euroconf/.

Erratum Vol. 5, No. 5

In the article "Using a Spatial Filter and a Geographic Information System to Improve Rabies Surveillance Data," by Andrew Curtis, there is an error in Figure 1 on page 604. The topmost and center maps have been transposed. The on-line article contains the correct figure, at URL: http://www.cdc.gov/ncidod/eid/vol5no5/curtis.htm

We regret any confusion this error may have caused.

Editorial Policy and Call for Articles

Emerging Infectious Diseases is a peer-reviewed journal established expressly to promote the recognition of new and reemerging infectious diseases around the world and improve the understanding of factors involved in disease emergence, prevention, and elimination.

The journal has an international scope and is intended for professionals in infectious diseases and related sciences. We welcome contributions from infectious disease specialists in academia, industry, clinical practice, and public health, as well as from specialists in economics, demography, sociology, and other disciplines. Inquiries about the suitability of proposed articles may be directed to the Editor at 404-371-5329 (tel), 404-371-5449 (fax), or eideditor@cdc.gov (e-mail).

Emerging Infectious Diseases is published in English and features the following types of articles: Perspectives, Synopses, Research Studies, Policy Reviews, and Dispatches. The purpose and requirements of each type of article are described in detail below. To expedite publication of information, we post journal articles on the Internet as soon as they are cleared and edited.

Spanish and French translations of some articles can be accessed through the journal's homepage at www.cdc.gov/eid. Articles by authors from non-English-speaking countries can be made simultaneously available in English and in the author's native language (electronic version of the journal only).

Instructions to Authors

Manuscript Preparation

Follow "Uniform Requirements for Manuscripts Submitted to Biomedical Journals" (Ann Intern Med 1997:126[1]36-47) (http://www.acponline.org/journals/annals/01jan97/unifreqr.htm).

Begin each of the following sections on a new page and in this order: title page, abstract, text, acknowledgments, references, tables, figure legends, and figures.

Title page. Give complete information about each author (i.e., full name, graduate degree(s), affiliation, and the name of the institution in which the work was done). Also provide address for correspondence (include fax number and e-mail address).

Abstract and key words. Avoid citing references in the abstract. Include up to 10 key words; use terms listed in the Medical Subject Headings from Index Medicus (http://www.nlm.nih.gov/mesh/meshhome.html).

Text. Double-space everything, including the title page, abstract, references, tables, and figure legends. Type only on one side of the paper and number all pages, beginning with the title page. Indent paragraphs 5 spaces; leave no extra space between paragraphs. After a period, leave only one space before beginning the next sentence. Use Courier font size 10 and ragged right margins. Italicize (rather than underline) scientific names when needed.

Electronic formats. For word processing, use WordPerfect or MS Word. Send graphics in either .TIF (Tagged Image File), or .EPS (Encapsulated Postscript) formats. The preferred font for graphics files is Helvetica. Convert Macintosh files into one of the suggested formats. Submit slides or photographs in glossy, camera-ready photographic prints.

References. Follow the Uniform Requirements style. Place reference numbers in parentheses, not in superscripts. Number citations in order of appearance (including in text, figures, and tables). Cite personal communications, unpublished data, and manuscripts in preparation or submitted for publication in parentheses in text. Consult List of Journals Indexed in Index Medicus for accepted journal abbreviations; if a journal is not listed, spell out the journal title in full. List the first six authors followed by "et al."

Tables and figures. Create tables within the word processing program's table feature (not columns and tabs within the word processing program). For figures, use color as needed; send files, slides, photographs, or prints. Figures, symbols, lettering, and numbering should be clear and large enough to remain legible when reduced. Place figure keys within the figure.

Manuscript Submission

Include a cover letter verifying that the final manuscript has been seen and approved by all authors.

Submit three copies of the original manuscript with three sets of original figures and an electronic copy (on diskette or by e-mail) to the Editor, Emerging Infectious Diseases, Centers for Disease Control and Prevention, 1600 Clifton Rd., MS D 61, Atlanta, GA 30333, USA; e-mail eideditor@cdc.gov.

Types of Articles

Perspectives, Synopses, Research Studies, and Policy Reviews: Articles should be approximately 3,500 words and should include references, not to exceed 40. Use of subheadings in the main body of the text is recommended. Photographs and illustrations are encouraged. Provide a short abstract (150 words) and a brief biographical sketch.

Perspectives: Articles in this section should provide insightful analysis and commentary about new and reemerging infectious diseases or related issues. Perspectives may also address factors known to influence the emergence of diseases, including microbial adaptation and change; human demographics and behavior; technology and industry; economic development and land use; international travel and commerce; and the breakdown of public health measures. If detailed methods are included, a separate section on experimental procedures should immediately follow the body of the text.

Synopses: This section comprises concise reviews of infectious diseases or closely related topics. Preference is given to reviews of new and emerging diseases; however, timely updates of other diseases or topics are also welcome. Use of subheadings in the main body of the text is recommended. If detailed methods are included, a separate section on experimental procedures should immediately follow the body of the text. Photographs and illustrations are encouraged.

Research Studies: These articles report laboratory and epidemiologic results within a public health perspective. Although these reports may be written in the style of traditional research articles, they should explain the value of the research in public health terms and place the findings in a larger perspective (e.g., "Here is what we found, and here is what the findings mean").

Policy Reviews: Articles in this section report public health policies that are based on research and analysis of emerging disease issues.

Dispatches: These brief articles are updates on infectious disease trends and research. The articles include descriptions of new methods for detecting, characterizing, or subtyping new or reemerging pathogens. Developments in antimicrobial drugs, vaccines, or infectious disease prevention or elimination programs are appropriate. Case reports are also welcome. Dispatches (1,000 to 1,500 words) need not be divided into sections. Provide a short abstract (50 words); references, not to exceed 10; figures or illustrations, not to exceed two; and a brief biographical sketch.

Book Reviews: Short reviews (250 to 500 words) of recently published books on emerging disease issues are welcome.

Letters: This section includes letters that give preliminary data or comment on published articles. Letters (500 to 1,000 words) should not be divided into sections, nor should they contain figures or tables. References (not more than 10) may be included.

News and Notes: We welcome brief announcements (50 to 150 words) of timely events of interest to our readers. (Announcements can be posted on the journal web page only, depending on the event date.) In this section, we also include summaries (500 to 1,500 words) of conferences focusing on emerging infectious diseases. Summaries may provide references to a full report of conference activities and should focus on the meeting's content.